TRANSPORTATION RESEARCH RECORD 666

Pavement Surface Properties, Evaluation, and Shoulders

TRANSPORTATION RESEARCH BOARD

COMMISSION ON SOCIOTECHNICAL SYSTEMS
NATIONAL RESEARCH COUNCIL

NATIONAL ACADEMY OF SCIENCES
WASHINGTON, D.C. 1978

Transportation Research Record 666
Price $4.00
Edited for TRB by Mary McLaughlin

subject areas
22 highway design
25 pavement design
26 pavement performance

Transportation Research Board publications are available by ordering directly from the board. They may also be obtained on a regular basis through organizational or individual supporting membership in the board; members or library subscribers are eligible for substantial discounts. For further information, write to the Transportation Research Board, National Academy of Sciences, 2101 Constitution Avenue, N.W., Washington, D.C. 20418.

Notice
The papers in this Record have been reviewed by and accepted for publication by knowledgeable persons other than the authors according to procedures approved by a Report Review Committee consisting of members of the National Academy of Sciences, the National Academy of Engineering, and the Institute of Medicine.

The views expressed in these papers are those of the authors and do not necessarily reflect those of the sponsoring committee, the Transportation Research Board, the National Academy of Sciences or the sponsors of TRB activities.

To eliminate a backlog of publications and to make possible earlier, more timely publication of reports given at its meetings, the Transportation Research Board has, for a trial period, adopted less stringent editorial standards for certain classes of published material. The new standards apply only to papers and reports that are clearly attributed to specific authors and that have been accepted for publication after committee review for technical content. Within broad limits, the syntax and style of the published version of these reports are those of the author(s).

The papers in this Record were treated according to the new standards.

Library of Congress Cataloging in Publication Data
National Research Council. Transportation Research Board.
Pavement surface properties, evaluation, and shoulders.

(Transportation research record; 666)

1. Pavements–Testing–Congresses. 2. Pavements–Skid resistance–Testing–Congresses. 3. Roads–Riding qualities–Testing–Congresses. 4. Roads–Shoulders–Congresses. I. Title. II. Series.
TE7.H5 no. 666 [TE250] 380.5'08s [625.8] 78-32008
ISBN 0-309-02805-1

Sponsorship of the Papers in This Transportation Research Record

GROUP 2—DESIGN AND CONSTRUCTION OF TRANSPORTATION FACILITIES
Eldon J. Yoder, Purdue University, chairman

Pavement Design Section
Carl L. Monismith, University of California, Berkeley, chairman

Committee on Surface Properties-Vehicle Interaction
Don L. Ivey, Texas A&M University, chairman
Glenn G. Balmer, Frederick E. Behn, A. Y. Casanova III, Peter M. W. Elsenaar, Robert D. Ervin, Michael W. Fitzpatrick, Kenneth D. Hankins, Rudolph R. Hegmon, Kenneth J. Law, David C. Mahone, James A. Matthews, W. E. Meyer, Thomas H. Morrow, Jr., W. Grigg Mullen, Arthur H. Neill, Jr., Bayard E. Quinn, John J. Quinn, Hollis B. Rushing, Richard K. Shaffer, Elson B. Spangler, James C. Wambold, M. Lee Webster, E. A. Whitehurst, Ross G. Wilcox

Committee on Pavement Condition Evaluation
K. H. McGhee, Virginia Highway and Transportation Research Council, chairman
Michael I. Darter, Edwin J. Dudka, Karl H. Dunn, Asif Faiz, Wouter Gulden, Ralph C. G. Haas, William H. Highter, W. Ronald Hudson, L. B. R. Hunter, David J. Lambiotte, J. A. Little, J. W. Lyon, Jr., R. D. Pavlovich, William A. Phang, Bayard E. Quinn, Freddy L. Roberts, Albert F. Sanborn III, Lawrence L. Smith, Paul N. Sonnenburg, Herbert F. Southgate, Elson B. Spangler, Robert J. Weaver, Loren M. Womack,

Committee on Shoulder Design
John F. Nixon, Texas State Department of Highways and Public Transportation, chairman
John S. Urban, Edwards & Kelcey, Incorporated, secretary
Donald K. Emery, Jr., Alvord C. Estep, Wade L. Gramling, Clinton L. Heimbach, R. G. Hicks, James W. Hill, John W. Hutchinson, Edwin C. Lokken, D. W. Loutzenheiser, Richard A. McComb, Leon M. Noel, R. D. Pavlovich, Josette M. Portigo, James F. Roberts, James A. Scherocman, F. W. Thorstenson, Graeme D. Weaver, W. A. Wilson, Jr.

Lawrence F. Spaine, Transportation Research Board staff

Sponsorship is indicated by a footnote at the end of each report. The organizational units and officers and members are as of December 31, 1977.

Contents

Pavement Texture: Its Significance and Development

Glenn G. Balmer, Federal Highway Administration, U.S. Department of Transportation

This paper discusses the influence of roadway surface textures on skid resistance, the skid resistance-speed gradient, accident rates on wet pavements, pavement wear, and the noise generated by tire-road interaction. The tendency of a vehicle to hydroplane is reduced by increasing the depth of the pavement texture. Appropriate textures are developed by using open-graded asphalt friction surface courses and by finishing portland cement concrete with steel tines or a vibrating float while the concrete is plastic. Hardened pavements can be textured by grooving with a diamond saw or by resurfacing with an overlay. More development is needed in techniques of texture measurement, especially in automating the stereophotographic interpretation method.

Water on the roadway is one of the major causes of highway accidents. It induces hydroplaning, reduces skid resistance, and adversely affects vehicle control (1). Modern high-speed traffic challenges the highway engineer to provide dynamic drainage at the tire-pavement interface and facilities for rapid removal of water from the pavement surface during precipitation. Construction of deep-textured surfaces can help in achieving these goals.

CLASSIFICATION OF SURFACE TEXTURES

The large-scale features of a pavement surface—known as the macrotexture—are commonly distinguished from the fine-scale features—the microtexture. Pavement surfaces can be analyzed in more detail by use of an American Society for Testing and Materials (ASTM) procedure, ASTM E 559. Four parameters are coded for the macrotexture: height, width, angularity, and density of the distribution of large projections. Two parameters describe the microtexture: harshness and the rugosity of the background. Kummer and Meyer (2) have classified the surface types as (a) smooth, (b) fine-textured and rounded, (c) fine-textured and gritty, (d) coarse-textured and rounded, and (e) coarse-textured and gritty.

MECHANISTIC ASPECTS OF TEXTURE

Effect of Texture on Friction and Speed Gradient

Figure 1 (3) shows the effects that road surfaces have on skid resistance and speed gradient. Both adhesion and hysteresis contribute to skid resistance. Adhesion is the shear force developed at the interface between the tire and the roadway, and hysteresis is the friction produced by damping losses in the rubber of the tire. Harsh or gritty pavement surfaces yield larger skid numbers (100 times the coefficient of friction) than rounded, polished, or smooth surfaces. This is true for both locked-wheel and peak braking. The sharp asperities of angular aggregates tend to penetrate the water film and grip the tires to provide better friction on wet pavements. The sharp, coarse texture is even more effective for peak braking than it is for locked-wheel braking.

The skid resistance-speed gradient (G) can be defined by

$$G_{(A-B)} = (SN_A - SN_B)/(B - A) \quad (1)$$

in which A and B are the test speeds at which the skid numbers SN_A and SN_B are measured. The gradient is often steeper at higher levels of skid resistance; therefore, a percentage gradient, which can be defined as

$$PG = [G/SN_{0.5(A+B)}] \times 100 \quad (2)$$

may correlate better with texture measurements (4) than does the speed gradient.

The speed gradient is not as steep for coarse surfaces as for fine-textured roadways because the large voids in coarse surfaces allow more rapid expulsion of water at the tire-road interface and because the coarse texture develops greater hysteretic effects in the tire, improving its friction characteristics. Skid resistance thus decreases more slowly with increasing speed. Open- or coarse-textured pavements are therefore excellent for safe, wet-weather travel at higher speeds. They decrease objectionable splash and spray, reduce hydroplaning, and diminish headlight glare by dispersing light (glare becomes intolerable at night when the roadway surface is smooth, wet, and reflective).

Gritty, fine-textured pavements usually yield larger skid numbers at lower speeds than do open-graded roadways. This makes them suitable for slow-speed traffic. Moyer (5) recognized the virtue of gritty, dense-graded surfaces many years ago. Surfaces of this type have been used successfully in Kentucky and Virginia and in other locations.

Influence of Texture Depth

Figure 2 shows significant increases in mean skid number with an increase in mean texture depth ("sand

Figure 1. Influence of different road surfaces on tire grip.

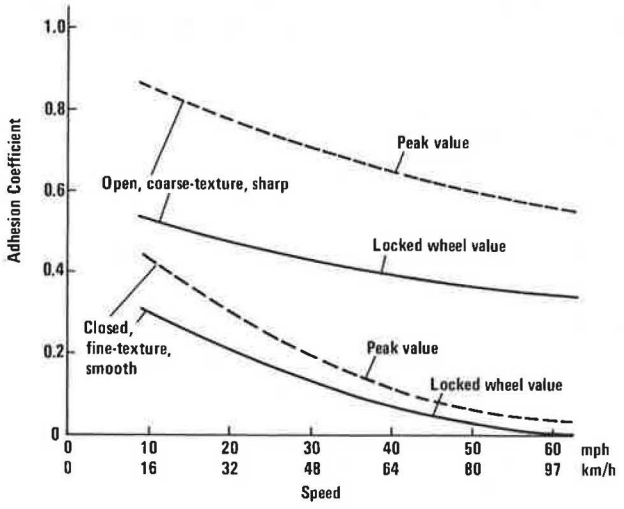

Figure 2. Effect of texturing methods on initial texture depth and skid resistance.

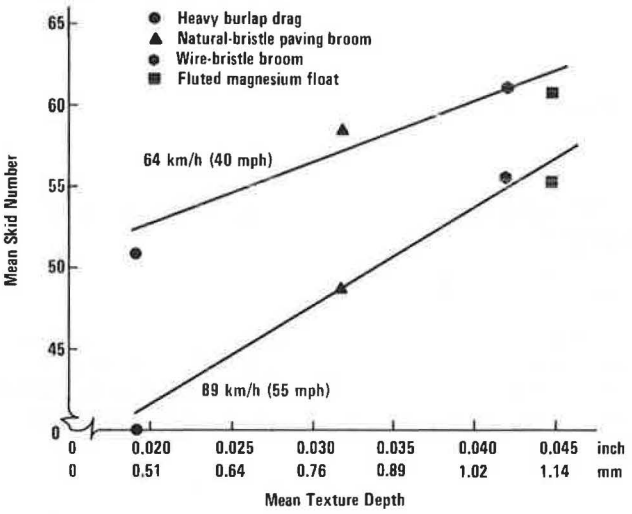

patch" method of texture measurement) on portland cement concrete (PCC) pavement in skid tests at 64 and 89 km/h (40 and 55 mph) (6). It should be noted that the slope is greater at the higher test speed. The coarse texture allows better drainage relief than the fine texture, particularly at the higher speed, and stimulates the hysteretic response of the tires.

Similar results have been obtained by others (7,8). One investigator's experiments extended linearly to a texture depth of nearly 2.5 mm (0.1 in). Both the sand-patch and "putty impression" methods (6,7,9) were used for measurement.

In a study of hydroplaning (10), experiments yielded more than a 16-km/h (10-mph) difference in speed for the initiation of hydroplaning for textures between 0.46 and 3.68 mm (0.018 and 0.145 in); this was determined by using the putty impression method and a 10 percent spin-down of the hydroplaning wheel. The more shallow texture was obtained by using a burlap drag on PCC pavement and the deeper one by using a seal coat with large, round river gravel. The deeper texture may be coarser than that generally used on highways, but it demonstrates the influence of texture on hydroplaning.

When the water depth on a pavement surface is measured from the top of the asperities, the depth is expressed as negative when the asperities are exposed and positive when they are inundated.

In Figure 3, the putty impression method has been used to show the depths of texture required to prevent

Figure 3. Combinations of cross slope and texture required to prevent significant water depths.

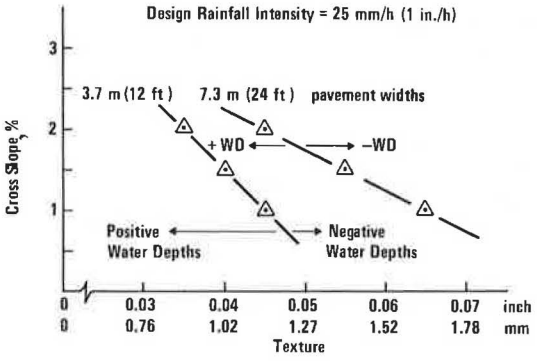

significant water depths for various cross slopes and for two pavement widths when a design rainfall intensity of 25 mm/h (1 in/h) reaches the steady state (11). It should be noted that the texture requirement increases as the width of the pavement increases and the cross slope decreases.

Skid Number Versus Accident Rate

Experimental results indicate that wet-pavement skid resistance usually increases with the depth of the pavement texture. Figure 4 shows that the wet-surface accident rate decreases as the skid number increases. These data were obtained from ASTM locked-wheel skid test measurements and from accident analysis on rural Interstate and parkway roads in Kentucky. Two analysis curves of similar shape are shown: one for roads with average daily traffic (ADT) of less than 3000 and one for roads with greater than 3000 ADT. The results are expressed in accidents per 161 million vehicle km (100 million vehicle miles).

Both curves reveal a significant decrease in the accident rate when the wet-pavement skid number is greater than 44. These data were obtained from an extensive analysis of wet-pavement accidents and a large number of highway skid tests conducted at 64 km/h (40 mph). Other analyses and tests conducted at a speed of 113 km/h (70 mph) show that a value of SN_{40} = 44 is equivalent to approximately SN_{70} = 27.

Open-Graded Asphalt Friction Courses

Western states recognized the merits of open-graded asphalt friction courses several years ago (12), and a number of these courses have been placed on roadways throughout the nation. Highway designers are recommending these surfaces to improve skid resistance and mitigate hydroplaning.

If quality aggregates are used, the skid resistance of open-graded courses is excellent when the plant-mix seals are new. In general, test results show improvement in friction characteristics as the bitumen wears and the harsh angular aggregates are exposed. The skid number decreases slightly with continued wear, but the surfaces continue to exhibit excellent skid resistance for several years.

The Louisiana Department of Highways has conducted tests on plant-mix seals with several different aggregates (13). A summary of test results on the performance of open-graded surfaces with time and traffic is given in Table 1. The test results indicate that the skid resistance of plant-mix seals is superior to that of a dense-graded hot-mix surface. The comparison would probably have favored plant-mix seals even more at higher speeds because the speed gradient of open-graded plant-mix seals is usually smaller than that of a dense-graded surface.

Smith, Rice, and Spelman (14) provide information on a new design method for open-graded asphalt friction courses, listing the following benefits for such courses:

1. Improved skid resistance at high speeds during wet weather,
2. Minimization of hydroplaning effects during wet weather,
3. Improved road smoothness [present serviceability index (PSI)],
4. Minimization of splash and spray during wet weather,
5. Minimization of wheel-path rutting,
6. Improved visibility of painted traffic markings,

7. Improved night visibility during wet weather (less glare),
8. Lower highway noise levels, and
9. Retardation of ice formation on the road surface.

These courses are desirable because their open texture provides channels for the escape of water from the surface. Air voids of 15 percent or greater are recommended in the design and construction of open-graded courses.

NOISE AND WEAR

Noise Produced by Tire-Road Interaction

The noise produced by tire-road interaction (15,16) increases with speed, depth of the pavement texture, and moisture, and it is the dominant traffic noise at higher vehicle speeds. It also increases with tire load and wear for many tire tread patterns. Tread vibration is a major source of tire-road noise. Irregularities in the road surface (asperities, texture, and roughness of the pavement) create an oscillation in the tread that emits sound waves. The modal responses of tires differ. At low frequencies most of the sound emanates from the contact area, whereas at higher frequencies carcass vibrations also contribute to the generation of sound.

Figure 5 (7) provides preliminary experimental highway data on sound pressure level versus texture depth for several finishing techniques at speeds of 64 and 97 km/h (40 and 60 mph). Noise was measured with a microphone near the left rear tire of a panel truck 1 m (3.3 ft) above the pavement. A conventional, worn highway tire was used as the test tire. Noise is expressed in decibels on the A scale, a measure of sound that is practical for modern highway vehicles and that correlates well with human evaluation of noise.

Notice that the sound level increases with texture depth for both speeds, but the noise is substantially greater at the higher speed. Steel comb or tine finishes for PCC pavements are rapidly gaining in favor, and this finishing technique has been used to develop the deeper textures.

Texture depth is not the only factor related to noise. The shape and the spacing of striations are other factors. Placing transverse grooves at irregular intervals in the road surface has prevented generation of a pure tone for concrete that was plastic grooved with a vibrating float (17). Random sizing of the discrete blocks or lugs of tire tread patterns is another way to reduce sound level. These methods diversify the sound frequencies developed and so decrease the intensity of individual tones.

Optimal tire performance and its relation to pavement texture, noise, polishing, and wear have been studied in England. Petrographic types of aggregates were subjected to polishing tests and then examined with a scanning electron microscope. A microtexture between 0.01 and 0.1 mm (0.0004 and 0.004 in) was recommended to penetrate a viscous water film and establish a harshness that is adequate for effective tire contact without excessive tire wear (18). Optimal macrotexture for sufficient bulk water drainage was provided by surface aggregates 6 to 12 mm (0.24 to 0.47 in) in diameter.

Another study suggests that a 0.4 ratio of groove to rib width for vehicle tires gives optimum tread drainage (19).

Wear of the Pavement Surface

Pavement surfaces wear by abrasion, degradation, and decomposition as a result of vehicle traffic and environ-

Table 1. Friction performance of open-graded surfaces (high traffic volume in exterior lane).

Age (months)	Cumulative Traffic (000s)	Skid Number at 64 km/h: Hot Mix	Gravel Plant-Mix Seal	Expanded Clay Plant-Mix Seal	Slag Plant-Mix Seal
0	0	36	42	60	52
4	0.68	37	47	60	56
12	2.11	42	46	59	51
18	3.90	39	45	55	51
32	5.83	46	46	57	51
40	6.83	44	44	56	50
48	7.83	41	43	52	52

Note: 1 km/h = 0.62 mph.

Figure 4. Skid number versus accident rate.

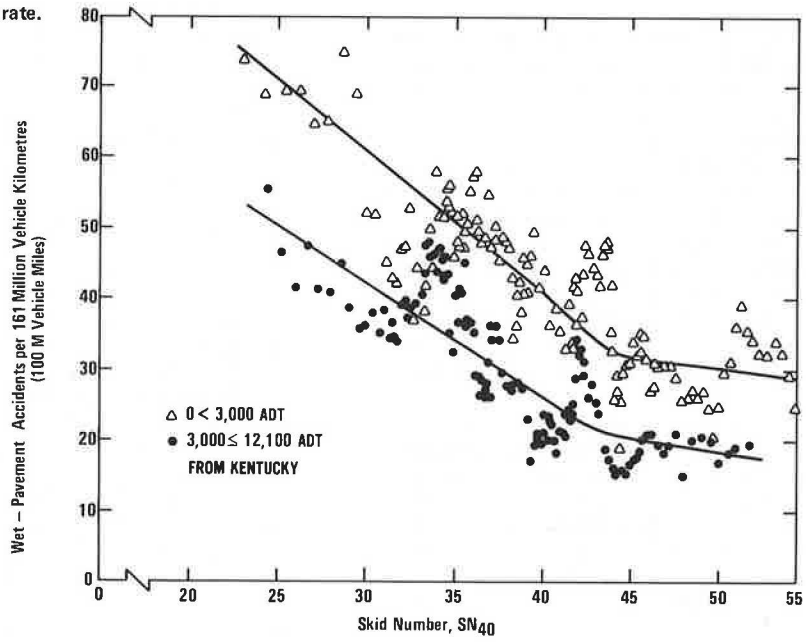

Figure 5. Effect of texture depth on sound pressure level.

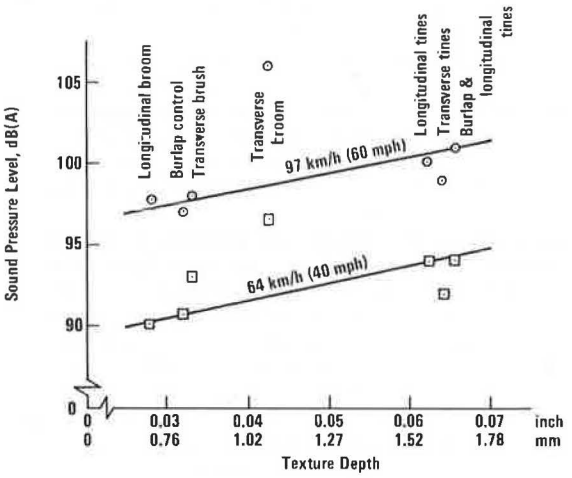

Figure 6. Skid resistance of various PCC pavement textures under traffic without studded tires.

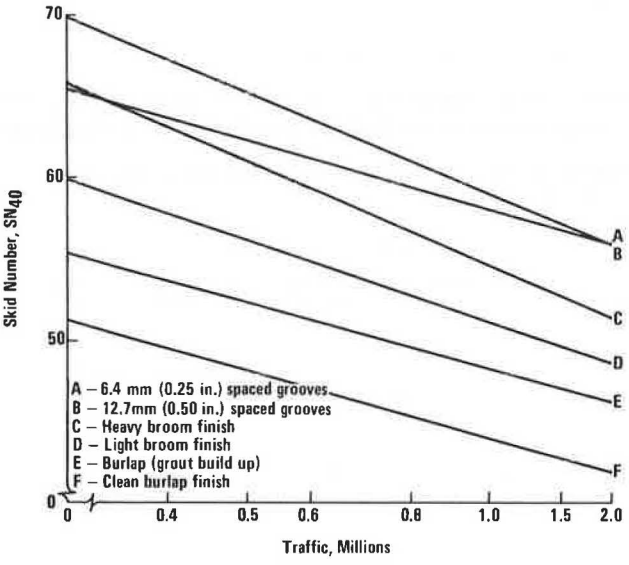

mental change. The rubber tires react with the detritus on the roadway to abrade homogeneous exposed rocks, degrade laminated stones or those with zones of weakness, and disintegrate the bonding medium, which in turn releases surface aggregates. The polishing of a pavement by traffic impairs the microtexture, and further wear reduces the texture depth of the surface (the macrotexture), decreases the void space of open-graded seal coats by degradation and compaction, and reduces the channels that permit the expulsion of surface water. Continued wear and the infiltration of dust, mineral particles, abraded rubber, oil drippings, and other foreign materials tend to clog the void spaces over a period of time and gradually reduce texture and skid resistance.

The release of sand-size mineral particles is not always a disadvantage. Dense-graded asphalt pavements have been designed to retain surface rugosity by attrition and thus continue to provide a skid-resistant surface. Eventually, it becomes necessary to rehabilitate the surface. When the pavement is wet, however, the open-graded asphalt friction course is usually superior to the dense-graded surface for higher vehicle speeds.

Studded tires and chains rapidly destroy the texture of both PCC and bituminous pavements. Heavy use of studded tires soon causes depressions or ruts in the wheel paths. Use of high-quality pavements with hard, durable surface aggregates retards the processes of wear, rutting, wheel-path compaction, and deterioration of skid resistance.

It is essential to use polish-resistant aggregates in pavement surfaces to provide enduring texture and skid resistance. Aggregates and pavement specimens can be evaluated before construction by means of polishing tests (ASTM D 3319, E 451, and E 510), petrographic analysis (ASTM C 294 and C 295), and chemical tests (ASTM D 3042) (20,21). The hardness of the mineral aggregates can be rated on the Mohs scale. Several types of circular test tracks have also been used for preevaluating the endurance characteristics of pavement surfaces. However, accelerated polishing tests do not account for weathering effects.

The Georgia Department of Transportation has used ASTM locked-wheel skid measurements to compare the wear of PCC pavement textures under traffic without studded tires (8). These results are shown in Figure 6, plotted as skid number versus traffic in millions (log scale) for a maximum of 2 million passes. It can be seen that grooves produced by steel comb or tine finishes gave the highest skid resistance and that the rate of wear for the surface with grooves spaced 12.7 mm (0.5 in) apart is less than that of all other finishes except the burlap finish with grout buildup (which has much lower skid resistance).

The rate of wear may decrease as the number of traffic passes increases. But even if wear for the tined finish with 12.7-mm (0.05-in) groove spacing continues at the same rate, it will remain above SN_{40} = 50 after 6.7 million passes.

FORMATION, RESTORATION, AND MEASUREMENT OF TEXTURE

Development of Texture on PCC Pavements

During the past few years, it has been recognized that the texturing methods for PCC pavements have been inadequate for allowing proper drainage relief, mitigating hydroplaning, exciting sufficient rubber hysteresis, and providing sufficient skid resistance for high-speed traffic. As a result, finishing techniques are being modified, and new methods are being introduced (22). Limited success has resulted from experiments conducted with finishing tools such as nylon brooms; flexible, fine wire brushes; wire drags; and modified burlap drags.

Greater success is being achieved by steel combing or grooving plastic concrete. Experiments have also been conducted with a fluted magnesium float (6). The steel comb or the vibrating groover has been incorporated in texturing and curing machines as a part of the paving train. This is desirable for mass producing textures with uniform high quality.

The deeper textures produced by the steel comb or the vibrating groover provide larger channels for water expulsion and drainage. This improves skid resistance, prevents hydroplaning, decreases splash and spray, and reduces wet-pavement highway accidents. These finishing techniques (8,17) permit coarse aggregates to remain near the surface of the pavement or between the grooves and minimally disturb the surface mortar, resulting in stronger, more durable textures. An additional benefit is that these grooves are placed in the

plastic concrete at the time of construction at a cost that is only a fraction of that for grooving hardened pavements. Grooving of hardened pavements, which is discussed below, can be very advantageous when surfaces have become slick as a result of wear by traffic or when they have an inadequate texture. It may be desirable to finish pavements with a burlap drag before grooving to produce a gritty texture between the grooves.

Recent research recommends a minimum macrotexture of 1.3 mm (0.05 in) for coarse-textured surfaces on high-speed highways (23). The texture can be measured by the sand patch or the silicone putty method.

Grooving Hardened Pavements

Grooving of hardened pavements to reduce wet-pavement accidents in locations that have high accident rates has increased rapidly in recent years. A before-and-after study on 55 lane-km (34 lane-miles) of grooved pavements in California has shown a 20 percent decrease in total accidents and a 70 percent reduction in wet-pavement accidents even with a 17 percent increase in traffic (24).

Transverse grooves furnish shorter escape routes for surface water, reduce splash and spray, and allow better wet-pavement braking distances than do longitudinal grooves. Presumably, longitudinal grooves increase the directional control and stability of vehicles because they improve lateral friction characteristics.

Because of the high cost of grooving hardened pavements, there is a tendency to minimize the grooving dimensions and increase the pitch or spacing. It is better to develop adequate pavement texture during construction and resurfacing—and thereby decrease the need for diamond sawing—than to groove hardened pavement. Grooving, however, is an effective means of reconditioning roadway surfaces that are smooth or worn from traffic.

Restoring or Retexturing Pavement Surfaces

Some common methods for restoring pavement surfaces are applying a seal coat, resurfacing, or placing a thin asphalt overlay (14,25). PCC pavements may be resurfaced with a PCC overlay (26) if the contractor is meticulous about resurfacing procedures. In any case, for the best results, the pavement should be structurally sound, patched, or repaired before resurfacing.

Pavements are often resurfaced to correct road roughness or to increase skid resistance. Adequate texture should be developed during resurfacing to obtain the best drainage relief and friction characteristics. Harsh, angular, properly graded aggregates are essential for these surface layers.

Measurement of Pavement Texture

Rose, Hutchinson, and Gallaway (9) summarize 26 methods for evaluating or measuring pavement texture. Of these, stereophotographic interpretation and the sand patch, silicone putty, and static drainage (outflow meter) methods or modifications of these procedures are most commonly used. Most of the measurements involve stationary procedures, but there is also a need to evaluate pavement texture from a vehicle moving at traffic speeds.

Pavement textures are complex, and many of the procedures measure only a single attribute such as depth, hydraulic radius, or drainage characteristics. This is why the correlation of skid resistance with texture measurements, which is commonly done today, is often imperfect.

RECOMMENDED TEXTURING METHODS

PCC pavement should be textured with a steel comb incorporated as a part of the paving train. The steel tines should be spaced 13 to 20 mm (0.5 to 0.8 in) apart center to center, and for high-speed roadways the average depth of the striations should be 5 mm (0.2 in). When pavements become worn or slick, they should be retextured by grooving with a diamond saw or resurfaced with an overlay that has a deep texture. The open-graded asphalt friction course—constructed from quality aggregates in accordance with procedures given by Smith, Rice, and Spelman—is recommended as a surface for new or hardened pavements.

CONCLUSIONS

Open-graded or coarse-textured roadway surfaces are advisable for high-speed, wet-weather traffic. They provide drainage relief at the tire-pavement interface, reduce the steepness of the speed gradient, decrease the likelihood of hydroplaning, minimize splash and spray, reduce the glare from wet pavements, and improve high-speed skid resistance. The skid number increases as the texture depth increases, and the wet-pavement accident rate diminishes as the skid number increases (the lowest rate occurring for values of 44 and greater).

Texture wear and tire-pavement noise usually become greater as the depth of the texture increases, but these factors depend on jaggedness, the contour of the surface, and the method used in finishing the pavements. The open-graded asphalt friction course is an exception. It is less noisy than many other surfaces. Adequate texture can be obtained by plastic grooving fresh concrete with a vibrating float or a steel comb. The surface is more durable when the grooves are spaced 13 mm (0.5 in) or more apart center to center. When it is well-designed and properly constructed, the open-graded asphalt friction course produces an excellent surface. Texture can be provided on hardened pavements by grooving or resurfacing. Polish-resistant aggregates must be used in resurfacing if durable textures are to be obtained. Harsh, angular aggregates give good results.

Pavement texture can be characterized by stereophotographic interpretation. Texture depths of 1.3 mm (0.05 in) or greater, measured by the sand patch method, are advocated for high-speed roads; however, measurements of this nature do not fully evaluate the characteristics of the texture. Textural requirements should probably be varied with the geometrics of the highway and with traffic demands. Deeper texture is needed in geographic locations where rainfall intensities are greater and vehicle speeds are faster.

ACKNOWLEDGMENT

This paper is a staff report condensation of research conducted for the Federal Highway Administration. The contents reflect my views, and I am responsible for the facts and the accuracy of the data presented. The contents do not necessarily reflect the official views or policies of the Federal Highway Administration. This paper does not constitute a standard, specification, or regulation.

REFERENCES

1. G. G. Balmer. The Significance of Pavement Texture. Federal Highway Administration, Rept. FHWA-RD-12, Feb. 1975, pp. 1-39; NTIS, Springfield, VA, PB 243 108/AS.
2. H. W. Kummer and W. E. Meyer. Tentative Skid-Resistance Requirements for Main Rural Highways. NCHRP, Rept. 37, 1967, pp. 1-80.
3. W. Hofferberth. Improved Grip of Tyres on Wet Roads. International Colloquium on the Interrelation of Skidding Resistance and Traffic Safety on Wet Roads, Verlag von Wilhelm Ernst und Sohn, Berlin, 1970, pp. 449-460.
4. W. E. Meyer, R. R. Hegmon, and T. D. Gillespie. Locked-Wheel Skid Tester Correlation and Calibration Techniques. NCHRP, Rept. 151, 1974, pp. 1-100.
5. R. A. Moyer. Skidding Characteristics of Road Surfaces. Proc., HRB, Vol. 13, 1934, pp. 123-168.
6. W. P. Chamberlin and D. C. Amsler. Pilot Field Study of Concrete Pavement Texturing Methods. HRB, Highway Research Record 389, 1972, pp. 5-17.
7. J. L. Davis, W. B. Ledbetter, and A. H. Meyer. First Progress Report on Concrete Experimental Test Sections in Brazos County, Texas. Texas Transportation Institute, College Station, Research Rept. 141-2, Aug. 1973, pp. 1-63; NTIS, Springfield, VA, PB 231 000/AS.
8. J. B. Thornton. Determination of Desirable Finish for Concrete Pavement. Georgia Department of Transportation, Forest Park, Final Rept., 1974, pp. 1-97; NTIS, Springfield, VA, PB 238 327/AS.
9. J. G. Rose, J. W. Hutchinson, and B. M. Gallaway. Summary and Analysis of the Attributes of Methods of Surface Texture Measurement. American Society for Testing and Materials, STP 530, 1973, pp. 60-77.
10. J. E. Martinez, J. M. Lewis, and A. J. Stocker. A Study of Variables Associated With Wheel Spin-Down and Hydroplaning. HRB, Highway Research Record 396, 1972, pp. 33-44.
11. A. J. Stocker, J. T. Dotson, and D. L. Ivey. Automobile Tire Hydroplaning—A Study of Wheel Spin-Down and Other Variables. Texas Transportation Institute, College Station, Research Rept. 147-3F, Aug. 1974, pp. 1-101; NTIS, Springfield, VA, PB 239 782/AS.
12. J. A. Mills III. A Skid Resistance Study in Four Western States. HRB, Special Rept. 101, 1969, pp. 3-17.
13. V. Adam and S. C. Shah. Evaluation of Open-Graded Plant-Mix Seal Surfaces for Correction of Slippery Pavements. TRB, Transportation Research Record 523, 1974, pp. 88-96.
14. R. W. Smith, J. M. Rice, and S. R. Spelman. Design of Open-Graded Asphalt Friction Courses. Federal Highway Administration, Rept. FHWA-RD-74-2, Jan. 1974; NTIS, Springfield, VA, PB 227 479/AS.
15. W. J. Galloway, W. E. Clark, and Jean S. Kerrich. Highway Noise Measurement, Simulation, and Mixed Reactions. NCHRP, Rept. 78, 1969, pp. 1-78.
16. R. K. Hillquist and P. C. Carpenter. A Basic Study of Automobile Tire Noise. Sound and Vibration, Feb. 1974, pp. 26-28.
17. J. Weaver. Deep Grooving of Concrete Roads. Cement and Concrete Association, London, Oct. 1972, and Second European Symposium on Concrete Roads, Bern, Switzerland, June 1973.
18. R. Bond, G. Lees, and A. R. Williams. An Approach Towards the Understanding and Design of the Pavement's Textural Characteristics Required for Optimum Performance of the Tyre. In The Physics of Tire Traction, Theory and Experiment (D. F. Hays and A. L. Browne, eds.), Plenum Press, New York, 1974, pp. 339-360.
19. G. Maycock. Experiments on Tyre Tread Patterns. British Road Research Laboratory, Crowthorne, England, RRL Rept. LR 122, 1967, pp. 1-11.
20. W. A. Goodwin. Pre-Evaluation of Pavement Materials for Skid Resistance—A Review of U.S. Techniques. HRB, Special Rept. 101, 1969, pp. 69-79.
21. W. G. Mullen, W. H. M. Dahir, and N. F. El Madani. Laboratory Evaluation of Aggregates, Aggregate Blends, and Bituminous Mixes for Polish Resistance. TRB, Transportation Research Record 523, 1974, pp. 56-64.
22. G. K. Ray and L. T. Norling. More Macrotexture in Concrete Pavement for Greater, Longer-Lasting Skid Resistance. Portland Cement Association, Skokie, IL, Paper TA034.01P, 1974, pp. 1-19.
23. B. M. Gallaway and others. Tentative Pavement and Geometric Design Criteria for Minimizing Hydroplaning. Federal Highway Administration, Rept. FHWA-RD-75-11, Feb. 1975, pp. 1-191; NTIS, Springfield, VA, PB 255 748/AS.
24. J. I. Karr. Evaluation of Minor Improvements—Grooved Pavements. Traffic Department, California Division of Highways, Sacramento, Pt. 8, Dec. 1972, pp. 1-72.
25. J. I. Karr. Thin Hot-Mix Wearing Courses (An Advisory). Asphalt Institute, College Park, MD, MISC-68-3, March 1968, pp. 1-20.
26. E. J. Felt. Resurfacing and Patching Concrete Pavements With Bonded Concrete. Proc., HRB, Vol. 35, 1956, pp. 444-469.

Publication of this paper sponsored by Committee on Surface Properties-Vehicle Interaction.

Prediction of Skid Resistance as a Function of Speed From Pavement Texture Measurements

M. C. Leu and J. J. Henry, Pennsylvania State University

A model that can be used to describe the variation of skid resistance with vehicle speed is presented. The model contains two constants: One is a measure of low-speed skid resistance, and the other accounts for the decrease in skid resistance as vehicle speed increases. It is demonstrated that the constants can be predicted from measurements of pavement microtexture and macrotexture. A significant feature of the model is that it clearly separates the effects of the two texture types. It can also be used to determine skid resistance-speed characteristics from a single speed measurement and a macrotexture measurement.

It is current practice in the United States to evaluate the skid resistance of highways by taking annual measurements of the locked-wheel skid number of the primary road system (1). These measurements are usually performed at one speed only—typically 64 km/h (40 mph)—but sometimes at the "prevailing traffic speed." Such measurements only partially characterize pavement safety in that they do not indicate the degree to which skid resistance changes with speed. The measurement of the relation between skid resistance and speed requires testing at two speeds or more, which would require three times the effort of conducting an annual survey.

The skid resistance of a pavement is determined by its surface texture. Kummer and Meyer (2) have reported the combined effects of microtexture and macrotexture. Microtexture, the fine-scale surface texture of the pavement aggregate, determines skid resistance at low vehicle speeds. Macrotexture, on the scale of the gradation of the aggregate, influences wet-pavement skid resistance by determining the rate at which water can escape from the tire footprint and therefore the rate at which skid resistance decreases as speed increases. Thus, it should be possible to predict the skid resistance-speed curve from suitable parameters for macrotexture and microtexture. An alternative method for determining the relation between skid resistance and speed for a pavement would be to perform a measurement at any convenient vehicle speed and combine the result with a macrotexture measurement to predict skid resistance at other speeds.

The objective of this research was to develop a model for characterizing the skid resistance-speed behavior of pavements and to relate this model to measures of pavement texture. Considerations are limited to measurements of skid resistance made according to the E 279-77 test method of the American Society for Testing and Materials (ASTM) (1). The effects of commercial tires, water-film thickness, and other test conditions are not considered here. Seasonal effects and variations in skid resistance caused by rain are also excluded from consideration because all data were obtained at the same time.

MODEL FOR THE RELATION BETWEEN SKID NUMBER AND SPEED

Three forms of the relation between skid number (SN) and speed (V) are considered; eventually, one is selected on the basis of how well it fits the experimental data and relates to the texture parameters.

A second-order relation is most frequently used to fit SN data (3):

$$SN = a_0 + a_1 V + a_2 V^2 \quad (1)$$

In this model, a_0 represents low-speed skid resistance and would therefore be expected to be related to some measure of microtexture. The skid number-speed gradient (SNG) for this model is

$$SNG \equiv -[d(SN)/dV] = -(a_1 + 2a_2 V) \quad (2)$$

and the percentage SNG (PSNG) is

$$PSNG \equiv (SNG/SN) \times 100 = [-(a_1 + 2a_2 V)100/a_0 + a_1 V + a_2 V^2] \quad (3)$$

The results of other investigations (4,5) have shown that PSNG is a function of macrotexture alone. The model in Equation 1 contradicts this observation because Equation 3 contains a parameter (a_0) that must be highly dependent on microtexture. Another deficiency of this model is that it often results in curve shapes that are concave downward (negative second derivative) or curves that indicate an increase of SN with speed at high vehicle speeds.

Majcherczyk (6) has plotted skid number versus speed data on log-log paper and obtained a linear fit, implying the following model:

$$SN = b_0 V^{b_1} \quad (4)$$

The gradient and percentage gradient for the model are as follows:

$$SNG = -b_0 b_1 V_1 \exp(b_1 - 1) \quad (5)$$

$$PSNG = (-b_1/V)100 \quad (6)$$

Majcherczyk found a correlation between b_1 and macrotexture that is consistent with earlier findings that PSNG at a given speed is a function of macrotexture alone. The deficiency of this model lies in its low-speed skid number behavior. The curve is so steep at low speeds that it predicts consistently high skid numbers at low speeds. The b_0 parameter, therefore, cannot be correlated with microtexture.

The model that was developed in the course of this research is

$$SN = c_0 \exp(c_1 V) \quad (7)$$

where c_0 is the zero speed intercept and the gradient and the percentage gradient are

$$SNG = -c_0 c_1 \exp(c_1 V) \quad (8)$$

and

$$PSNG = -100\, c_1 \quad (9)$$

As in Equation 1, low-speed skid resistance is indicated by the zero speed intercept of the curve fitting the data. It would therefore be anticipated that c_0 would be strongly correlated with parameters of microtexture. The c_1 parameter is proportional to the PSNG and should therefore be related to macrotexture parameters. It is interesting to note that the PSNG for this model is a constant that is independent of speed. In fact, the model in Equation 7 was suggested as a result of the observation that the PSNG of actual data did not vary significantly with speed. The model can be derived from the following definition of PSNG:

$$PSNG \equiv (-100/SN)\,[d(SN)/dV] \quad (10)$$

which can be rearranged to obtain

$$[d(SN)/SN] = (-PSNG/100)\,dV \quad (11)$$

Integrating from zero to any speed and assuming the PSNG is independent of speed,

$$\ln (SN_V/SN_{V=0}) = -(PSNG/100)V \quad (12)$$

which yields the Pennsylvania State University (PSU) model for skid resistance-speed behavior:

$$SN = SN_0 \exp[-(PSNG/100)V] \quad (13)$$

where

SN_0 = zero speed intercept (related to microtexture) and
PSNG = percentage skid number-speed gradient (related to macrotexture).

A significant advantage of this model is that it separates the effects of macrotexture and microtexture.

Figure 1 shows the results of a least squares fit of the three models to three sets of skid resistance-speed data. Although the three models fit the data equally well, only the PSU model (Equation 13) consistently provides the expected shape and low-speed behavior. Further evidence of the superior ability of this model to fit skid resistance-speed data may be found in the treatment of data for six pavements where the vehicle speed ranged from 16 to 80 km/h (10 to 50 mph) (7).

The speed gradient from Equation 13 is

$$SNG = SN_0\,(PSNG/100)\exp[-(PSNG/100)V] \quad (14)$$

If it is assumed that SN_0 is a function of microtexture and PSNG is a function of macrotexture, then SNG is a function of both macrotexture and microtexture. For two surfaces with the same macrotexture, the one with a better microtexture will have a steeper gradient.

Findings in earlier research appear to be consistent with the PSU model. Sabey (8) and Gallaway and Rose (9) both found a higher correlation between macrotexture and PSNG than between macrotexture and SNG. Schulze (10), using model surfaces, concluded that surfaces with high microtexture produce high skid numbers at low speeds and a steeper SNG than do surfaces with low microtexture. Mahone (11), in research on actual pavements, found that surfaces that originally had a steep gradient would have an intermediate gradient after polishing (wearing away of the microtexture).

DATA BASE

The skid resistance data used in this study were obtained by the West Virginia Department of Highways on

Figure 1. Test of three models for relation between skid number and vehicle speed.

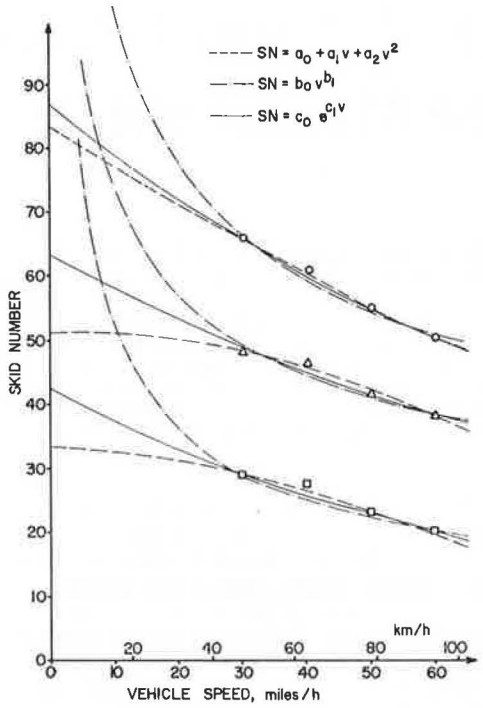

20 test sections in West Virginia in July 1976. The tests were conducted in accordance with ASTM E 274-77 at speeds of 48, 64, 80, and 96 km/h (30, 40, 50, and 60 mph). Twelve tests were made at each speed, and the average values were used in the study. A least squares fit of the data to the PSU model (4) was performed to provide values of SN_0 and PSNG for each pavement.

At the time the skid resistance measurements were made, two core samples were taken from each section and sand-patch measurements (8) were performed by personnel of the West Virginia Department of Highways. During the same week, PSU personnel recorded macrotexture and microtexture profiles. PSU personnel subsequently analyzed the profile data to obtain root mean square values for the heights of the macrotexture and microtexture profiles ($RMSH_{MA}$ and $RMSH_{MI}$ respectively) (7) and obtained British portable numbers from the core samples.

PAVEMENT MACROTEXTURE AND PSNG

To test the hypothesis that macrotexture parameters can be used to predict PSNG, two parameters were considered: root mean square height ($RMSH_{MA}$) from profile analysis and sand-patch mean texture depth (MD). A high degree of correlation was found between these two parameters (Figure 2). Therefore, either of the two can be selected with similar results.

Figure 3 shows the correlation of PSNG with MD. The relation

$$PSNG = 4.1(MD)^{-0.47} \quad (15)$$

is seen to fit the data well. Similar results were obtained when $RMSH_{MA}$ and other profile-derived parameters were used (7).

Although the sand-patch method is relatively simple, it has two disadvantages as a method for measuring macrotexture: (a) It is somewhat lacking in precision, and (b) it requires closing the pavement to traffic. Noncontacting methods that can be used at traffic speeds are under development (5) and should be considered as substitutes for sand-patch or profiling techniques.

PAVEMENT MICROTEXTURE AND SN_0

Two microtexture parameters, root mean square height ($RMSH_{MI}$) from profiles and British portable number (BPN) from core samples, are available to test the hypothesis that SN_0 can be predicted from microtexture data. The values of $RMSH_{MI}$ depend on the definition of the size range of microtexture. Values for $RMSH_{MI}$ were computed as a function of the largest wavelength considered. The cutoff wavelengths ranged from 0.05 to 2.54 mm (0.002 to 0.10 in). A correlation between the resulting values of $RMSH_{MI}$ and SN_0 was then attempted for each cutoff wavelength. The highest correlations, with correlation coefficients of 0.69 and 0.87 for two data sets, were obtained for the cutoff wavelength of 0.5 mm (0.02 in) (7). Microtexture is therefore defined here as consisting of asperities whose width is less than 0.5 mm.

The correlation between the $RMSH_{MI}$ of asperities less than 0.5 mm (0.02 in) wide and the BPN from the core samples is shown in Figure 4. The fact that only two core samples were obtained at each test section could account for some of the scatter.

In Figure 5, SN_0 is plotted versus BPN for 20 test sites. A least squares regression analysis yields the following:

$$SN_0 = -31 + 1.38\ BPN \quad (16)$$

with a correlation coefficient of 0.75. Other data obtained at six sites in Pennsylvania, for which BPN measurements were taken at five rather than two locations at each site, are given by Leu (7). For these data, the regression equation was

$$SN_0 = -35 + 1.32\ BPN \quad (17)$$

with a correlation coefficient of 0.95.

PREDICTION OF SNs FROM TEXTURE PARAMETERS

By combining Equations 13, 15, and 16, a relation can be obtained for SN, MD, BPN, and V:

$$SN = (-31 + 1.38\ BPN) \exp[-0.041\ V(MD)^{-0.47}] \quad (18)$$

Values of SN_{40} and SN_{60}, calculated from the texture data by using Equation 18, are compared with the mea-

Figure 2. Mean texture depth versus root mean square macrotexture height.

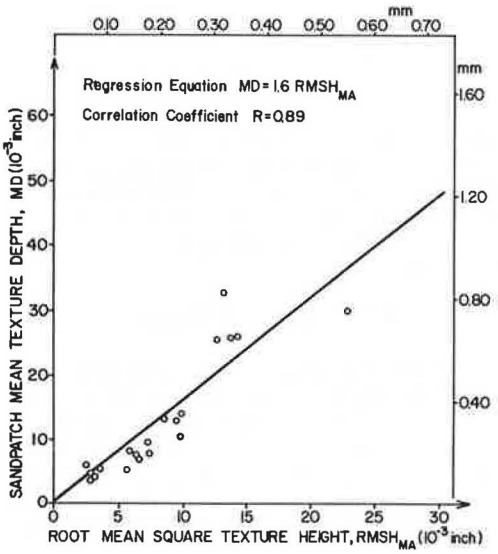

Figure 3. Percentage skid number-speed gradient versus mean texture depth.

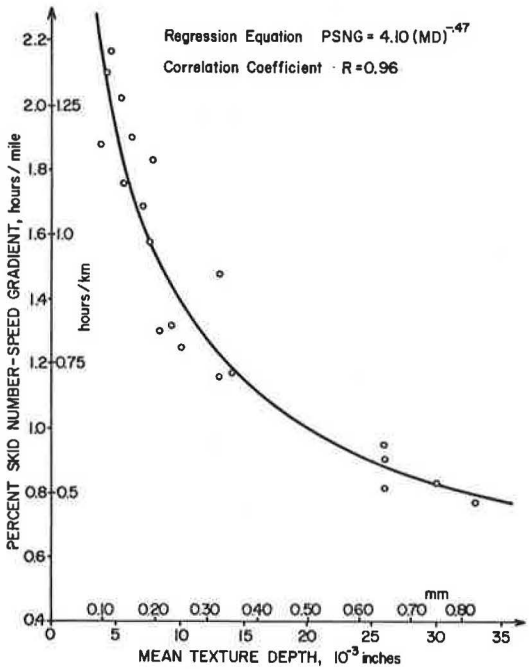

Figure 4. British portable number versus root mean square microtexture height.

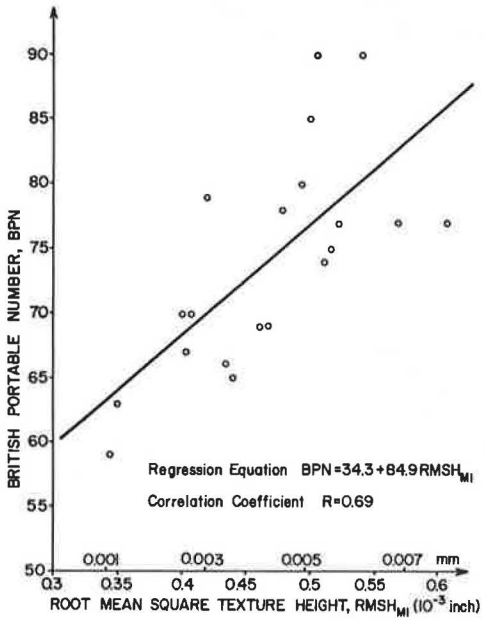

Figure 5. Zero speed intercept skid number versus British portable number.

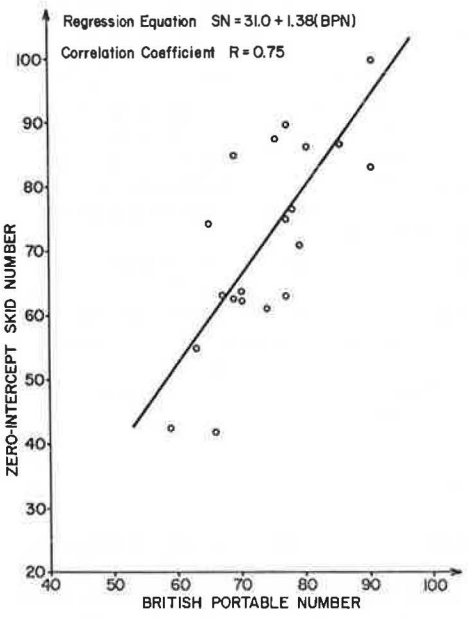

sured skid numbers shown in Figure 6. Although the method provides good prediction of skid resistance, better results could be expected if more extensive BPN data were available.

The combination of an SN measurement and a macrotexture measurement can also be used to predict SNs at other speeds. For example, SN_{40} [64 km/h (40 mph)] and MD could be used by combining Equations 13 and 15 to yield

$$SN = SN_{40} \exp[-0.041(V - 40)(MD)^{-0.47}] \quad (19)$$

Figure 7 shows excellent agreement between measured SN_{60} [96 km/h (60 mph)] and the predictions from Equation 19. Noncontacting methods for measuring macrotexture at traffic speeds would provide a more convenient technique for use in an equation of the form of Equation 19; such methods are now being developed (5).

Figure 6. Measured skid number versus predicted skid number for British portable number and mean texture depth.

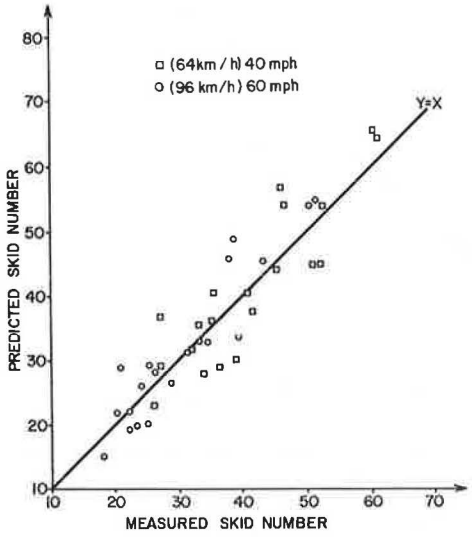

Figure 7. Skid number at 96 km/h (60 mph) as measured and predicted from skid number at 64 km/h (40 mph) and mean texture depth.

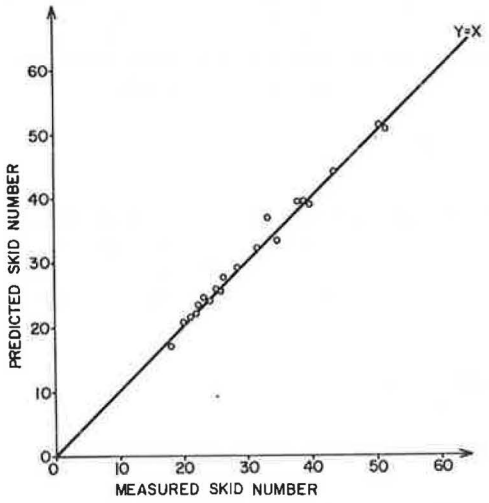

The relation between SN and V for various macrotextures and microtextures is shown graphically in Figure 8. In designing pavements for good skid resistance at low speeds, it is important to provide high BPN levels; for adequate skid resistance at high speeds, it is necessary to have high MD values.

CONCLUSIONS AND RECOMMENDATIONS

Skid resistance at any speed can be predicted from one microtexture and one macrotexture parameter by using the Pennsylvania State University model for skid resistance-speed behavior. An advantage of this model is that it clearly distinguishes the roles of macrotexture and microtexture. Another application of this model permits the prediction of skid resistance at any speed

Figure 8. Relation between skid number and vehicle speed for various conditions of pavement texture.

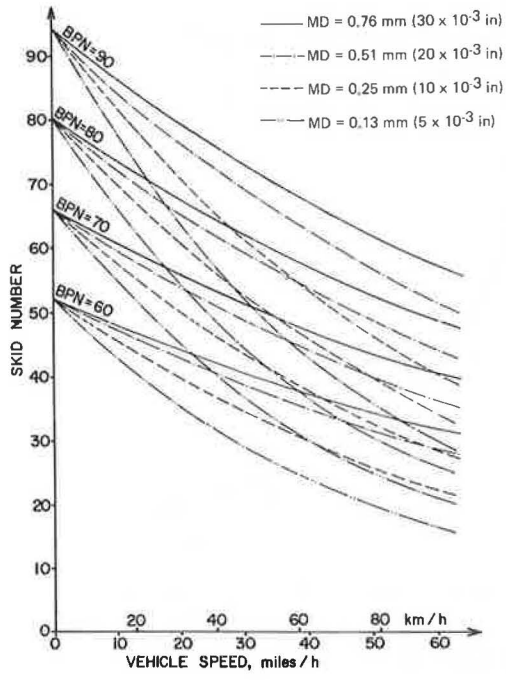

from a measured skid number at one speed and a macrotexture measurement.

Although British portable number and sand-patch texture depth are adequate measures of microtexture and macrotexture, they do require the interruption of traffic. It is unlikely that microtexture can be measured at high vehicle speeds. Progress is being made, however, in the development of noncontacting, high-speed methods for measuring macrotexture. The development of these methods should be encouraged so that a simultaneous macrotexture measurement and skid number measurement can be obtained that will make it possible to determine the skid resistance-speed characteristics of a pavement from a single test.

ACKNOWLEDGMENTS

This work was sponsored by the Federal Highway Administration (FHWA). We wish to express our gratitude to R. R. Hegmon of FHWA and E. Howerter of Ensco Corporation for their assistance in obtaining the experimental data used in this work. The suggestions and advice of W. E. Meyer contributed significantly to the research. The contents of this paper do not necessarily reflect the opinions of the sponsoring agency.

REFERENCES

1. Road, Paving, Bituminous Materials; Skid Resistance. Annual Book of ASTM Standards, Pt. 15, 1977.
2. H. W. Kummer and W. E. Meyer. Tentative Skid Resistance Requirements for Main Rural Highways. NCHRP, Rept. 37, 1967.
3. W. E. Meyer and others. Locked Wheel Pavement Skid Tester Correlation and Calibration Techniques. NCHRP, Rept. 151, 1974.
4. J. J. Henry and R. R. Hegmon. Pavement Texture Measurement and Evaluation. ASTM, Philadelphia, Special Technical Publ. 583, 1974.
5. R. E. Veres and others. Use of Tire Noise as a Measure of Pavement Macrotexture. ASTM, Philadelphia, Special Technical Publ. 583, 1974.
6. R. Majcherczyk. Influence de la Rugosité Géométrique d'un Revêtement sur l'Evacuation de l'Eau à l'Interface Pneu-Route et sur le Dérapage des Véhicules. Annales de l'Institut Technique du Batiment et des Travaux Publics, No. 318, 1974, pp. 37-68.
7. M. C. Leu. The Relationship Between Skidding Resistance and Pavement Texture. Pennsylvania State Univ., Automotive Research Program Rept. S78, 1977.
8. B. E. Sabey. Road Surface Texture and Change in Skidding Resistance With Speed. British Road Research Laboratory, RRL Rept. 20, 1966.
9. B. M. Gallaway and J. G. Rose. Macro-Texture Friction, Cross Slope and Wheel Track Depression Measurements on 41 Typical Texas Highway Pavements. Texas Transportation Institute, Texas A&M Univ., Research Rept. 138-2, 1970.
10. K. H. Schulze. Typen der Oberflächenfeingestalt und Ihre Wirkung auf den Reibungswiderstand bei Nässe. Internationales Colloquium Über Strassengriffigkeit und Verkehrssicherheit bei Nässe am 5. und 6.6., Berlin, Beitrag 15, 1968.
11. D. C. Mahone. Skid Number and Speed Gradients on Highway Surfaces. TRB, Transportation Research Record 602, 1976, pp. 69-71.

Discussion

William P. Chamberlin, New York State Department of Transportation

One of the mathematical models proposed by Leu and Henry allows prediction of a skid number at one vehicle speed from a combination of a skid number at another vehicle speed and a macrotexture measurement. Equation 19 is an expression of this model in which the constants were derived from tests on 20 bituminous pavements in West Virginia. For the West Virginia pavements, SN_{40} varied from 26 to 61 and mean sand-patch texture depth from 0.08 to 0.83 mm (0.003 to 0.032 in). It has recently been shown (12) that Equation 19 is also valid for 31 experimentally textured bituminous pavements in Texas (13) for which the range in SN_{40} is comparable to that in West Virginia but the range in texture depth is much greater [0.25 to 3.15 mm (0.01 to 0.12 in)]. The purpose of this discussion is to show that Equation 19 applies equally to a group of experimentally textured concrete pavements in New York State.

The New York data were collected at five different experimental sites, and each was textured by the same four methods—burlap drag, natural bristle paving broom, wire brush, and fluted float (14,15). Skid resistance at 64.5 and 88.5 km/h (40 and 55 mph) and sand-patch texture depths were measured immediately after construction and at various times over the next 4 years. SN_{40} in the New York data varied from 20 to 72 and sand-patch texture depth from 0.20 to 1.65 mm (0.008 to 0.064 in).

The New York data were first used to develop the relation between MD and PSNG (Figure 3). Fitting an exponential curve of the form of Equation 15 to these data resulted in the regression shown in Figure 9. Although the scatter of data points about this regression is greater than that found by Leu and Henry, the correlation coefficient (0.61) is significant at the 0.01 level and, more important, the constants in the regression equation are similar.

Because of this similarity, Equation 19 was used with the authors' constants (4.1 and 0.47) to estimate values of SN_{55} from measured values of SN_{40}. Comparison of the estimated and measured values of SN_{55} is shown in Figure 10 in which the 0.95 prediction limits for the regression and the line of equality are shown as broken lines. The regression itself is not plotted because of its close correspondence with the line of equality. The prediction limits correspond to a standard error of estimate of 2.6 skid numbers, a value only slightly larger than the measurement error associated with typical skid tests performed according to ASTM E 274 (16).

Thus, experience with bituminous pavements in Texas and concrete pavements in New York, which represent textures produced by a variety of methods, supports the authors' contention (based on experience in West Virginia) that skid resistance at one speed can be estimated with reasonable accuracy from a combination of skid resistance measured at another speed and a measurement of pavement macrotexture.

REFERENCES

12. Pavement Texture and Available Skid Resistance. Office of Research, Federal Highway Administration, Nov. 1977.
13. J. F. Nixon and others. Sprinkle Treatment for Skid Resistance Surfaces. Texas State Department of Highways and Public Transportation, Research

Figure 9. Percentage skid number-speed gradient versus mean texture depth for experimental concrete textures in New York.

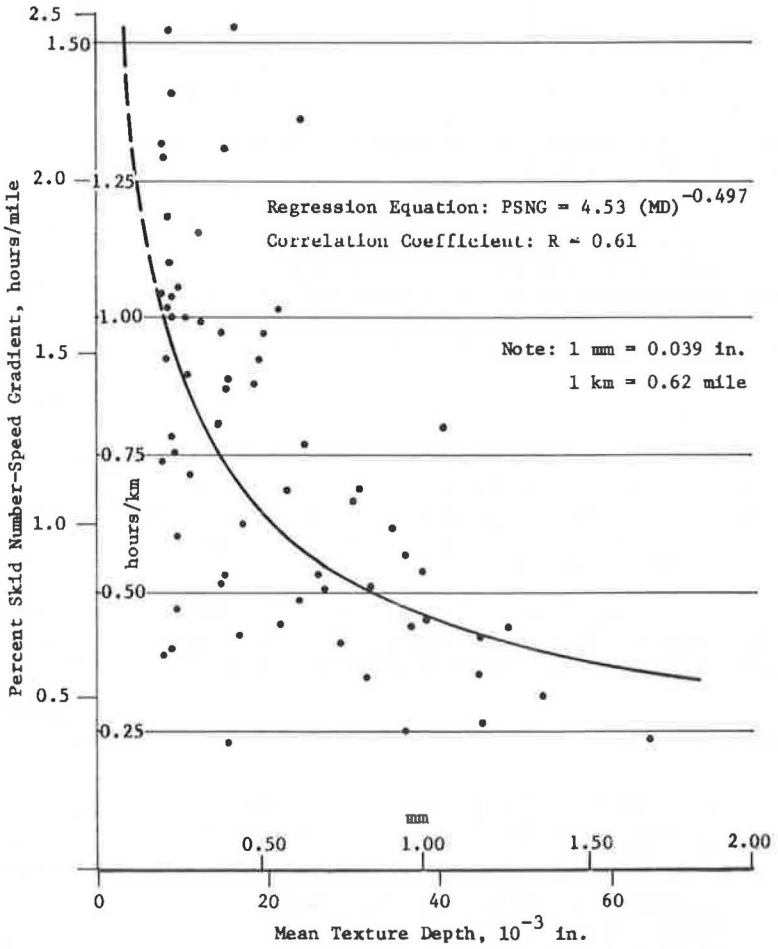

Figure 10. Prediction of SN_{55} by use of the Leu and Henry model.

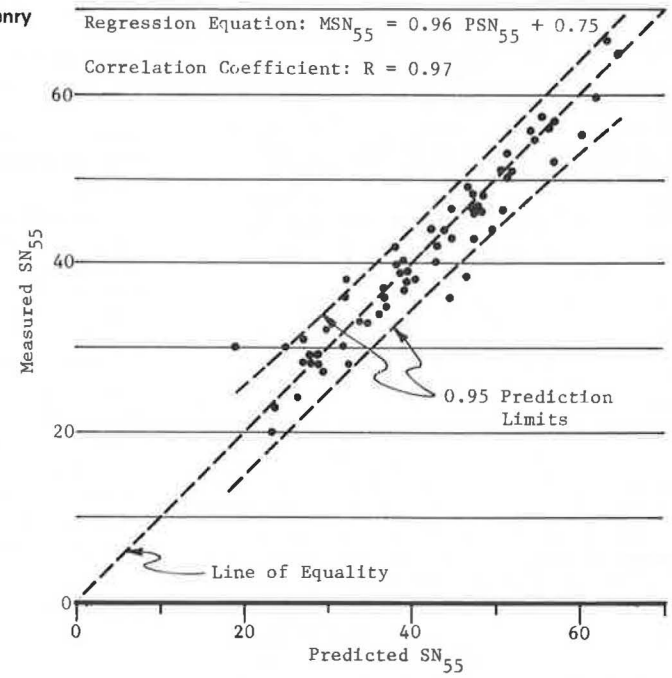

Rept. 510-IF, Vol. 1, Dec. 1976.
14. W. P. Chamberlin and D. E. Amsler. A Pilot Field Study of Concrete Pavement Texturing Methods. HRB, Highway Research Record 389, 1972, pp. 5-17.
15. W. P. Chamberlin. Concrete Pavement Texturing Methods—A Review of Experience in New York. Engineering R&D Bureau, New York State Department of Transportation, Feb. 1978.
16. R. R. Hegmon. Seasonal Variations in Pavement Skid Resistance—Are They Real? Public Roads, Vol. 42, No. 2, Sept. 1978.

Authors' Closure

We would like to express our appreciation to Chamberlin for making available additional data in support of one aspect of our research. Chamberlin's regression coefficients of 4.53 and 0.497 are in good agreement with ours of 4.10 and 0.47 respectively, considering the precision of the correlated data (SN_{40} and mean depth measured by the sand-patch method). Research that will consider 20 sites in Pennsylvania is planned for 1979, so we would welcome similar data from others.

Equation 19 eliminates the parameter SN_0 from our model (Equation 13). We have found that this parameter is affected by both microtexture and short-term variations in weather. Weather-related effects are eliminated by conducting all skid measurements in one weather area at the same time. However, it is probably not possible to compare data sets taken at different locations at different times without correcting for weather-related factors such as rainfall history. The differences between Equations 16 and 17 can be attributed in part to these effects, and larger differences might be expected. Research into seasonal and short-term variations is under way and, if it is successful, we may be able to account for microtexture and weather in a generalized model.

Publication of this paper sponsored by Committee on Surface Properties-Vehicle Interaction.

Determination of Skid Resistance-Speed Behavior and Side Force Coefficients of Pavements

V. R. Shah, Dorr-Oliver Company, Stamford, Connecticut
J. J. Henry, Pennsylvania State University

Pavement friction characteristics including skid resistance-speed dependence, side force coefficients, and brake slip numbers are seen to be derivable from data obtained in the transient slip test. The transient slip test is described, and it is noted that any friction tester with force-measuring transducers can be used for these measurements. The brake slip numbers are shown to be independent of the rate of wheel lockup, which leads to the observation that brake slip numbers obtained during a transient slip test are equivalent to locked-wheel skid numbers at the same sliding speed. Side force coefficients can be computed from transient slip data with the help of a model. The data and conclusions apply to the standard skid-test tire operating under fixed test conditions and normal load, water film thickness, and inflation pressure.

Highway safety in the United States is currently evaluated by using locked-wheel skid numbers (1). During the lifetime of a pavement wearing course, the skid number (SN) is measured at least once a year at a single vehicle speed—usually 65 km/h (40 mph)—although sometimes at the "prevailing traffic speed." Because vehicles are operated on highways at a variety of speeds and only rarely in the locked-wheel mode, the ranking of pavement safety by means of a locked-wheel test at a single speed can be questioned. Furthermore, vehicles require adequate lateral forces to maintain directional stability in cornering maneuvers. In a complete evaluation of pavement safety, it is necessary to measure the complete frictional characteristics of a pavement at various speeds, cornering angles, and wheel stop rates. It would clearly be impractical to do this for each pavement in the country on an annual basis.

Research was initiated at the Pennsylvania Transportation Institute (PTI), Pennsylvania State University, to determine the degree of interrelationship among slip, side force, and locked-wheel data (2,3). The objective of this research was to determine the most efficient means of evaluating the frictional capability of pavements. As a result of this research, a methodology was developed for processing data from a single measurement at one vehicle speed to obtain the speed dependence and side force frictional characteristics of a pavement.

EXPERIMENTAL PROCEDURE

The Penn State Mark III Road Friction Tester (4) was used in this study. The tester has a single wheel, a six-component force-torque measuring hub, and a hydraulic system that can steer the test wheel into angles of up to 12° in relation to the forward velocity of the towing vehicle. Two rotary variable differential transformers measure the angle of the test trailer and the angle of the free-trailing fifth wheel relative to the truck axis. In this way, the actual yaw angle of the test trailer—including the correction for any yaw it induces in the

direction of the towing vehicle—is determined. Both the test-wheel and fifth-wheel speeds are measured. All signals are recorded on an oscillograph recorder that has sufficient response so that friction force and velocities can be recorded as the test tire is being locked up. In addition, side force and yaw angle can be recorded as the trailer sweeps from free trailing to a 12° yaw angle at a rate of about 24°/s.

The pavements used in this study (six sites at the PTI Skid Test Facility) are described below:

Pavement	Type
3	Dense-graded asphalt concrete with thick application of Jennite and low-friction surface
4	Dense-graded asphalt concrete with a sand-epoxy overlay and fine-grained texture
5	Portland cement concrete lightly dragged in transverse direction with burlap drag
6	Dense-graded asphalt concrete (Pennsylvania Specification 1D2A)
8	Open-graded asphalt concrete with river bottom gravel aggregate (Pennsylvania Specification SR1A)
Tangent	Dense-graded asphalt concrete (same as site 6 but subjected to wear as part of PTI Pavement Durability Track)

Some supporting data were also obtained on public roads in the State College, Pennsylvania, area.

Three test tires were included in the study: the ASTM E 249 five-ribbed tire (5), the ASTM E 501 seven-ribbed tire (6), and the ASTM E 524 blank tire (7). Data are reported here only for the E 501 seven-ribbed tire, which is the current standard test tire. Data for the other tires are given elsewhere (3).

In all tests, the on-board watering system delivered a nominal 0.50-mm (0.02-in) water film thickness. Tire inflation pressure was 165 kPa (24 lbf/in^2) (measured cold), and the vertical load was 4670 N (1050 lb).

Locked-wheel skid numbers were obtained at 16, 24, 32, 48, 64, and 80.5 km/h (10, 15, 20, 30, 40, and 50 mph). Side force coefficients with a free rolling wheel were obtained at yaw angles up to 12°. Transient slip data were obtained at 48, 64, and 80.5 km/h. The test procedure for transient slip consists of operating the strip chart recorder fast enough so that the friction force can be read as a function of the rotational velocity of the test tire from the free rolling to the fully locked condition. In all other respects, this test is the same as a locked-wheel test. The lockup rates for the road friction tester are between 0.25 and 0.5 for the pavements tested.

Because all data reported here were collected during the first two weeks of August 1975, seasonal variations and their possible effects on the data are not considered.

TEST RESULTS

In the procedure used in this research, the locked-wheel skid number (SN) is the special case of the transient slip brake slip number (BSN) at 100 percent slip. The BSN is the ratio of friction force to normal load multiplied by 100 at a specified wheel slip. Percentage slip is defined as the deficiency in angular velocity caused by braking expressed as a percentage of free-rolling angular velocity. Any skid tester equipped with a force-measuring hub and sufficiently responsive instrumentation can be used to obtain data on transient slip.

The BSN is a function of the percentage slip and the test speed. In other investigations of the effect of lockup rate, it has been found that peak and slide coefficients are not significantly affected by lockup from 0.25 to 1 s (8). Some tests were performed by using a constant slip tester on loan from the Federal Aviation Agency (9). At the same time, data were obtained with the road friction tester on the transient slip mode. The constant slip test has an effective zero lockup rate compared with the rapid lockup rate of the transient slip test. Figure 1 shows the results of these tests. The slight difference in the results can be attributed to the calibration of the two testers. The effect of wheel lockup rate is therefore considered to be negligible.

A significant discovery resulted from plotting the BSN data versus sliding speed rather than percentage slip. Sliding speed can be determined by multiplying the percentage slip by the test speed and represents the velocity of the tire tread relative to the pavement. Locked-wheel data can also be plotted on these coordinates because SN is equivalent to BSN at 100 percent slip. Figures 2 through 7 show the plots for reduced

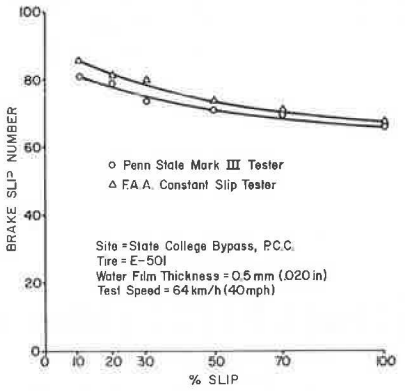

Figure 1. Brake slip number versus percentage slip for constant and variable speed testers.

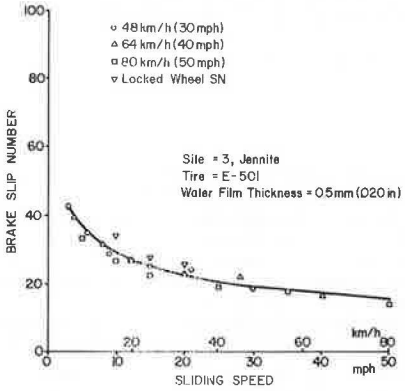

Figure 2. Reduced brake slip number versus sliding speed for site 3.

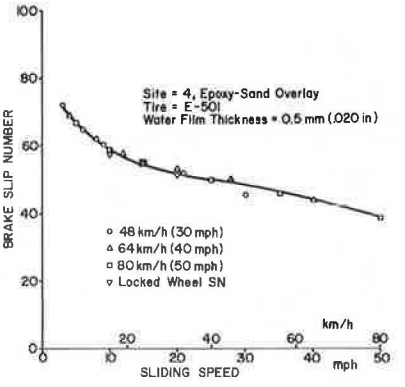

Figure 3. Reduced brake slip number versus sliding speed for site 4.

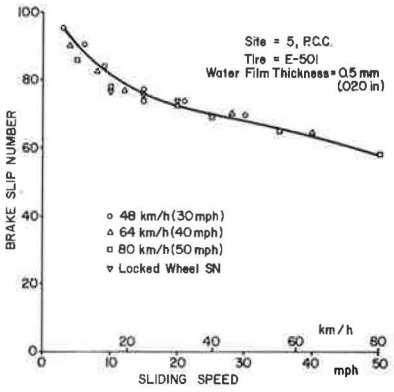

Figure 4. Reduced brake slip number versus sliding speed for site 5.

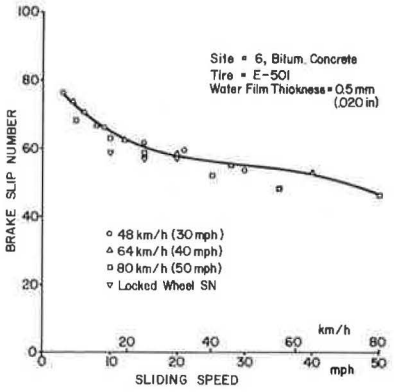

Figure 5. Reduced brake slip number versus sliding speed for site 6.

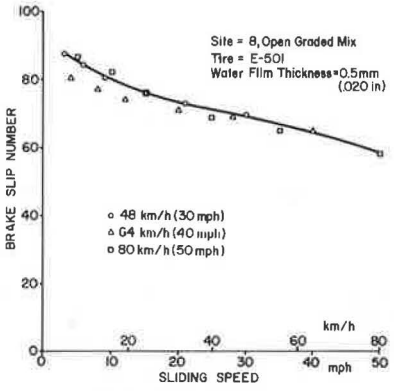

Figure 6. Reduced brake slip number versus sliding speed for site 8.

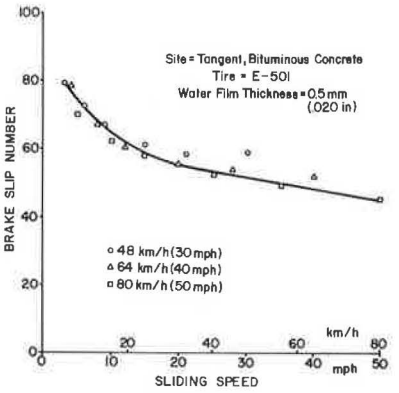

Figure 7. Reduced brake slip number versus sliding speed for site tangent.

brake slip number (BSN versus sliding speed) for the six test sites. Each datum point for the transient slip data represents the average of at least 15 measurements; the low-speed locked-wheel data are averages of five measurements.

A single curve drawn through the data in the plots of reduced brake slip number can be used to determine the speed-related friction performance of a pavement. For example, a locked-wheel test at 48 km/h (30 mph) will produce the same result for SN_{30} as a transient slip test result at 80.5 km/h (50 mph) with 60 percent slip. The curves for reduced brake slip number can be obtained from transient slip tests at a single test speed and used to determine the skid number-speed behavior up to that test speed.

Prediction of Side Force Coefficients From Transient Slip Data

A model designed to predict side forces generated by a cornering tire requires parameters that describe the behavior of the tire and the friction force in the tire-pavement contact area as a function of sliding speed. The friction forces depend on the combination of tire and pavement and can be measured by the transient slip method described above. The other parameters, those that describe the tire, depend on the tire only and are thus fixed when the tire is selected. It is possible then to predict side force coefficients (the ratio of the lateral force on a cornering tire to the normal load times 100) for a given tire given the reduced brake slip number plot for that tire-pavement combination.

The following assumptions were made for the model:

1. The tire behaves as an elastic beam representing the tread base, supported on an elastic foundation represented by the carcass, which permits simulation of vertical and longitudinal carcass motion.
2. A pressure distribution in the tire contact region is parabolic along the contact length and uniform across it.
3. The contact region is approximated by a rectangle.
4. The friction coefficient is isotropic.
5. The carcass has a bending stiffness EI.

In general, the tire motion during braking, traction, or cornering is a combination of slipping, sliding, and rolling. The tire-pavement contact surface can be divided into sliding and nonsliding regions, which are analyzed separately. The coordinate system defined here is similar to the one adopted by the Society of Automotive Engineers (10) except that the system discussed here takes into account finite deformation of a tire in the region of contact with the pavement. Figure 8 shows the coordinate system for a freely rolling, yawed tire. The analysis is an extension of analyses

Figure 8. Coordinate axes for tire model.

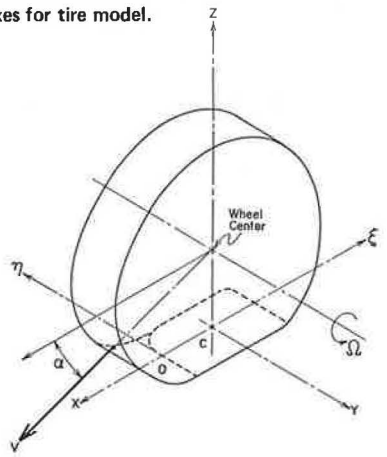

made by Fiala (11) and Sakai (12), which do not account for the dependence of friction on speed and are valid only for small yaw angles.

Nonsliding Region

Figure 9 shows the shear deformation of a single portion of the tire tread for a freely rolling, yawed tire. (Deformation and shear stress are averaged across the tire tread, and the resulting kinematic and force expressions depend on the ξ coordinate only.) In Figure 9, B is a point on the carcass whereas A is a corresponding point on the tread element that is in contact with the road surface. O represents the leading edge of the tire in contact with the road surface. The diagram of tire velocity shown in Figure 8 shows the wheel yawed at an angle α to the direction of motion. It can be seen in the figure that V_r represents the free-rolling velocity of the tire whereas V_y represents the lateral elastic slip or slide of the tire. In time t, the base point B of a tread element will move into the contact region a longitudinal distance ξ as determined by rolling velocity V_r.

Then,

$$\xi = -V_r \cdot t \tag{1}$$

where V_r is in the negative ξ direction. The velocity of the contacting tip A is V. During the same time interval t, A will be laterally displaced by a distance given by

$$\eta = -V_y \cdot t \tag{2}$$

t can be eliminated between Equations 1 and 2 to give

$$\eta = (V_y/V_r) \cdot \xi \tag{3}$$

The preceding analysis assumes that there is no sliding or slipping of the tire with respect to the road surface. In the region of adhesion, lateral deformation is produced by the static coefficient of friction with a limiting value μ°. The friction force required to produce this displacement depends on the lateral stiffness of the element (C_y in pounds force per cubic inch) (because the equations were formulated in U.S. customary units, no SI equivalents are given). The force per unit area is

$$F_\eta = C_y (\eta - \eta_b) \tag{4}$$

where η_b is the carcass deformation.

The maximum static friction force available from a particular tire-pavement combination depends on the limiting friction coefficient (μ°) and the vertical contact pressure distribution (P_z). Friction force varies linearly until the limiting condition is reached when

$$F_\eta/(\xi = \xi_a) = \mu^\circ P_z/(\xi = \xi_a) \tag{5}$$

where ξ_a is the limit of the adhesion region.

The curve of carcass deflection is given by Hartranft (4):

$$\eta_b = bS \cdot (\xi/L)[1 - (\xi/L)] \tag{6}$$

where b is the beam constant (0.015×10^{-3} in/lbf for the E 501 tire) determined experimentally according to the Hartranft procedure (4) and S is the side force. Assuming a parabolic pressure distribution in the contact region gives

$$P_z = (6N/wL^2) \cdot (\xi/L)[1 - (\xi/L)] \tag{7}$$

where

- N = static wheel load (1050 lbf for the tests reported here);
- w = tire contact patch width, the width of the tire minus the total width of the grooves (4.62 in for the E 501 tire); and
- L = tire contact patch length (6 in for the E 501 tire).

At the point of incipient slip,

$$\xi = \xi_a \tag{8}$$

Substituting for F_η and R_z in Equation 5 from Equations 4 and 7 gives

$$C_y (\eta - \eta_b) = (6\mu^\circ N/wL^2) \cdot (\xi_a/L)[1 - (\xi_a/L)] \tag{9}$$

But $\eta = \xi_a \tan \alpha$. Substituting for η and η_b and solving the expression for ξ_a give

$$\xi_a = [(6\mu^\circ N/wL^2 C_y) + (bS/L) - \tan \alpha] \cdot [(L/6\mu^\circ N/wL^2 C_y) + (bS/L)] \tag{10}$$

Sliding Region

Beyond the adhesion limit, the tread element begins to slide back to its original undeformed position and the sliding velocity changes from zero at the limiting adhesion point to its maximum at the exit of the contact region. The side force per unit area in this region is given by

$$F_\eta = \mu P_z \tag{11}$$

The total side force S is given by

$$S = S_{adhesion} + S_{sliding} \tag{12}$$

which can be obtained by integrating over the entire contact region. Thus,

$$S = \int_0^{\xi_a} w \cdot F_\eta \cdot d\xi + \int_{\xi_a}^{L} w \cdot \mu p_z \cdot d\xi \tag{13}$$

Substituting for F_η and P_z and simplifying give

$$S = ([\tfrac{1}{2} \cdot w \cdot C_y \cdot \xi_a^2 \cdot \tan \alpha] + \{\mu N[1 - 3(\xi_a/L)^2 \; 2(a/L)^3]\})/ \{1 + (b/L)\xi_a^2 [\tfrac{1}{2} - (\xi_a/3L)]\, w C_y\} \tag{14}$$

where the first term in the numerator represents the contribution by the adhesion region and the second the contribution by the sliding region. Thus, the expres-

Figure 9. Tire deformation in the contact patch.

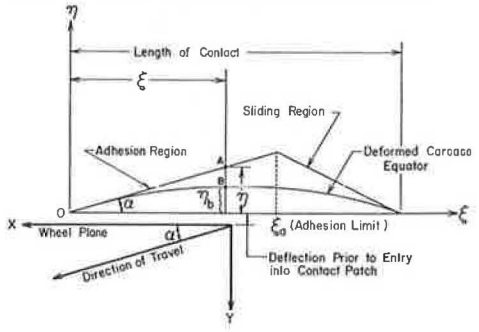

sion for S permits evaluation of S for any yaw angle α. μ is a function of sliding velocity and can be obtained from plots for BSN and sliding speed. In the present case, values are obtained from Figures 2 to 7 for the particular surfaces.

C_y can be obtained as follows: In the adhesion region, the side force is given by

$$S = S_{adhesion} = \tfrac{1}{2} \cdot w \cdot C_y \cdot \xi_a^2 \cdot \tan \alpha \quad (15)$$

For the limiting condition of α approaching zero, this expression becomes

$$S = \tfrac{1}{2} \cdot w \cdot C_y \cdot \xi_a^2 \cdot \alpha \quad (16)$$

and

$$(\partial S/\partial \alpha) = \tfrac{1}{2} \cdot w \cdot C_y \cdot \xi_a^2 \quad (17)$$

But ξ_a = L = contact length (in that no slip takes place in this condition), which gives

$$(\partial S/\partial \alpha) = \tfrac{1}{2} \cdot w \cdot C_y \cdot L^2 \quad (18)$$

$$C_y = 2(\partial S/\partial \alpha)/w \cdot L^2 \quad (19)$$

From the experimentally obtained plots of side force versus yaw angle, the value of $\partial S/\partial \alpha$ at α approaching zero was calculated. This gives C_y = 250 lbf/in^3 for the E 501 tire. The length of the contact region was determined by obtaining tire footprints under statically loaded conditions. The values of side force obtained from Equation 14 are compared with the experimentally obtained results for the six test sites in Figures 10 to 15.

Figure 10. Side force coefficient versus yaw angle for site 3.

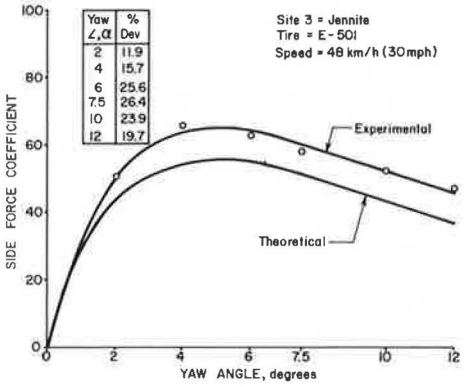

Figure 11. Side force coefficient versus yaw angle for site 4.

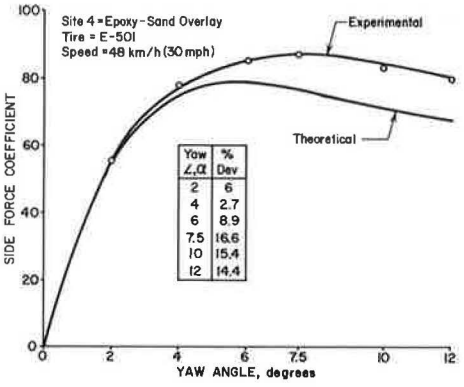

Figure 12. Side force coefficient versus yaw angle for site 5.

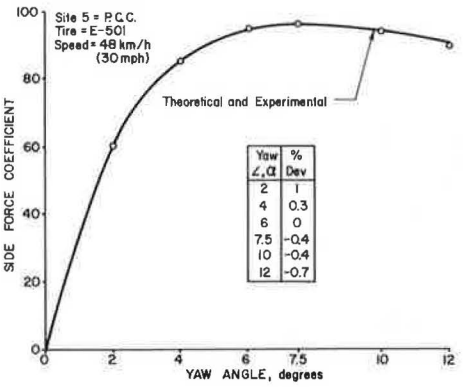

Figure 13. Side force coefficient versus yaw angle for site 6.

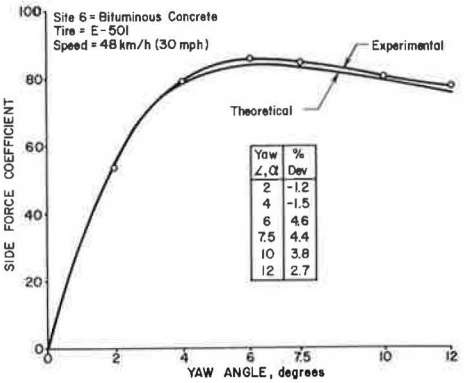

Figure 14. Side force coefficient versus yaw angle for site 8.

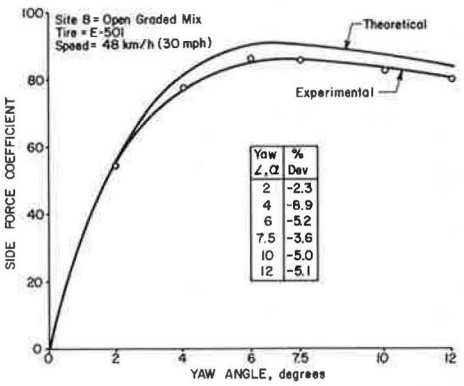

Figure 15. Side force coefficient versus yaw angle for site tangent.

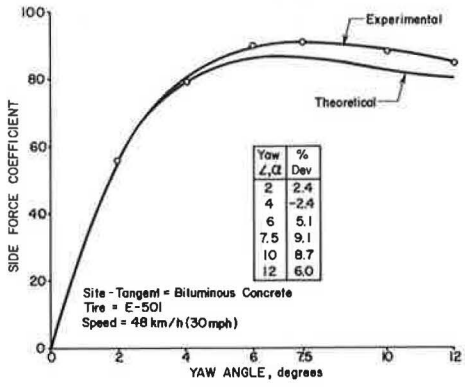

The results show a good agreement between experimental and theoretical results for sites 5, 6, 8, and tangent but poorer agreement for sites 3 and 4. The cause of this poor agreement lies in the assumption that the friction coefficient is isotropic. Although it is not possible to obtain SNs perpendicular to the direction of travel, the British Portable Tester (13) was used to determine British portable numbers (BPNs) in relation to direction of travel to determine whether the assumption of isotropic friction is valid. The results obtained are given in the table below, which shows that the assumption is least valid for sites 3 and 4:

	BPN		
Site	Parallel to Road	Perpendicular to Road	Deviation (%)
3	53.2	58.4	+9.8
4	65	70.3	+8.2
5	86	83	-3.5
6	81	81	0
8	82.1	81.7	-0.5

Thus, the calculated results for these sites would be expected to differ from experimental results and, because friction is greater in the lateral direction, the experimental results are greater than the predictions.

CONCLUSIONS

It has been shown that collecting data during the transient portion of a locked-wheel skid test as the test tire undergoes the transition from freely rolling to fully locked can provide useful information. During the transition, instantaneous friction force and corresponding sliding speed (relative velocity of the tread and the pavement) can be measured and are found to be independent of test speed and wheel lockup rate. Data on brake slip number and sliding speed characterize the relation between pavement friction and speed and can be used, with the help of a model, to determine side force coefficients.

Transient slip tests do not require unique equipment. Any locked-wheel skid tester provided with a force-measuring hub and instrumentation that has sufficient response to measure forces and angular velocities during the transition can be used.

ACKNOWLEDGMENTS

This research was sponsored by the Pennsylvania Department of Transportation and the Federal Highway Administration. We would like to express our gratitude to R. K. Shaffer and R. R. Hegmon of those agencies for their cooperation in project coordination and for their constructive criticism and guidance during the conduct of this work. Consultation with and the suggestions of W. E. Meyer of Pennsylvania State University provided a valuable contribution to the project. The contents and the conclusions of this presentation do not necessarily reflect the opinion of the sponsors.

REFERENCES

1. Standard Test Method for Skid Resistance of Paved Surfaces Using a Full-Scale Tire. Annual Book of ASTM Standards, Pt. 15, E 274-70, 1977.
2. J. J. Henry and W. E. Meyer. Relationship of Locked Wheel Friction to That of Other Test Modes. Bureau of Materials, Testing and Research, Pennsylvania Department of Transportation, 1975.
3. V. R. Shah and J. J. Henry. Relationship of Locked Wheel Friction to That of Other Test Modes. Bureau of Materials, Testing and Research, Pennsylvania Department of Transportation, Final Rept. 72-7, March 1977.
4. T. J. Hartranft. Theoretical and Experimental Correlation Between Locked Wheel and Other Friction Modes. Pennsylvania State Univ., PTI Rept. 7502, Feb. 1975.
5. Specification for Standard Tire for Pavement Tests (Discontinued 1973). Annual Book of ASTM Standards, Pt. 15, E 249, 1973.
6. Standard Specification American Tire for Pavement Skid-Resistance Tests. Annual Book of ASTM Standards, Pt. 15, E 501, 1977.
7. Standard Specification for Smooth-Tread Standard Tire for Special-Purpose Pavement Skid-Resistance Tests. Annual Book of ASTM Standards, Pt. 15, 1977.
8. J. L. Bradisse, A. F. Ramsey, and S. R. Sacia. Mobile Truck Tire Test System. SAE, Paper 741138, 1974.
9. W. A. Hiering and C. R. Grisel. Friction Effects Due to Runway Grooving. Federal Aviation Agency, U.S. Department of Transportation, Interim Rept. on Project 510-003-07X, 1968.
10. Vehicle Dynamic Technology. SAE, Recommended Practice J670C, Handbook Supplement, Jan. 1973.
11. E. Fiala. Seitenkräfte am Rollenden Luftreifen. Zeitschrift des Vereins Deutscher Ingenieure, No. 29, Oct. 1974.
12. H. Sakai. Theoretical Study of the Effect of Tractive and Braking Forces on the Cornering Characteristics of a Tire. Safety Research Tour in the U.S.A., Bulletin, Japan Society of Automotive Engineers, No. 3, Paper 4, March 1971, 1969, pp. 64-74.
13. Standard Test Method for Measuring Pavement Surface Frictional Properties Using the British Portable Tester. Annual Book of ASTM Standards, Pt. 15, E 303, 1977.

Publication of this paper sponsored by Committee on Surface Properties-Vehicle Interaction.

Nondestructive Pavement Evaluation: The Deflection Beam

G. Y. Baladi, Michigan State University
M. E. Harr, Purdue University

The prediction of the effects of vehicle motion on pavements is time dependent. Current design procedures, however, account for this motion as a sequence of equivalent static conditions reduced to passes or coverages. A solution to this problem was obtained by verifying the following hypothesis. A pavement system operated on by a vehicular input produces an output response. Relating the two is a time-dependent transfer function that contains within it the properties of the system. This function is obtained, in a mathematical sense, by using Laplace transformations without the need to simulate respective material performance or to determine values for preselected descriptors. The time-dependent transfer functions can be used to predict the response and the performance of a pavement system when it is subjected to an imposed load. The investigation was carried out by extending transfer function theory in connection with a finite convolution procedure to define the time-dependent transfer functions of a pavement. Moving trucks and aircraft were used in full-scale dynamic tests in service environments (six highway and two runway cross sections). It was shown that the time-dependent transfer functions obtained represent the characteristics of flexible pavements. Changes in parameters of the functions reflect changes in the performance and the condition of the pavement.

The major problem that faces the highway engineer today is not how to design and construct new pavements but how to evaluate, maintain, and upgrade existing pavement systems to meet today's demand for higher magnitudes of traffic loading and frequency.

The closing of a highway to permit the use of conventional destructive evaluation methods (such as test pits and plate load tests) may have catastrophic consequences. The need for rapid, nondestructive methods of pavement evaluation has been recognized in recent years (28,29), and different methods of nondestructive pavement evaluation have been developed (12,30,31). These methods, however, do not simulate actual traffic loading or take into account the complexity of the mechanism of pavement-subgrade interaction.

This paper introduces equipment for the rapid, nondestructive evaluation of pavement and a test procedure that was used at nine highway and airfield sites to measure flexible pavement deflections caused by the passage of a conventional vehicle.

DEVELOPMENT OF TESTING METHOD

The need for remedial measures to upgrade pavements so that they meet today's traffic demands has led many investigators to agree that a closer look must be taken at the materials that make up the pavement structure. Researchers concerned with fatigue failures have long recognized the need for a testing method that would simulate the action of traffic (8):

> Irrespective of the theoretical method of evaluation of load tests, there remains the important question as to what extent individual static load tests reflect the results of thousands of dynamic load repetitions under actual traffic. Tests have already indicated that various types of soils react differently and that the results of static load tests by no means bear a simple relation to pavement behavior.

In 1947, Campen and Smith (7), Hittle and Goetz (17), McLeod (20), and Phillipe (23) had all begun investigations of repeated-load tests on model pavement sections in which the number of load repetitions was on the order of 10. But these tests were destructive, time consuming, and costly, and experimentation with repeated-load testing in the conventional triaxial cell was soon recognized as a better method (32). Cyclic (repeated) plate load tests could only evaluate soil parameters under one set of conditions—those that existed at the time of testing—whereas critical soil conditions could be reproduced in the triaxial cell. Consequently, the effects of many different parameters (such as density, water content, degree of saturation, confining pressure, and deviatoric stresses) were soon being investigated (1,4,5,9,10,11,14,15,16,18,19,21,22,24,25,26,27).

Terrel and Awad (25) stressed the continuation of research to develop a newer theoretical technique and refine existing test procedures so that adequate material parameters could be obtained. Recently, investigators recognized that pavement deflection was one such technique, and a search was begun for a method of accurately predicting pavement deflection.

In 1970, Harr introduced the transfer function concept as a method of determining pavement parameters. Ali (33) applied transfer function theory to the study of flexible pavement under controlled laboratory conditions. Boyer and Harr, extending transfer function theory to in-service pavement systems, conducted field tests at Kirtland Air Force Base, New Mexico, and concluded that the characteristics of flexible pavements could be represented by a time-dependent transfer function (6). They were successful in their prediction of pavement deflections, but their method of testing was destructive.

In response to ambient conditions, volume changes cause pavement surfaces to curl and warp with time and location (13). Portions of the surface may therefore not be in contact with underlying materials when the pavement is subjected to vehicle loadings. Thus, any apparatus used to evaluate a pavement system must not alter the conditions that prevail before loading. All devices in use today—such as the Benkelman beam and vibrators—suffer from this shortcoming. In the Benkelman beam test procedure, the beam is set up next to a stationary load vehicle and the rebound of the pavement is measured as the vehicle moves away. Vibrators must seat the pavement before introducing steady-state vibrations. It should be noted that the nature of loading (the magnitude and frequency) of steady-state vibrators bears little resemblance to the transient input of an actual vehicle. Although Benkelman beams treat vehicle loads, they monitor only residual deflections after the pavement surface has been seated by vehicles at creep speeds.

If developed hardware is to gain widespread acceptance and use, it must (a) be inexpensive; (b) be operable with minimal or no training on the part of the user; (c) be lightweight, self-contained, and mobile; and (d) be able to accommodate available vehicles at the test site.

FIELD INVESTIGATION

The field phase of this study had as its objective the development, design, and use of rapid, nondestructive techniques for obtaining the data needed to determine

1. A time-dependent deflection response function for pavement,
2. An equivalent forcing function for the vehicle, and
3. The attenuation of energy in the pavement section.

Boyer's work at Kirtland Air Force Base, New Mexico (6), provided the technical guidance for the early phases of these investigations. Boyer reported that accurate deflection measurements could be obtained by using linear variable differential transformer (LVDT) gauges embedded in the pavement system. He also noted that accelerometer gauges are inadequate for the task because of their slow response and electrical drift. Based on Boyer's tests, it was decided to use LVDTs with an accuracy of 0.0025 mm (0.0001 in).

The initial LVDT installations were made on a line perpendicular to the wheel path at a gravel pit road near the West Lafayette, Indiana, campus of Purdue University. The objectives of these installations were (a) to determine the width of the dynamic deflection basin of the pavement section for a wide variety of trucks that enter the gravel pit plant and (b) to help in designing and checking the nondestructive measurement system. Results of this test program indicated that the width of the deflection basin extends less than 1.5 m (5 ft) laterally from the outside edge of the wheel for highway pavements.

The time-dependent deflection response functions of the pavement were recorded under varying ambient conditions for a wide variety of truck gear configurations by using the installed LVDT gauges at the gravel pit road. Analyses of these results led to the construction of a lightweight aluminum beam that carried six LVDTs (so that there would be no need to install gauges in subsequent tests). Figure 1 shows a schematic representation of the LVDT beam. It should be emphasized that measurements made with the LVDT beam are nondestructive.

The LVDT beam was first placed over the installed gauges, and pavement deflections were recorded by both systems. Figure 2 shows a plot of pavement deflections recorded by the LVDT beam versus those recorded by the installed LVDT gauges at the same lateral distances from the edge of the tire. Deflection measurements made by the beam were also checked against data from two other sets of installed LVDT gauges at Eglin Air Force Base, Florida. In those tests, an F-4 aircraft with a 111.2-kN (25 000-lb) wheel load was used as a loading vehicle, and tests were performed on a parking area as well as on an active taxiway. Pavement deflections at the same lateral distances from the wheel path showed the same relative equivalence as those shown in Figure 2.

Scope

The field investigations were conducted at seven sites. Locations of four of those sites are given below (1 m = 3.3 ft):

Site	Road	Indiana Location
1	Gravel Pit Road	West Lafayette, entrance to gravel plant after railroad bridge (installed LVDT gauges 45 m inside the gate)
2	Happy Hollow Road	West Lafayette, 182 m north of Happy Hollow Park entrance
3	North 9th Street	Lafayette, at exit of a small road leading to an old bridge
4	County Road 200 North	West Lafayette

Cross-sectional characteristics of these four sites are shown in Figure 3. Information about the other three

Figure 1. LVDT beam.

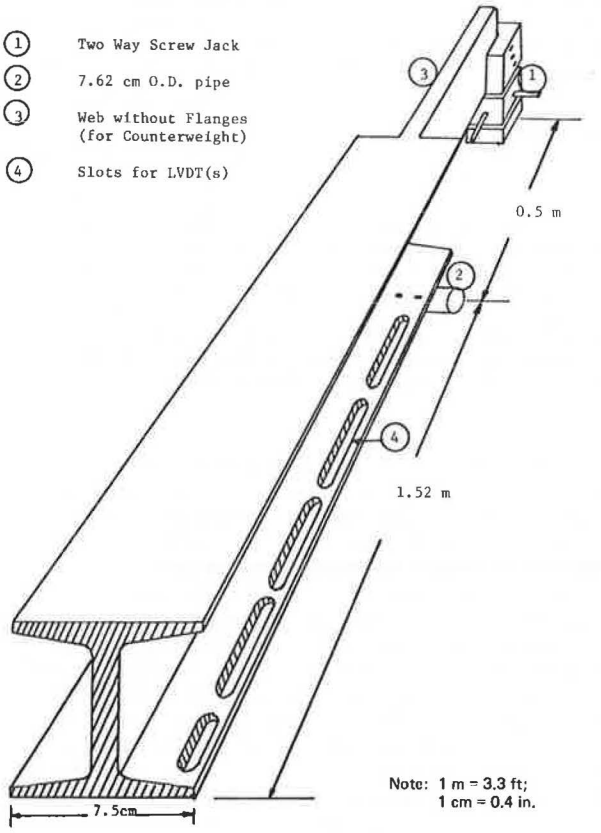

Figure 2. Pavement deflection responses of LVDT beam and LVDT gauges.

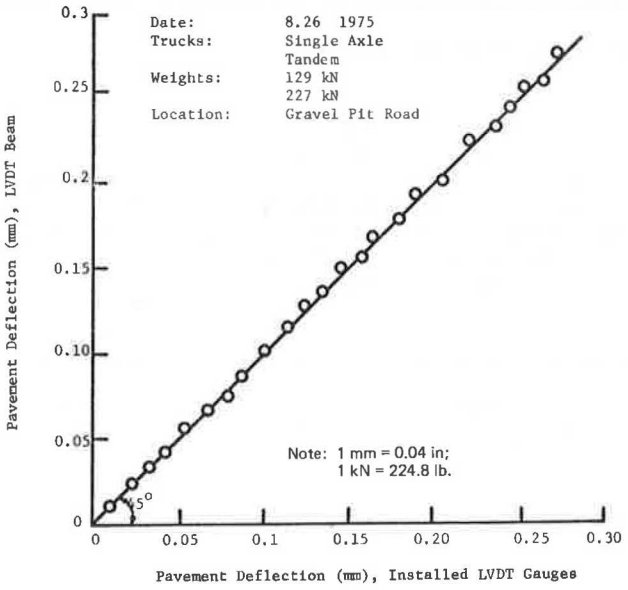

Figure 3. Cross sections of sites 1, 2, 3, and 4.

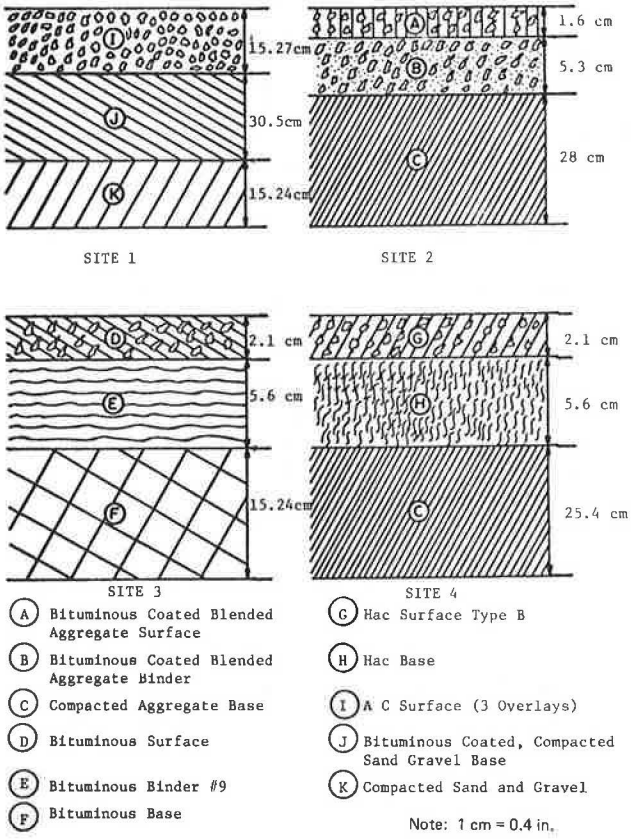

sites may be obtained elsewhere (3). Investigations were designed and tests were performed to account for various factors that were thought to influence the performance and response of pavement. These factors include (a) ambient conditions (Table 1), (b) gear configuration (Table 2), (c) load variation (Table 2), (d) tire pressure (Table 2), and (e) load repetitions (Table 3).

Signature

The signature of a vehicle is defined here as the pavement's time-dependent deflection response function that is measured or calculated at the edge of the tires of the loading vehicle. The symbol for the signature is y(0,t).

The overhang of the LVDT beam and the bulge of the side of the tire prevented the direct measurement of vehicle signature. However, pavement deflections were measured at different lateral distances from the edge of the tire. A study of the deflection basin at the embedded LVDT gauges determined that the deflection would follow the expression

$$y(x,t) = y(0,t)\exp[-(1/B)x^N] \quad (1)$$

where

- $y(x,t)$ = measured deflection at lateral distance x from the tire edge at time t,
- $y(0,t)$ = calculated deflections [signature at the tire edge (x = 0) and at time t],
- x = lateral distance from the tire edge to the LVDT gauge at which y(x,t) was measured, and
- B and N = parameters of the equation.

The LVDT beam was placed at the side of the embedded LVDT gauges at site 1 (gravel pit road). The loading vehicle was then driven so that the intermediate and rear tires passed over one of the embedded gauges. Pavement deflections were recorded under the tire and at various gauge positions on the LVDT beam. The vehicle signature was calculated by using Equation 1.

Table 1. Ambient test conditions.

Date	Time	Temperature (°C)	Wind (km/h)	Sky	Precipitation
3/12/75	9:00 a.m.-1:00 p.m.	2.8	North at 16	Cloudy	1 d after rain
3/13/75	9:00 a.m.-1:00 p.m.	-3.9	North at 11	Cloudy	Snowing
4/10/75	9:00 a.m.-2:00 p.m.	-2.2	Southwest at 16	Cloudy	Snowing
4/12/75	9:00 a.m.-2:00 p.m.	4.4	South at 16	Cloudy	2 d after snow
8/26/75	9:00 a.m.-3:00 p.m.	23.9	Southwest at 16	Partly cloudy	1 d after rain
10/10/75	10:00 a.m.-3:00 p.m.	7.2	North at 13	Clear	3 d after rain
1/5/76	9:00 a.m.-1:00 p.m.	-24.4	North at 16	Clear	1 d after snow
1/10/76	9:00 a.m.-11:00 a.m.	-23.3	North at 13	Clear	1 d after snow
3/17/76	9:00 a.m.-2:00 p.m.	-5.6	Southeast at 8	Clear	2 d after snow
5/13/76	9:00 a.m.-1:00 p.m.	17.8	Northwest at 16	Partly cloudy	5 d after rain
7/30/7	9:00 a.m.-1:00 p.m.	25.6	Southwest at 13	Partly cloudy	Hours after rain
8/12/76	9:00 a.m.-4:00 p.m.	26.7	South at 13	Partly cloudy	5 d after rain
9/13/76	12:00 n.-1:00 p.m.	26.7	Southwest at 16	Clear	10 d after rain

Note: 1°C = (1°F - 32)/1.8; 1 km = 0.62 mile.

Table 2. Data for truck types at site 1.

Gear Configuration	Gross Load (kN)		Speed Range (km/h)	Tire Pressure Range (kPa)
	Empty	Loaded		
Double tandem	111	325	18-40	483-621
Tandem	89	222	10-40	517-689
Single axle	36	89	16-48	517-621
Automobile	18	19	6-16	138-172
Pickup	27	40	16-24	172-241
Concrete truck	133	289	16-32	552-689
Tandem	93	231	16-48	483-695

Note: 1 kN = 225 lb; 1 km = 0.62 mile; and 1 kPa = 0.145 lbf/in^2.

Table 3. Average count of load repetitions at sites 1, 2, 3, and 4.

Site	Average Load Repetition[a]	Vehicle Type	Counting Days
1	200 000	90 percent trucks[b] 10 percent automobiles	Monday, Wednesday, Friday[c]
2	250 000	5 percent trucks 95 percent automobiles	Monday, Wednesday, Saturday
3	300 000	10 percent trucks 20 percent pickups 70 percent automobiles	Monday, Wednesday, Saturday
4	200 000	5 percent trucks 15 percent pickups 80 percent automobiles	Monday, Wednesday, Saturday

[a] Number of wheels that passed over one point in the pavement.
[b] Checked at the scale with the bookkeeper of the gravel road plant.
[c] Plant closes over weekends.

Figure 4. Calculated versus measured signature at site 1.

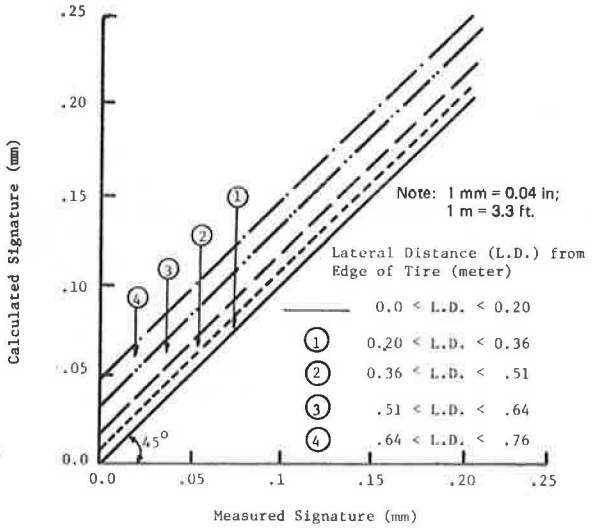

The region between the straight lines shown in Figure 4 designates the locus of the pairs of calculated and measured signatures for various lateral positions of loading vehicles. The solid line represents the correspondence between the measured and calculated signatures within the accuracy of the measurements. This last condition was found to hold for all tests when the intermediate and rear tires of the loading vehicles passed within 20 cm (8 in) of the front of the LVDT beam. Discrepancies between calculated and measured values were noted for vehicle paths at greater lateral distances.

Figure 5 shows typical measured deflections and calculated signature as a function of time at different lateral distances from the wheel path. Figure 6 shows measured and calculated deflections as a function of lateral distances.

The values of the parameters N and B of Equation 1 were calculated for sites 1 through 7 and are given in Table 4. Figure 7 shows plots of the values of N (to an arithmetic scale) against the corresponding values of B (to a logarithmic scale) for sites 1, 2, 3, and 4. The

Figure 5. Typical measured deflection and calculated signature (G_o) versus time for standard highway truck at site 2.

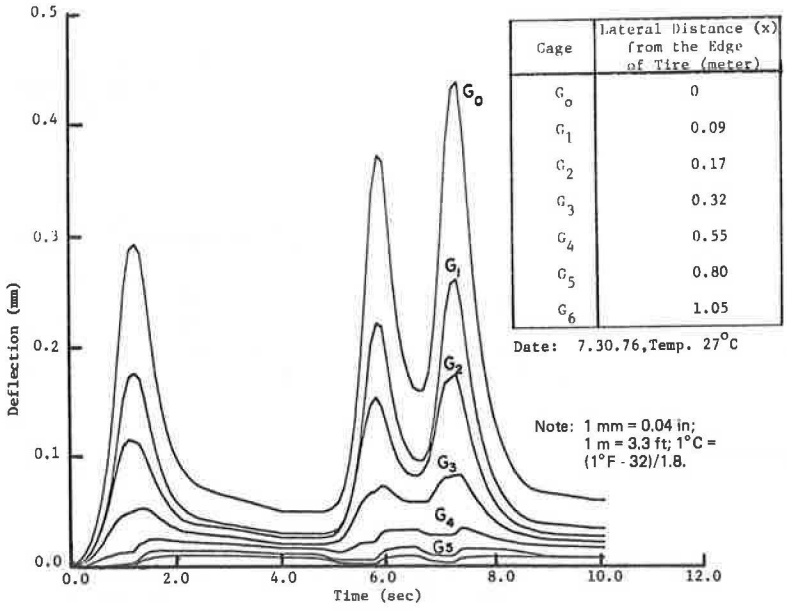

Figure 6. Measured and calculated peak deflection versus lateral distance for standard highway truck at site 2.

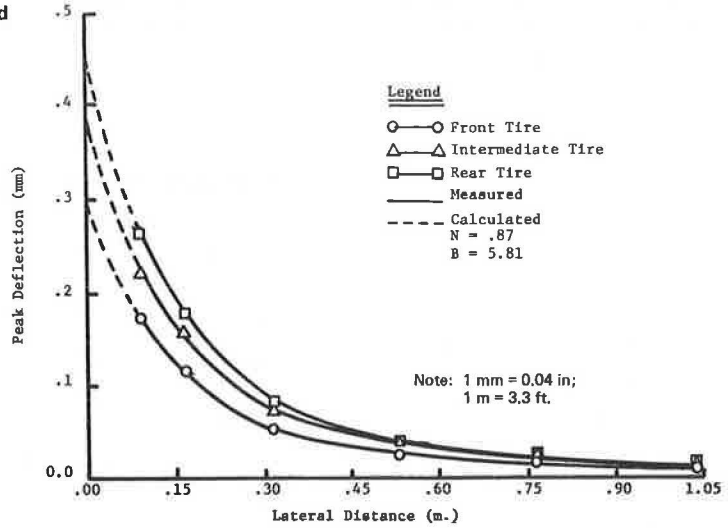

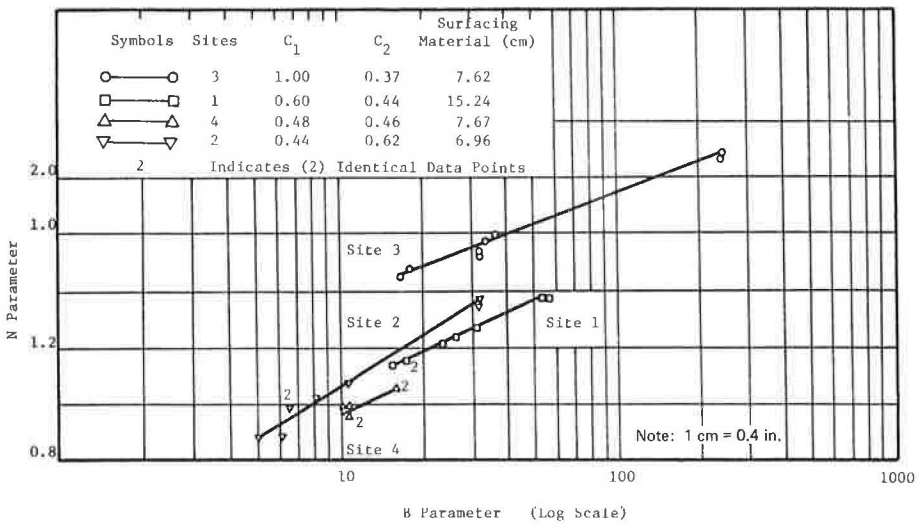

Figure 7. N versus log B for sites 1, 2, 3, and 4.

Table 4. Data for standard highway truck at all seven sites.

Site	Date	Air Temperature (°C)	Wheel Load (kN)			Peak Deflection (mm)			Vehicle Velocity (m/s)	Deflection Basin Parameters	
			Front	Intermediate	Rear	Front	Intermediate	Rear		N	B
1	8/26/75	24	29	30	30	0.17	0.17	0.17	0.81	1.26	31.64
		24	29	30	30	0.17	0.17	0.17	0.86	1.26	31.82
	1/05/76	-24	29	30	30	0.00	0.00	0.00	0.82	-	-
		-24	29	30	30	0.00	0.00	0.00	0.88	-	-
	3/17/76	-5.6	28	39	42	0.13	0.18	0.19	1.08	1.38	53.30
		-5.6	28	38	42	0.13	0.18	0.19	0.99	1.38	52.28
	5/13/76	17.8	29	37	39	0.14	0.19	0.19	0.77	1.22	26.28
		17.8	29	37	39	0.14	0.19	0.19	0.72	1.22	23.62
	7/30/76	25.6	30	38	39	0.17	0.21	0.21	1.09	1.14	17.25
		25.6	30	36	41	0.17	0.20	0.22	1.27	1.15	17.04
	9/13/76	26.7	20[a]	12	16	0.14	0.08	0.11	0.67	1.128	15.62
		26.7	4[b]	-	4	0.03	-	0.02		1.13	15.60
2	8/25/75	27.8	28	32	31	0.26	0.29	0.28	0.95	1.01	8.46
		27.8	29	33	30	0.34	0.39	0.35	1.10	1.07	10.70
	1/05/76	-24	28	31	30	0.00	0.00	0.00	0.80	-	-
		-24	28	32	29	0.00	0.00	0.00	0.89	-	-
	3/17/76	-5.6	31	35	36	0.30	0.34	0.35	0.91	1.37	31.95
		-5.6	31	37	37	0.29	0.34	0.35	0.80	1.34	32.24
	5/13/76	20	31	36	35	0.40	0.46	0.43	0.77	0.99	6.54
		20	31	36	35	0.40	0.46	0.43	0.91	0.99	6.54
	7/30/76	26.7	28	36	36	0.25	0.49	0.50	0.91	0.87	5.81
		26.7	28	35	37	0.25	0.46	0.51	0.77	0.88	6.75
3	8/26/75	24	27	33	34	0.83	1.02	1.05	1.01	1.60	37.29
		24	27	34	37	0.68	0.92	0.92	0.34	1.57	34.67
	1/5/76	-24	29	35	36	0.00	0.00	0.00	1.10	-	-
		-24	29	35	36	0.00	0.00	0.00	0.58	-	-
	3/17/76	-5	29	39	44	0.26	0.34	0.39	0.63	1.86	241.39
		-5	29	39	44	0.26	0.34	0.39	0.63	1.88	252.09
	5/13/76	20	29	39	39	0.59	0.78	0.78	0.78	1.52	32.01
		20	29	40	38	0.62	0.84	0.80	0.74	1.53	32.39
	7/30/76	27	31	35	43	0.96	1.13	1.37	1.03	1.45	16.77
		27	31	35	44	0.86	0.99	0.67	1.27	1.48	18.28
4	8/25/75	28	25	36	32	0.82	0.98	0.87	0.89	1.05	16.15
		28	25	36	36	0.82	0.97	0.87	0.95	1.05	16.16
	1/5/76	-24	29	36	36	0.00	0.00	0.00	0.28	-	-
		-24	29	35	36	0.00	0.00	0.00	1.26	-	-
	5/13/76	20	29	40	41	0.96	1.30	1.30	0.84	0.99	10.11
		20	29	39	39	0.98	1.32	1.33	0.83	0.99	10.64
	7/30/76	27	31	36	44	1.01	1.15	1.41	0.86	0.93	10.81
		27	31	36	44	1.01	1.16	1.41	0.80	0.93	10.80
5	8/12/76	27	31	38	42	0.44	0.53	0.58	0.45	1.15	20.17
6	8/12/76	27	28	39	41	0.21	0.28	0.29	0.38	0.87	6.87
7	8/12/76	27	28	39	41	0.58	0.80	0.84	0.40	0.50	2.08

Note: 1°C = (1°F - 32)/1.8; 1 kN = 225 lb; 1 mm = 0.04 in; and 1 m = 3.3 ft.
[a]Standard (empty) highway truck.
[b]Ford automobile.

figure suggests that N and B may be related functionally as

$$N = C_1 + C_2 \log B \quad (2)$$

where C_1 and C_2 are constants that depend on the characteristics of the pavement section at each site. Analyses of the data have indicated the constants to be independent of temperature, number of load repetitions, and loading vehicle. Corresponding values of the constants calculated for each of the four sites are shown in Figure 7.

The N and B parameters of Equation 1 may be thought

of as descriptors of the distribution of deflections from the edge of a loading tire. For example, if N = 2, Equation 1 resembles the normal (Gaussian) distribution with B proportional to the variance. Thus, changes in values of N and B for a pavement section reflect changes in the distribution of deflections and structural characteristics of that section.

Figure 8 represents four typical, normalized peak deflection curves as a function of lateral distance for sites 1, 2, 3, and 4. The corresponding values of N and B parameters and the values of $(B^{1/N})$ are indicated in the figure. It can be seen that the higher the value of $(B^{1/N})$ is, the greater is the lateral spread of the deflection. Again, the analogy to the normal distribution should be noted for N = 2. For this state, $(B^{1/N})$ is seen to be proportional to the standard deviation. Most tests were conducted by using the same loading vehicle traveling at creep speed; the input energy was thus fairly constant and the amount of lateral spread may be thought of as a measure of the lateral attenuation of energy in the pavement. These observations gave rise to the use of the N and B parameters as indicators of pavement performance.

Plots of the B parameter as a function of the number of load repetitions for sites 1, 2, 3, and 4 are shown in Figure 9, and corresponding data are given in Table 5. The solid symbols in the figure designate conditions at a temperature of -5.5°C (22°F). Open symbols indicate the temperature range of 18° to 27°C (64° to 80°F). The straight lines between the data points were obtained from a least squares analysis. The coefficients of correlation (R^2), the y-intercepts, and the slopes of the lines are given in Table 5. The table also gives the numbers of trucks, pickups, and automobiles that traveled over each of the road sites (as a percentage of the total traffic at the site). Figure 9 and Table 5 indicate that in all cases the B parameter decreases with increasing load repetitions during the period of

Figure 8. Normalized peak deflection versus lateral distance for sites 1, 2, 3, and 4.

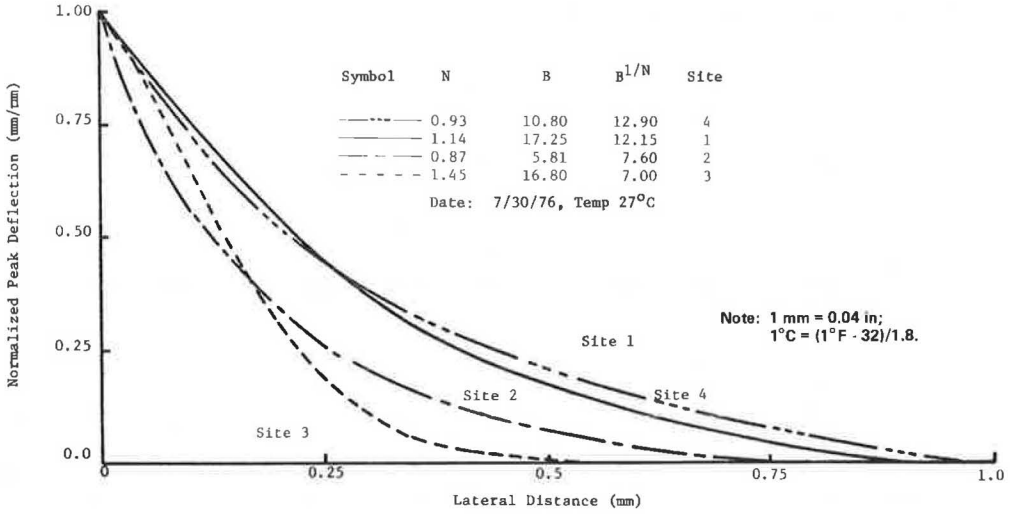

Figure 9. B versus load repetition for sites 1, 2, 3, and 4.

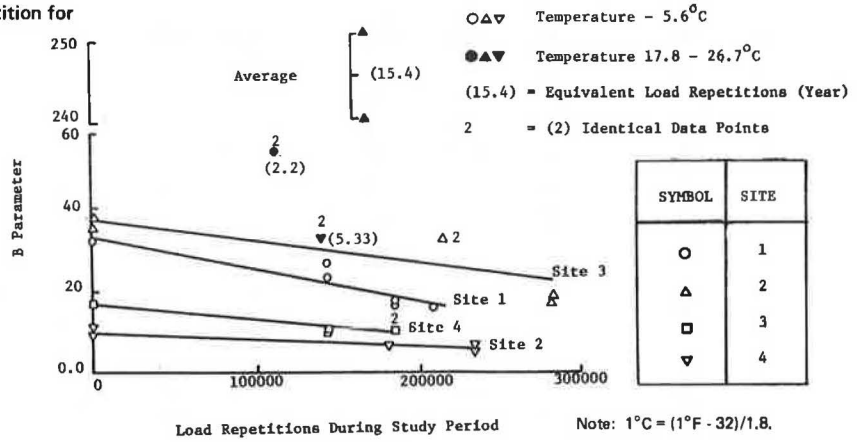

Table 5. Data for B versus load repetition (Figure 9).

Symbol	Site	Slope x 10^{-8}	Y-Intercept	R^2 (%)	Percentage of Total Traffic		
					Truck	Pickup	Automobile
○	1	-7.4	32.51	94.6	90	0	10
△	2	-5.4	37.45	80.4	10	20	70
□	3	-3.2	15.93	95.8	5	15	80
▽	4	-1.5	9.51	89.6	5	0	95

study. In addition, the steeper the slope of the line is, the higher is the percentage of trucks traveling over the site.

Plots of the N parameter with load repetitions are shown in Figure 10. The N parameter also decreases with increasing load repetitions, but the slopes of the lines—obtained from a least squares analysis—show much less variation than did those for the B parameter.

Figure 11 shows a schematic representation of the typical deflection basin with corresponding relative values of the N and B parameters at one site. The figure show that, the smaller the value of the parameters is, the more rapid is the lateral attenuation of energy and the deeper it penetrates under the wheel. As noted above, implicit in this is that, as N and B decrease, more work is done to the pavement section in the vicinity of the wheel load. As a result, greater distress might be expected to occur with fewer passes.

Table 5 indicates that, at an air temperature of -5.5°C (22°F), the values of N and B parameters are larger than those listed at higher temperatures. This is a consequence of the more uniform deflection for the colder pavement. Conditions for this temperature are designated in Figures 9 and 10 by the solid symbols. The number shown in brackets next to each of these symbols indicates the equivalent number of years of traffic that must travel over the road site so that the data point will fall back on the straight line representing the site. These numbers were calculated by using the noted slopes of the lines and relating observed load repetitions and time.

SUMMARY AND CONCLUSIONS

Equipment for rapid, nondestructive pavement evaluation was designed and used on nine different highway and airfield sites. Time-dependent deflection response functions were measured, and deflections under the edge of the loading wheel were calculated by using Equation 1. Analyses of the data indicated the following conclusions:

1. The results obtained from the LVDT beam (nondestructive system) were found to be in extremely close agreement with those obtained by the embedded LVDT gauges.
2. The lateral extent of the deflection basin was found in all cases to be less than 1.5 m (5 ft) from the edge of the loading tire.
3. The deflection basin extending laterally from the edge of a tire of a loading vehicle was found to follow an exponentially decaying function (Equation 1).
4. The parameters of Equation 1 were found to be independent of gear configuration, tire pressure, and wheel load. They did depend on the number of load repetitions and temperature.

Figure 10. N versus load repetition for sites 1, 2, 3, and 4.

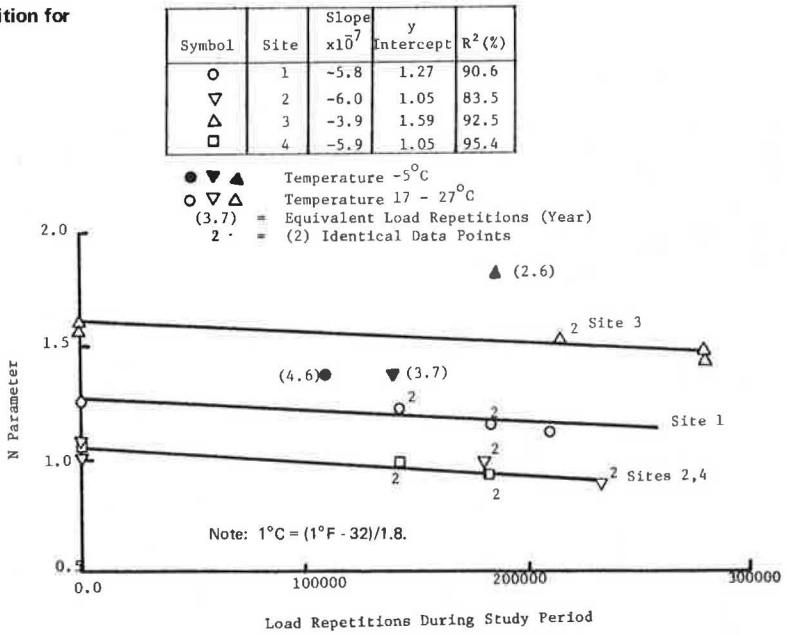

Figure 11. Typical deflection basin.

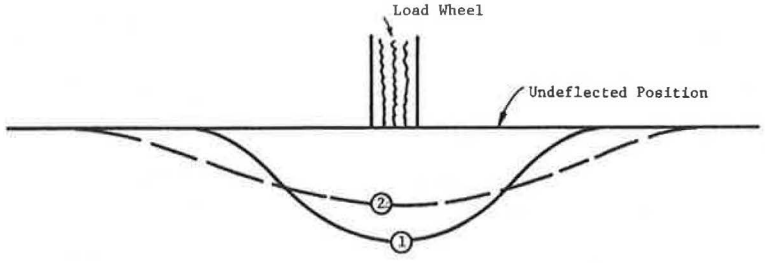

ACKNOWLEDGMENT

Sincere thanks are extended to the U.S. Air Force, the Federal Aviation Administration, the Federal Highway Administration, and the Indiana State Highway Commission for the financial assistance needed to conduct the research and for the facilities made available. The opinions, findings, and conclusions expressed are ours and do not necessarily reflect those of the sponsoring agencies.

REFERENCES

1. S. B. Ahmed and H. G. Larew. A Study of the Repeated Load Strength Moduli of Soils. Proc., International Conference on Structural Design of Asphalt Pavements, Univ. of Michigan, 1962.
2. J. J. Allen and M. R. Thompson. Resilient Response of Granular Materials Subjected to Time-Dependent Lateral Stresses. TRB, Transportation Research Record 510, 1974, pp. 1-13.
3. G. Y. Baladi. Invariant Properties of Flexible Highway Pavements. Purdue Univ., PhD thesis, Dec. 1976.
4. R. D. Barksdale and R. G. Hicks. Evaluation of Materials for Granular Base Courses. Proc., Third International Conference on Materials Technology, Rio de Janeiro, Aug. 1972.
5. J. Biarez. Contribution et l'Étude des Propriétés Mécaniques des Sols et des Matériaux Pulvérulents. Univ. of Grenoble, France, DSc thesis, 1962.
6. R. D. Boyer. Predicting Pavement Performance Using Time-Dependent Transfer Functions. Purdue Univ. and Indiana State Highway Commission, Joint Highway Research Project, No. 32, Sept. 1972.
7. W. C. Campen and J. R. Smith. Use of Load Tests in the Design of Flexible Pavements. ASTM, Special Technical Publ. 79, 1947.
8. A. Casagrande and W. L. Shannon. Research on Stress-Deformation and Strength Characteristics of Soils and Soft Rocks Under Transient Loading. Harvard Univ., Engineering Soil Mechanics, Series 31, 1948.
9. B. S. Coffman, D. C. Kraft, and J. Tamayo. A Comparison of Calculated and Measured Deflections for the AASHO Road Test. Proc., AAPT, Vol. 33, 1964.
10. J. A. Deacon. Equivalent Passages of Aircraft With Respect to Fatigue Distress of Flexible Airfield Pavements. Proc., AAPT, Vol. 40, 1971.
11. W. A. Dunlap. A Report on a Mathematical Model Describing the Deformation Characteristics of Granular Materials. Texas Transportation Institute, Texas A&M Univ., Technical Rept. 1, 1963.
12. R. Guillemin and J. C. Gramsammer. Dynamic Nondestructive Testing of Pavements in France. Proc., Third International Conference on Structural Design of Asphalt Pavements, London, 1972.
13. M. E. Harr and G. A. Leonards. Analysis of Concrete Slab on Ground. Journal of Soil Mechanics and Foundations Division, Proc., ASCE, Vol. 85, No. SM3, June 1959.
14. W. Heukelom and A. J. G. Klomp. Road Design and Dynamic Loading. Proc., AAPT, Vol. 33, 1964.
15. R. G. Hicks and C. L. Monismith. Factors Influencing the Resilient Response of Granular Materials. HRB, Highway Research Record 345, 1970, pp. 15-31.
16. R. G. Hicks. Factors Influencing the Resilient Properties of Granular Materials. Univ. of California, Berkeley, PhD thesis, 1970.
17. J. D. Hittle and W. H. Goetz. A Cyclic Load Test Procedure. ASTM, Special Technical Publ. 79, 1947.
18. B. F. Kallas and J. C. Riley. Mechanical Properties of Asphalt Pavement Materials. Proc., Second International Conference on Structural Design of Asphalt Pavements, Univ. of Michigan, 1967.
19. D. A. Kasianchuk, R. L. Terrel, and C. G. Haas. A Design Subsystem for Minimizing Fatigue, Permanent Deformation, and Shrinkage Fracture Distress of Asphalt Pavements. Proc., Third International Conference on Structural Design of Asphalt Pavements, London, Vol. 1, Sept. 1972.
20. N. W. McLeod. A Canadian Investigation of Load Testing Applied to Pavements Design. ASTM, Special Technical Publ. 79, 1947.
21. F. G. Mitry. Determination of the Modulus of Resilient Deformation of Untreated Base Course Materials. Univ. of California, Berkeley, PhD thesis, 1964.
22. L. W. Nijboer and C. T. Metcalf. Dynamic Testing at the AASHO Road Test. Proc., International Conference on Structural Design of Asphalt Pavements, Univ. of Michigan, 1963.
23. R. R. Phillipe. Field Bearing Tests Applied to Pavement Design. ASTM, Special Technical Publ. 79, 1947.
24. H. B. Seed, C. K. Chan, and C. D. Lee. Resilience Characteristics of Subgrade Soils and Their Relation to Fatigue Failures in Asphalt Pavements. Proc., International Conference on Structural Design of Asphalt Pavements, Univ. of Michigan, 1962.
25. R. L. Terrel and I. S. Awad. Resilient Behavior of Asphalt Treated Base Course Materials. Washington State Highway Department, Research Program Rept. 6.1, Aug. 1972.
26. C. Van der Poel. A General System Describing the Visco-Elastic Properties of Bitumens and Its Relation to Routine Test Data. Journal of Applied Chemistry, Vol. 4, 1954.
27. C. Van der Poel. Road Asphalt. In Building Materials, Their Elasticity and Inelasticity (M. Reiner, ed.), Interscience, 1954.
28. C. J. Vantil and B. A. Vallerga. Application of a Theoretical Procedure to Airfield Pavement Evaluation and Overlay Design. Proc., Third International Conference on Structural Design of Asphalt Pavements, London, 1972.
29. D. A. Voss and R. L. Terrel. Structural Evaluation of Pavements for Overlay Design. HRB, Special Rept. 116, 1971, pp. 199-210.
30. R. A. Weiss. Nondestructive Vibratory Testing of Airport Pavements. Federal Aviation Administration, U.S. Department of Transportation, Rept. FAA-RD-73-205-II, Vol. 2, April 1975.
31. G. Wiseman. The Interpretation of Surface Deflection Measurements Using the Model of an Infinite Plate on an Elastic Foundation. Symposium on Nondestructive Test and Evaluation of Airport Pavements, Vicksburg, MS, Nov. 1975.
32. M. A. Young and G. Y. Baladi. Repeated Load Triaxial Testing, State of Art. Division of Engineering Research, Michigan State Univ., Rept. 1, March 1977.
33. G. A. Ali. A Laboratory Investigation of the Application of Transfer Functions to Flexible Pavements. Purdue Univ., PhD thesis, Aug. 1972.

Publication of this paper sponsored by Committee on Pavement Condition Evaluation.

Measurement of Road Roughness in Australia

D. W. Potter, Australian Road Research Board

After the introduction of vehicle-based systems of road roughness measurement in the United States, a survey was made of such systems in Australia. The qualities sought were simplicity, trouble-free operation, and ability to predict the present serviceability rating of pavements (as determined by a panel of drivers). Two systems were selected for field trials: the PCA road meter and the Mays road meter. An apparatus was then developed that combines features of both meters. This apparatus and its operation are described in this paper. Development of improved methods of displaying, recording, and storing data as well as a method of obtaining a continuous trace of body-axle displacement is also described. Current use of roughness data in Australia and possible future applications are discussed. An area of concern common to all systems that are based on the measurement of body-axle displacement is the establishment of a standard against which vehicles can be periodically checked. Efforts made in Australia to overcome this problem are described.

To determine the extent to which individual sections of a road network are fulfilling their functions and to determine those sections of the network that need improvement, a method of quantitative assessment of condition is required. Carey and Irick (1), in the design stage of the AASHO Road Test, developed the concept of the condition of a section of road as its "ability to serve the needs of the user." Condition defined in this manner depends predominantly on the quality of the ride experienced by the road user. The changing performance of a road is then reflected by change of condition with time and traffic.

The term present serviceability rating (PSR) was introduced to quantify this measure of condition. To determine the PSR of a section of road, a panel of drivers representative of the driving population travel over the section. Each driver is asked to rate the section on a scale from 0 (very poor) to 5 (excellent). The mean of the panel's ratings is the PSR of the section.

Because of the time and expense involved in conducting such a rating exercise over substantial lengths of a road network, considerable effort has been expended in developing instruments capable of measuring characteristics of the road that can be correlated with PSR. The estimate of PSR from such a measure is called the present serviceability index (PSI). Several types of instruments are currently being used by highway organizations throughout the world. Australian experience in this field is described in this paper.

DEVELOPMENT OF ROUGHNESS MEASURING DEVICES

The first instrument developed to quantify a road surface profile was the CHLOE profilometer (2). This instrument, which was developed in association with the AASHO Road Test, measures the surface slope for each 150 mm (6 in) of travel by means of two rigid wheels in contact with the road surface. A computer calculates the variance of the slopes. The system is based in a long trailer and operates at a travel speed of 8 km/h (5 mph). Because of the slow travel speed and the effect on the results of coarse surface texture (sprayed seals), the instrument has been little used in Australia. However, the Australian Road Research Board (ARRB) possesses an instrument for research purposes (3).

Another device developed was the U.S. Bureau of Public Roads (BPR) roughometer—a single-wheel trailer towed in a wheel path (usually the outer) and capable of a travel speed of 32 km/h (20 mph). The roughometer sums displacements in one direction between trailer wheel and frame, expressing roughness in (U.S. customary) terms of inches of displacement per mile traveled (2).

General Motors (GM) developed a considerably more elaborate and expensive device—the GM road profilometer (4)—a vehicle-based system capable of determining road profile. The acceleration of a solid wheel in contact with the road surface is measured relative to an inertial reference. Double integration of this acceleration with respect to time produces the required profile. The vehicle is capable of operation at 80 km/h (50 mph).

Because of the advantages of a vehicle-based system that operates at highway speed and the cost and complexity of the GM profilometer, other, simpler systems were soon developed. The two most widely used are the Mays road meter (5) and the Portland Cement Association (PCA) road meter (6).

Output of the Mays meter is in the form of a graph of individual displacement between vehicle body and axle versus total body-axle displacement. Thus, the roughness of a section of road is determined by measuring the length of the graph generated by the section. The PCA meter also measures body-axle displacement in a vehicle. The amplitude of each individual displacement is measured to the nearest 3.1 mm (0.125 in) by means of a roller traversing a plate segmented in 3.1-mm intervals; the roller is attached to the vehicle axle, and the plate is attached to the vehicle body. A common configuration uses a plate composed of 23 segments. The segments are electrical conductors, and those equidistant from the central segment are connected together. Associated with each pair of segments is a digital counter (total of 11 counters). When the roller contacts a segment, an electrical connection is made and the count on the corresponding counter is increased by 1.

Before fieldwork begins, the plate is adjusted to bring the central segment in contact with the roller (the vehicle is stationary on level ground). Testing is conducted at 80 km/h (50 mph). The PCA value of a section is determined from the counts by means of the following formula:

$$\text{PCA value} = [(1 \times \text{counter } 1) + (2 \times \text{counter } 2) + \ldots + (N \times \text{counter } n)] \times (1/8) \div \text{distance} \quad (1)$$

where distance is derived in miles. This value is related to the time-based variance of the axle-body displacements. Scala (3) has reported early Australian experience with this device.

AUSTRALIAN DEVELOPMENTS

The development of roughness meters was followed with considerable interest by road authorities in Australia, and in 1969 the National Association of Australian State Road Authorities (NAASRA) and ARRB established a joint subcommittee to report on currently available systems with a view to adopting a system for use in Australia.

The subcommittee was also asked to make recommendations on any modifications it considered desirable. Because a considerable portion of the Australian road network is in sparsely populated areas, emphasis was placed on reliability and simplicity of operation in addition to ability to predict PSR.

A detailed investigation of the PCA meter was carried out and reported by Scala (3). Two major difficulties were experienced: The zero position of the meter (and thus the roughness value) changed with grade and with fuel use, and it was found that the shortest interval of distance in which counter readings could be continuously recorded was approximately 0.8 km (0.5 mile). However, for maintenance and reconstruction programming applications, it was considered desirable to monitor roughness in intervals as short as 0.2 km (0.12 mile). Maintaining satisfactory electrical contact between roller and plate segments, particularly in dusty conditions, was also a problem. In the case of the Mays meter, the main objection centered on the office work involved in measuring up to 1000 strips of paper for each day's field testing.

To overcome these difficulties a device was developed (with the guidance of the subcommittee) that translated the axle-body displacement into rotation of a shaft. Clutches were incorporated to allow one-way-only rotation of the shaft (corresponding to downward displacement of the axle relative to the body), and a mechanical revolution counter similar to a vehicle odometer was attached to the shaft. By means of this system, the degree of roughness of a section of road is obtained by subtracting the reading of the revolution counter at the start of the section from the reading at the end of the section. This difference divided by the section length in kilometers gives a roughness value in counts per kilometer. Details of the meter, designated the NAASRA roughness meter, are given in a technical manual that contains full operating instructions (7).

The meter is mounted in a "station sedan" (i.e., station wagon), directly over the differential. A thin steel cable, attached to the housing of the differential, passes through the vehicle floor and is attached to a length of bicycle chain. The latter passes over a sprocket to a tension spring attached to the vehicle body (Figure 1). The sprocket is attached to a shaft by a sprag clutch, which allows rotation of the shaft in only one direction. A second sprag clutch is incorporated between shaft and meter housing to eliminate backlash. A speedometer type of flexible drive connects the shaft to the counter, which is located in the glove compartment of the vehicle. An accurate mechanical odometer is also housed in the glove compartment adjacent to the roughness counter (Figure 2).

After successful preliminary trials, a detailed study was conducted to determine the effect on roughness count of vehicle type, test speed, ballast, tire type and pressure, road surface texture, and vehicle driver (8).

Correlation of NAASRA Meter With PSR

Studies were carried out in four of the six Australian states to determine the correlation of the NAASRA roughness meter with PSR. Panels consisting of approximately 15 highway engineers were selected. Each panel member rated approximately 30 rural and 30 urban sections. Each section was approximately 0.8 km (0.5 mile) long and of uniform roughness. Sections differed in roughness over a smooth to rough range and encompassed a representative range of pavement widths and types. Rural sections were traversed at 80 km/h (50 mph) and urban sections at 50 km/h (30 mph).

In rating a section, a panel member was required to assign a number between 0 (very poor) and 5 (excellent) to the section. The PSR of the section was the mean rating for the sections. NAASRA roughness values (counts per kilometer) for each section were taken as the mean of four runs. Figures 3 and 4 (8) show typical results obtained. On the basis of these studies, it was concluded that the correlation of the NAASRA roughness meter with PSR was comparable to that of other systems based on the measurement of body-axle displacement. Further details are given elsewhere (8).

Tolerability Rating of Pavements

During the PSR rating of pavements outlined above, additional information was sought from each panel member.

Figure 1. NAASRA roughness meter fitted in vehicle.

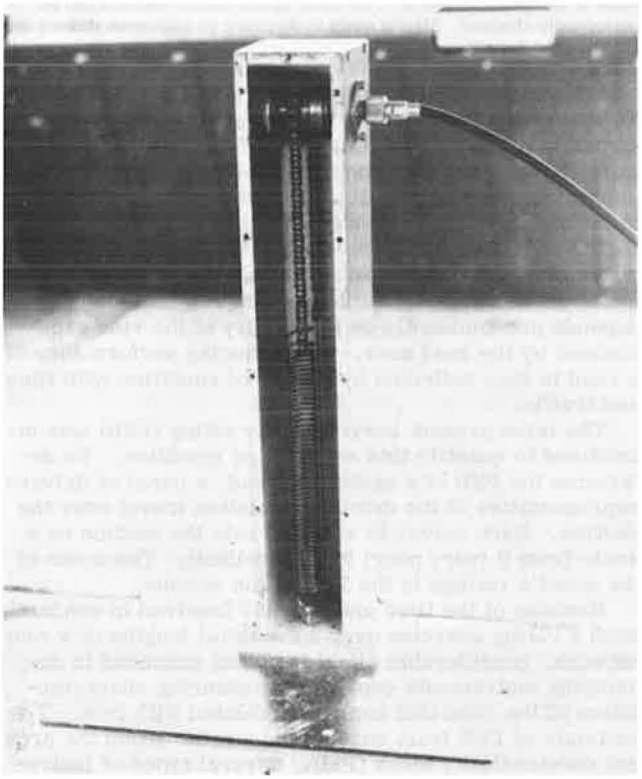

Figure 2. Roughness counter and odometer in glove compartment of vehicle.

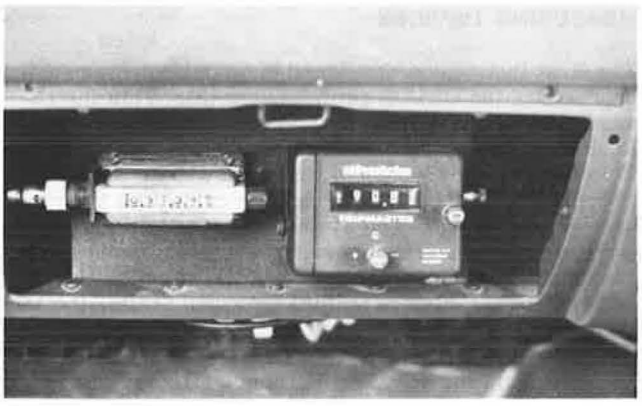

Figure 3. PSR versus NAASRA roughness values at 80 km/h (50 mph).

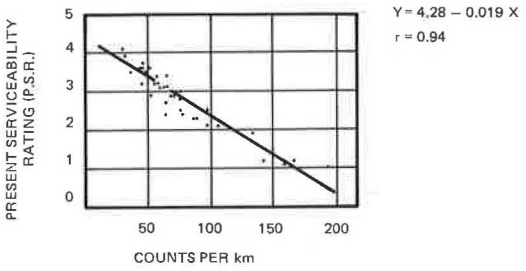

Figure 4. PSR versus NAASRA roughness values at 50 km/h (30 mph).

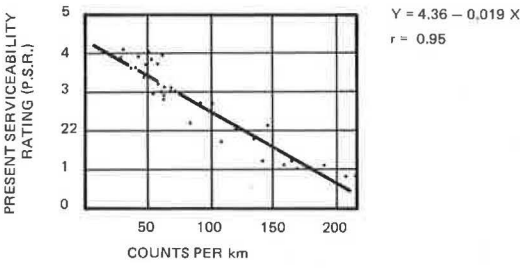

After the panel members traversed each rural section, they were asked the following questions:

1. Assuming that you have to drive at 80 km/h (50 mph) for 320 km (200 miles) on a highway, is the pavement of acceptable quality?
2. Assuming that you have to drive at 80 km/h (50 mph) for 80 km (50 miles) on a main road, is the pavement of acceptable quality?

After the panel members traversed each urban section, the following question was posed:

3. Assuming that you are on an urban arterial that has a 60-km/h (35-mph) speed limit and you have to drive 32 km (20 miles) in heavy traffic, is the pavement of acceptable quality?

The purpose of this exercise was to determine the maximum NAASRA roughness value (or minimum PSI) for each class of road that could be considered a tolerable limit. Responses to the questions were analyzed, and 50th percentile values (i.e., NAASRA roughness values considered acceptable by 50 percent of the rating panels) were determined. These values were adopted by the NAASRA subcommittee as tentative maximum tolerability limits (1 km = 0.62 mile):

Class of Road	NAASRA Roughness (counts per kilometer)
Highways	110
Main roads	150
Urban arterials and subarterials	175

Roughness Data

Recording and Storage

After the NAASRA roughness meter was accepted by the state road authorities, the device gained rapid acceptance as a routine road survey tool. During this phase it became apparent that, because of the large quantities of data being generated, more sophisticated methods of data collection and analysis were needed. A fully automated system was developed and constructed by ARRB in 1971 and 1972. In this system, the desired distance interval for roughness measurement (0.1, 0.2, 0.5, or 1.0 km) may be preset. Travel time, roughness, and distance from the starting point are automatically recorded for each interval on computer-compatible punched paper tape. This information can also be recorded at any mid-interval position by use of a manual keyboard that consists of 16 alphabet characters. During operation, a record of the alphabet character and the time, roughness, and distance information are placed on the punched tape by the pressing of a key.

A coding system is used that associates each alphabet character with a road feature of special interest. Thus, by use of a suitable computer program for processing the data, roughness associated with special road features such as railway level crossings, stock grids, bridges, culverts, and construction zones can be isolated. This feature can also be used to indicate a change in pavement surfacing or test speed. A printer is supplied with the equipment so that data can be assessed on the spot. Figure 5 shows a schematic diagram of the system, which has been used in Australia for routine survey work for approximately 4 years (7).

A prototype that performs the same function but incorporates improved electronic circuitry and cassette tape recording is currently undergoing field evaluation. This unit is considerably smaller in size and requires significantly less power to operate.

Two additional recording systems have also been developed that, in sophistication, fall somewhere between the standard NAASRA roughness meter and the fully automated system. The first of these has the ability to "hold" on a digital display the roughness reading for the preceding distance interval. The additional time afforded the operator to record the roughness value considerably reduces operator fatigue. The unit is compact [approximately 75 × 100 × 125 mm (3 × 4 × 5 in)] and is mounted under the glove compartment of the vehicle. The second system has capabilities similar to those of the fully automated version except that output data are available only in a printed (not computer-compatible) form. This unit is also compact and is located in front of the operator.

Continuous Trace Recording

A disadvantage associated with the methods of recording road roughness outlined above is that a single roughness value is assigned to each distance interval. However, the roughness for an interval may be attributable mainly to one or two isolated bumps or a short, very rough subsection (e.g., transverse construction joints and bridge expansion joints or uneven settlement of embankments and isolated pavement failures). To enable distinctions of this nature to be made, ARRB has developed equipment that continuously records the body-axle displacement of a vehicle.

Two types of devices are currently in use. Installation of both systems is simple and rapid (9).

The first system uses a paper drive assembly and heated pens from a commercially available (Watanabe Mini-Writer model 711) chart recorder (Figure 6). The pen that records displacement is directly attached to the chain of the roughness meter; the recorder trace is thus direct reading (with a 1:1 displacement scale). A second pen is used to provide event marks on the trace. The paper trace is driven by means of a mechanical cable

Figure 5. Automatic recorder equipment and interconnecting cables.

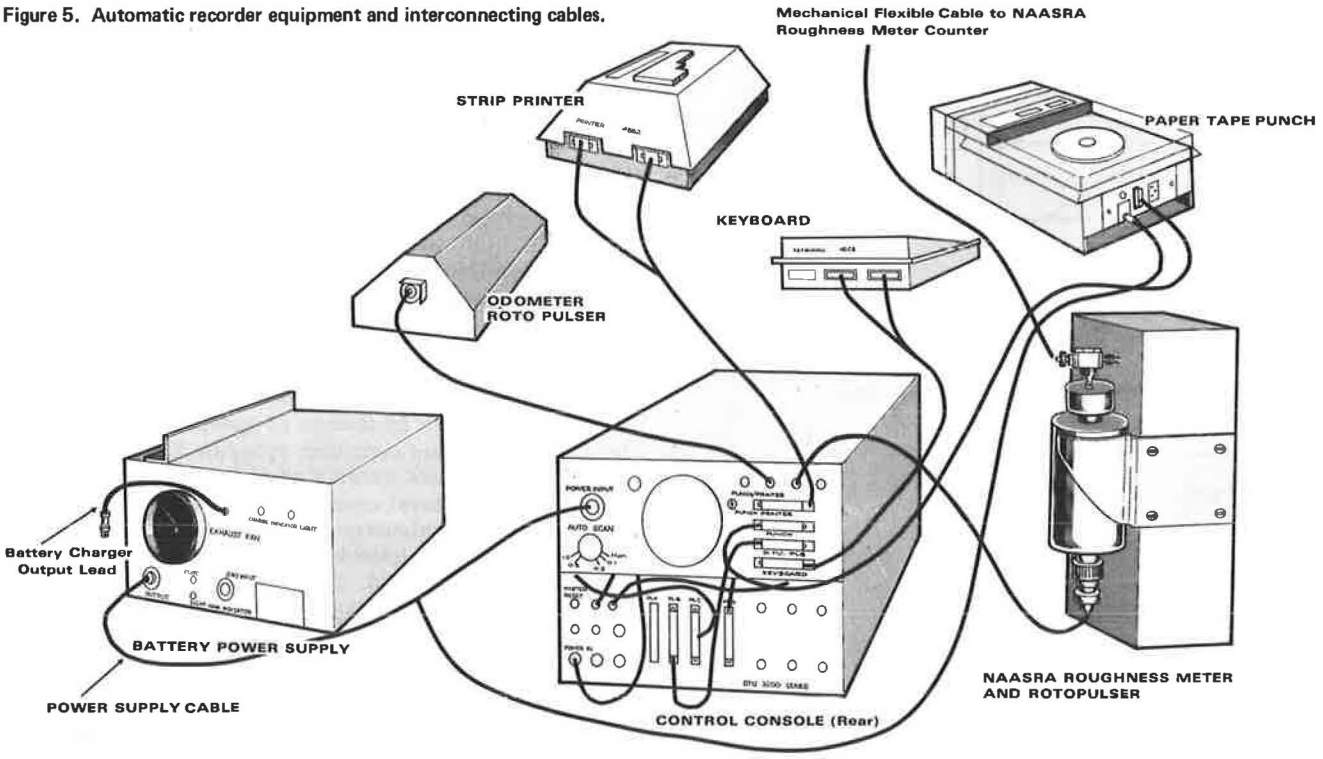

linked to the vehicle speedometer cable. This produces a record of body-axle displacement versus distance traveled. Controls for pen temperatures and the event marker are housed in a small box that is carried on the front seat between the driver and the operator of the device. The recorder does not affect the operation of the roughness meter and thus may be used as an adjunct to routine testing. The device is installed in a few minutes and has proved to be trouble free in operation.

A second system was developed to allow direct entering of comments and items such as section identification on the trace during testing. A displacement transducer is mounted so that its central core is attached to the roughness meter chain and its body is attached to the meter frame (Figure 7). Output voltage is fed to a conventional chart recorder. The recorder gain is adjusted to give direct-reading body-axle displacements. Again, the paper trace is driven by a mechanized cable. The

Figure 6. Direct link recorder.

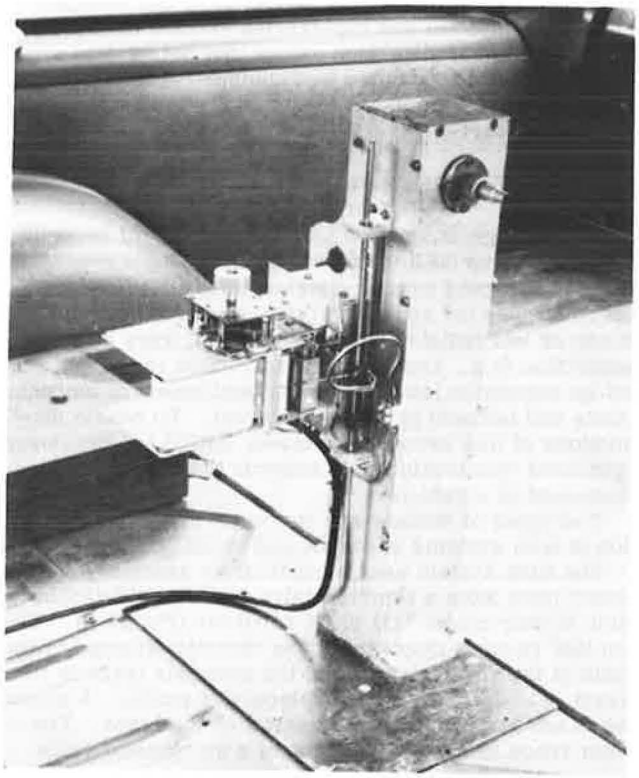

Figure 7. Remote recording apparatus.

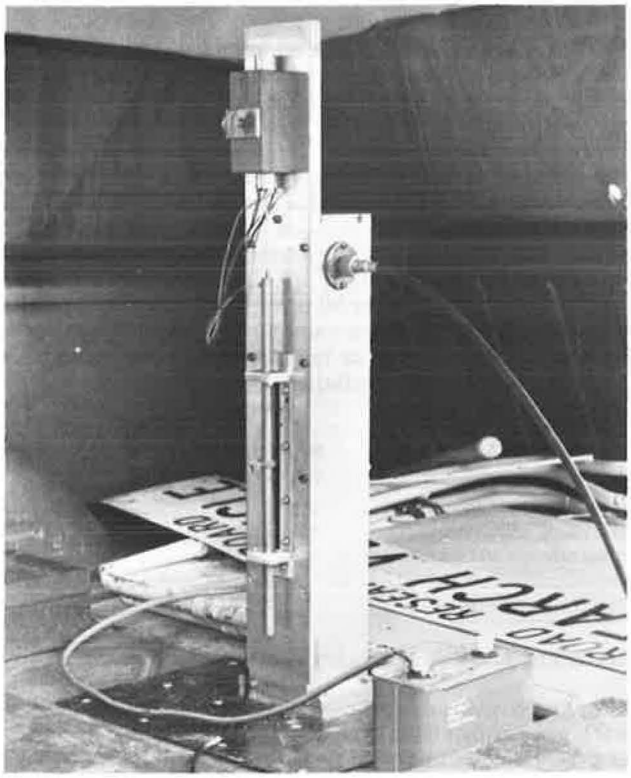

recorder can be comfortably carried on the operator's lap, and comments can be directly recorded on the trace.

Current Use

In Australia, roughness data are currently collected at two levels. Each state road authority collects data for the entire road system under its control. These data, categorized according to road class, are used by the state to support its application for financial assistance from the federal government. They are also used within the road authority as input for long-range rehabilitation programming and, in the short term, to assist in assigning priorities in maintenance and overlay programs. Such data were used in a recent major study that assessed the overall economic impact of changes in current restrictions on road vehicles (such as limits on axle load, gross weight, and size). Roughness data and pavement age were used to determine performance relations for each class of road. By use of the "fourth power law" derived from AASHO Road Test results (i.e., the destructive effect of an axle is proportional to the fourth power of the axle load), estimates could be made of the additional expenditures that would be required to maintain the road system in its current condition if it were subjected to increased axle loads (10).

The second major use of roughness data is at the operating, or district, level. To determine specific remedial measures on a section of road to be upgraded, roughness levels are usually determined at 0.2-km (0.1-mile) intervals. This detailed information helps the engineer to locate possible problem areas—such as poor drainage and embankment consolidation—that require attention before overlaying. The continuous trace recorder is also put to considerable use at this level.

Future Applications

It is anticipated that roughness data will increasingly be used in Australia during roadwork construction. A continuous trace of roughness on each successive pavement layer during construction would help in rapidly indicating those areas that require further work. It is also felt that, as the concept of rideability becomes more widely accepted as a criterion of pavement condition, current longitudinal profile requirements based on deviation from a straight edge will be supplanted by maximum acceptable roughness levels.

Roughness data collected from periodic surveys of the entire road system will make possible a continued refinement of estimates of pavement performance, providing information required for the development of pavement management systems and maintenance management subsystems.

ESTABLISHMENT AND MAINTENANCE OF A ROUGHNESS STANDARD

The response to a road profile of a vehicle-based system of roughness measurement depends on, among other things, the response characteristics of tires, springs, and shock absorbers. As vehicles age, these characteristics change, and so does the roughness value determined for a fixed road profile. If meaningful comparisons are to be made between roughness data obtained at different times, a standard is required against which vehicles can be periodically calibrated. Australian studies directed toward establishing a standard started with the selection of standard sections of road, which were chosen on the basis of uniformity of roughness within a section and a range of roughnesses between sections. Other requirements were light traffic (low rate of deterioration with time) and assurances from the controlling authorities that no rehabilitation or major maintenance work on the sections was projected. In addition, an ARRB roughness vehicle was designated as a standard vehicle; its use was restricted to the establishment of correlations with other roughness vehicles.

The limitations of this approach soon became apparent. When the roughness levels of the standard sections recorded by the standard vehicle varied with time, it was impossible to determine what proportion of this change was attributable to changes in road profile and what proportion to changes in vehicle response. After considering the problem, the NAASRA subcommittee recommended that ARRB develop a secondary standard system based on a two-wheel trailer. It was considered that a trailer-based system would offer the following advantages:

1. When the trailer was required to travel interstate for calibration of state road authority vehicles, wear on suspension components would be minimized by transporting the trailer on a flatbed truck.
2. When the trailer was not in use, it could be conveniently stored so that there was no load on its wheels and spring sag was reduced.
3. Fewer components affect the response characteristics of a two-wheel system than affect a four-wheel system. This point was considered relevant because an attempt would be made to determine the response characteristic of each major component.
4. The use of two standards (the trailer and the ARRB vehicle) in conjunction with standard sections of road would overcome the problem presented in item 3. If, on a given standard section of road, both trailer and vehicle responses changed but the relation between trailer response and vehicle response remained unchanged, one could attribute the change in response to a change in section roughness. However, if the response of only one standard changed or if both changed by different amounts, laboratory checking of the suspension components of the trailer should enable the extent of the changes to be determined and the necessary corrections to be made.

Following the recommendations of the subcommittee, ARRB constructed a trailer by using the rear suspension of a station wagon (11, 12). The use of adjustable shock absorbers makes it possible to obtain trailer roughness values that are in close agreement with vehicle roughness values. After establishing this relation, ARRB intends to determine the static load deflection characteristics of the springs and the load displacement characteristics of the shock absorbers under repeated sinusoidal displacements of fixed amplitude and frequency. Tests will be conducted at 1, 2, 5, 10, and 20 Hz.

It is expected that use of the trailer response system will help to achieve a more permanent standard of roughness measurement.

CONCLUSIONS

As a result of the development by ARRB and the acceptance by NAASRA of a simple, vehicle-based device for the measurement of road roughness, roughness values are now used as routine inputs into rehabilitation programming and maintenance scheduling in Australia. Recording systems of varying complexity have been developed to expedite data manipulation. A long-term program is currently being undertaken that, it is believed, will

allow meaningful comparison of roughness values measured at different times.

ACKNOWLEDGMENTS

The work reported in this paper was carried out by ARRB under the guidance of a joint ARRB-NAASRA committee. The committee's assistance is gratefully acknowledged. Special acknowledgment is made to A. J. Scala of ARRB, who has been directly involved in all phases of the work.

REFERENCES

1. W. N. Carey, Jr., and P. E. Irick. The Pavement Serviceability Performance Concept. HRB, Bulletin 250, 1960, p. 40.
2. F. N. Hveem. Devices for Recording and Evaluating Pavement Roughness. HRB, Bulletin 264, 1960, pp. 1-26.
3. A. J. Scala. Use of the PCA Roadmeter for Measuring Road Roughness. Proc., 5th Australian Road Research Board Conference, Vol. 4, 1970, pp. 348-67.
4. R. W. Hudson. High Speed Road Profile Equipment Evaluation. HRB, Highway Research Record 189, 1967, pp. 150-164.
5. F. Lively. Mays Meter Smooths the Way. Texas Highways, Vol. 16, No. 2, 1969.
6. M. P. Brokaw. Development of the PCA Roadmeter: A Rapid Method for Measuring Slope Variance. HRB, Highway Research Record 189, 1967, pp. 137-149.
7. A. J. Scala and D. W. Potter. Measurement of Road Roughness. Australian Road Research Board, Technical Manual ATM 1, 1977.
8. R. L. Kaeshagen, O. A. Wilson, A. J. Scala, and A. Leask. The Development of the NAASRA Roughness Meter. Proc., 6th Australian Road Research Board Conference, Vol. 4, 1972, pp. 303-330.
9. D. W. Potter. Development and Use of Continuous Recorders for Measurement of Road Roughness. Australian Road Research Board, Internal Rept. AIR 088-1, 1976.
10. A. T. Fry, J. M. Stevenson, and S. G. Servais. Report on the Development of the Pavement Performance Relationships. National Association of Australian State Road Authorities, Economics of Road Vehicle Limits Study, Task 25-P1, 1975.
11. D. W. Potter. Development and Assessment of a Road Roughness Trailer. Australian Road Research Board, Internal Rept. AIR 088-2, 1977.
12. D. W. Potter. Report to NAASRA Sub-Committee on Modified PCA Meter Concerning Extended Testing of ARRB Roughness Trailer. Australian Road Research Board, Internal Rept. AIR 088-5, 1977.

Publication of this paper sponsored by Committee on Pavement Condition Evaluation.

Use of Road Rater Deflections in Pavement Evaluation

M. C. Wang and Thomas D. Larson, Pennsylvania State University
Amar C. Bhajandas and Gaylord Cumberledge, Pennsylvania Department of Transportation

There is a need to predict the future performance of pavements by using deflections measured at any time so that deflection data can be used to determine the strategy for pavement maintenance. The road rater is a relatively new instrument for evaluating pavement performance. This paper presents some basic principles of road rater operation, its method of measuring pavement response, and criteria for evaluating the future performance of flexible pavements that contain bituminous concrete base courses. The response of experimental pavements to 80-kN (18 000-lb) axle loads and road rater loading is analyzed and is related to the actual performance of the experimental pavements. A model 400 road rater was operated at a frequency of 25 Hz. The BISAR computer program was used to obtain spring pavement temperature and subgrade moisture condition. Critical responses analyzed include maximum vertical compressive strain at the top of the subgrade, maximum tensile strain at the bottom of the base course, and maximum surface deflection. Based on the results of the analysis, equations are developed that interrelate various pavement responses and permit the calculation of critical responses to 80-kN axle loads from the road rater deflection basin. A permissible ratio of surface curvature index to maximum deflection is also established based on the fatigue property determined in the laboratory. This value may be used to evaluate pavements for rehabilitation purposes.

Predicting pavement performance is an essential step in the development of maintenance programs to extend the service life of a pavement beyond its original design life. Warrants for overlays are currently based mainly on the functional performance of a pavement, which is essentially a measure of riding comfort. The design of overlays, however, is based on surface deflection data, which primarily measure the structural performance of the pavement. There is thus a need to predict the future performance of pavements by using deflections measured at any time so that deflection data can be used to determine the strategy for pavement maintenance.

Various types of instruments are available for measuring the deflections of a pavement surface under load. The Benkelman beam was developed during the WASHO Road Test in 1952. The underlying principles of operation for this instrument are relatively simple and have been well defined (1, 2). One disadvantage of the Benkelman beam test is the limited rate of progress that can be achieved in the routine evaluation of roads. This has prompted the development of mechanized versions of the instrument that are aimed at providing a much greater rate of progress. The most common of these instruments are the traveling deflectometer developed by the California Division of Highways (3) and the Lacroix de-

flectograph developed in France (4). Other types of instruments have been developed for measuring specific features of the deflection basin, such as the curvature meter developed in South Africa (5) and the slopemeter (6). All of these instruments are used in measuring the deflection characteristics of a pavement surface under a dual wheel load that is either stationary or moving at a very slow speed.

Dynamic testing techniques have been developed to simulate the effect of vehicle speed in reproducing repeated impulsive loadings at a point in the pavement. One method that has the advantage of fast operation uses a stationary vibrating load to replace the moving wheel load; the response of the pavement is monitored through a number of geophones (accelerometers). The road rater (7), the Dynaflect (8), and other instruments (9) have been developed for this purpose. Because of its relatively high degree of mobility, the road rater has been adopted by the Pennsylvania Department of Transportation (PennDOT) for the routine evaluation of state highway pavements.

The road rater technique for measuring pavement response is simple, but use of the instrument for evaluating pavement performance is by no means well established. This paper presents some basic principles of road rater operation, its method of measuring pavement response, and criteria for evaluating the future performance of flexible pavements that contain bituminous concrete base courses. The evaluation criteria were developed based on the results of an analysis of road rater deflections and performance data collected at the Pennsylvania Transportation Research Facility (10).

PAVEMENT RESPONSE UNDER ROAD RATER LOADING

The road rater is composed of three basic types of elements: loading, sensing, and monitoring. The loading element consists of a vibrating weight and two rectangular steel plates that rest on the pavement surface. The weight varies from 72 to 295 kg (160 to 650 lb), depending on the model, and vibrates vertically at various frequencies. The loading plates have dimensions of 10.2 by 17.8 cm (4 by 7 in) each and are spaced 26.7 cm (10.5 in) apart center to center. The sensing element consists of four geophones 0.33 m (1 ft) apart; one sits at the middle of the two loading plates, as shown in Figure 1. The monitoring element is simply a readout unit for the four geophones. The road rater is mounted at the front of a van. A more detailed description of the components and the operation of the road rater is given by Bhajandas, Cumberledge, and Hoffman (11).

The vibratory motion of the weight induces a simple harmonic loading. The peak force of the road rater loading is

$$F_{peak} = 19.73\,Wf^2D \quad (1)$$

where

W = weight (kg),
f = frequency of vibration (Hz), and
D = peak-to-peak displacement (cm).

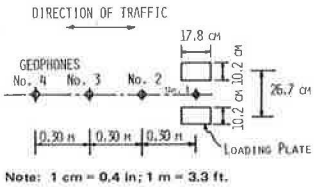

Note: 1 cm = 0.4 in; 1 m = 3.3 ft.

Figure 1. Arrangement of geophones and loading plates of a road rater.

Equation 1 is derived as follows. The weight (W) vibrates sinusoidally in the vertical direction at a frequency f. Displacement at any time t can be expressed in terms of the angular velocity ($\omega = 2\pi f$), as follows:

$$\chi = \chi_o \cdot \sin \omega t \quad (2)$$

where

χ = displacement at time t and
χ_o = peak displacement.

The acceleration of motion can be obtained from

$$\ddot{\chi} = -\chi_o \omega^2 \sin \omega t \quad (3)$$

The maximum values of displacement and acceleration occur when the sine function equals unity. Thus,

$$\chi_{max} = \pm \chi_o \quad (4)$$

and

$$\ddot{\chi}_{max} = \pm \chi_o \omega^2 \quad (5)$$

The peak force is induced by the maximum acceleration, which equals

$$F_{peak} = m\ddot{\chi}_{max} = m(\pm \chi_o \omega^2) \quad (6)$$

Substituting $m = (W/g)$, $\chi_o = (D/2)$, and $\omega = 2\pi f$ into Equation 6 yields

$$F_{peak} = \pm 0.0511\,Wf^2D \quad (7)$$

where D is the peak-to-peak displacement that can be measured directly from the road rater.

The road rater used in Pennsylvania is a model 400, which has a vibrating weight of 72 kg (160 lb). The device is commonly operated at a frequency of 25 Hz, but other frequencies used have ranged between 10 and 40 Hz. The peak-to-peak displacement for the model 400 road rater is 1.803 mm (0.071 in). In these conditions, peak force is 1615 N (362.8 lbf), and the contact pressure under each plate is 89.6 kPa (13 lbf/in^2). During testing, the loading plates are subjected to a downward static force. A static force of 6672 N (1500 lbf) is used for the road rater and the van. Because only the difference in pavement response to maximum and minimum downward forces is monitored, the magnitude of the static force has no direct influence on monitored pavement response. Thus, the pavement response under the road rater loading can be analyzed by using the peak force alone.

In this analysis, the 10.2- by 17.8-cm (4- by 7-in) loading plates were approximated by two circular areas spaced 26.7 cm (10.5 in) apart center to center; each has a 7.6-cm (3-in) radius. The contact pressure for a frequency of 25 Hz is 89.6 kPa (13 lbf/in^2). In these conditions, surface deflections at four geophones can be determined, and surface curvature index (SCI) and base curvature index (BCI) can be computed. SCI is defined as the difference between the first and second geophone readings and BCI as the difference between the third and fourth geophone readings (12).

The deflection profiles of pavement systems were analyzed for the loading conditions described above by using the BISAR (bitumen structures analysis in roads) computer program. The pavement systems analyzed were composed of an elastic layer that had a finite thickness overlaying the elastic half space. Results of the analysis are shown in Figures 2 and 3. Figure 2 indicates that the ratio of SCI to maximum surface deflection

(δ_{max}) increases as the moduli ratio of lower to upper portions of the pavement structure (E_2/E_1) increases; the slope of the curves decreases slightly as the E_2/E_1 ratio increases. Figure 3 shows that the BCI/SCI ratio decreases as the E_2/E_1 ratio increases. Both figures imply that, when the upper portion of a pavement structure undergoes deterioration faster than the lower portion, the SCI/δ_{max} ratio will increase and the BCI/SCI ratio will decrease. Therefore, the deflection profile determined from road rater measurements can be used to evaluate the relative strength between the upper and lower portions of a pavement structure.

EXPERIMENTAL PAVEMENTS AND FIELD TESTING

Field studies of road rater deflections were conducted at the Pennsylvania Transportation Research Facility. This accelerated live testing facility—a 1.6-km (1-mile), one-lane highway constructed in August 1972—is composed of sections of various lengths and thicknesses and different types of base materials (Figure 4). Four different base course materials were used: bituminous concrete, aggregate cement, aggregate-lime-pozzolan, and aggregate bituminous base. The subbase material was a crushed limestone natural to central Pennsylvania. The subgrade soil had classifications that ranged from A-4 to A-7 but was predominantly A-7. The wearing surface for the entire facility was constructed of one type of material. This paper deals only with the pavements that contain bituminous concrete base.

By the end of December 1974, the pavement sections constructed during the first cycle of research had been subjected to about 1 million applications of equivalent 80-kN (18 000-lb) axle loads (EAL_{18}). By the end of May 1977, a total of about 1.5 and 0.5 million axle loads respectively had been applied to pavement sections constructed during the first research cycle and pavement sections constructed during the second cycle. Traffic loading was provided by a conventional truck tractor that pulled a semitrailer and a full trailer. Complete information on design, construction, material properties, and traffic operation has been given in several research reports (13, 14).

Field performance measurements of the test pavements were conducted periodically; these included measurements of surface deflection (by use of the Benkelman beam and the road rater), rut depth, surface roughness, and surface cracking. In addition, data on subgrade moisture, pavement temperature, and meteorological conditions were collected regularly. Table 1 gives the results of the crack survey for the pavement sections that contain bituminous concrete base. A complete record of the field data accumulated so far is available elsewhere (15).

Material Properties

The modulus of elasticity of each constituent pavement material was determined by using repeated-load laboratory tests on laboratory-compacted test specimens. The specimens were 15.2 cm (6 in) in diameter and 25.4 cm (10 in) high. The repeated loading had a frequency of 20 cycles/min and a duration of 0.1 s. For the range of confining pressures and deviator stresses that occurred under loading by the test vehicle, the resilient modulus of the crushed limestone subbase material was 331 MPa (48 000 lbf/in^2). At 23 percent water content, the subgrade modulus was about 55 MPa (8000 lbf/in^2). Modulus values of surface and base materials for various temperatures are given elsewhere (14).

Fatigue properties of the surface and base course materials were determined by conducting fatigue tests on laboratory-compacted beam specimens. The repeated loading had the same frequency and duration as that used in the testing of the resilient modulus. These test results are given by Root (17).

Data on the change of moduli values with number of axle load applications were required to determine the variation in pavement response during pavement service life. For this purpose, regression analyses were performed for the Benkelman beam deflection data for the

Table 1. Results of crack survey.

Section	Layer Thickness (cm)			Number of Equivalent 80-kN Axle Loads at First Appearance of Significant Cracking (000 000s)
	Surface	Base	Subbase	
1B	3.8	15.2	35.6	-
1C	3.8	15.2	20.3	1.37
1D	3.8	15.2	15.2	1.32
2	6.4	15.2	20.3	-
6	6.4	20.3	20.3	-
7	3.8	20.3	20.3	-
8	3.8	10.2	20.3	0.386
9	6.4	10.2	20.3	1.052
14	3.8	20.3	0	0.906
H	3.8	12.7	0	0.359

Note: 1 cm = 0.39 in; 1 kN = 224.8 lb.

Figure 2. SCI/δ_{max} versus E_2/E_1.

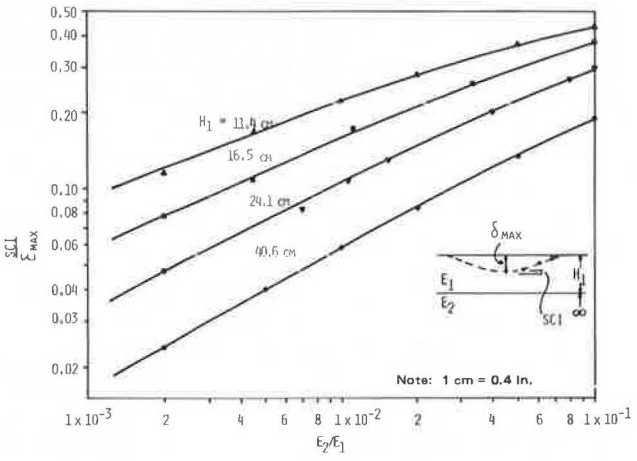

Figure 3. BCI/SCI versus E_2/E_1.

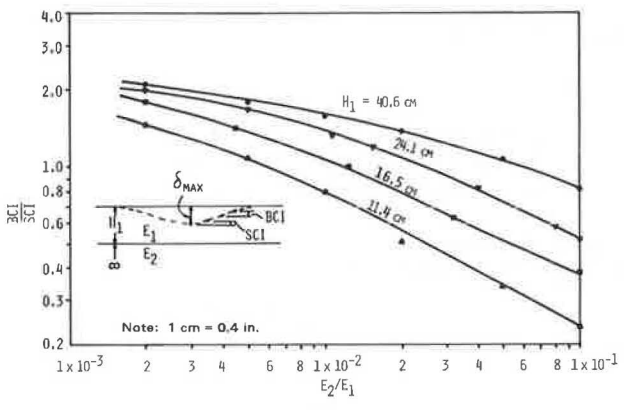

Figure 4. Plan view and longitudinal profile of test track.

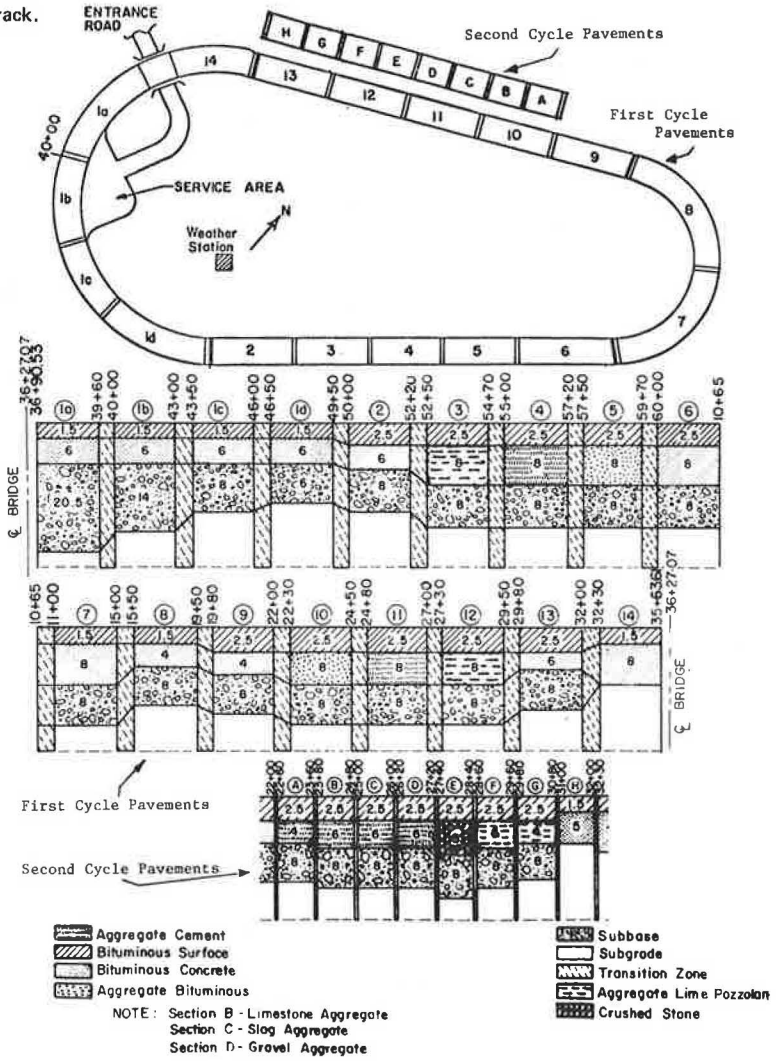

sections that contained bituminous concrete base. Results of the regression analyses give deflection equations for these pavement sections.

Benkelman beam spring season deflection equations for the bituminous concrete base sections at the Pennsylvania Transportation Research Facility are as follows (because the values are derived in U.S. customary units of measurement, no SI units are given): For bituminous concrete base sections 1C, 2, 6, 7, 8, 9, and 13,

$$\delta \times 10^3 = 86.632 - 15.898H_1 - 89.739(\log H_2) + 18.219H_1(\log H_2) - 2.460H_1(\log H_2)(EAL)^2 + 7.818(EAL)^2 \quad (8)$$

For full-depth bituminous concrete sections 14 and H,

$$\delta \times 10^3 = 20.145 - 0.650H_2 - 15.989H_2\sqrt{EAL} + 144.580\sqrt{EAL} \quad (9)$$

where

δ = Benkelman beam deflection (in 0.001 in);
H_1 = surface layer thickness (in);
H_2 = base layer thickness (in); and
EAL = 18 000-lb equivalent axle loads.

Note that the original deflection model contains several other influential factors. These equations are reduced from the original model to spring temperature and moisture conditions. A pavement temperature of 15.6°C (60°F) and a subgrade moisture of 23 percent were used because these are the most critical conditions that affect pavement performance. These equations permit the calculation of spring season deflections at any time during the service life of the experimental pavements.

The field data for subgrade moisture indicate that the subgrade moisture content reached a maximum of approximately 23 percent for all test sections. Thus, it would be conservative to assume that the subgrade modulus in the spring season remains constant throughout the entire service life of the experimental sections. Subbase modulus is also assumed to be independent of the number of axle load applications. It is generally recognized that, during the early stages of pavement service life, a pavement will undergo some degree of compaction that will cause a slight increase in the modulus. But results of field plate load tests conducted during the construction of the research facility and after termination of traffic at the end of the first cycle of study did not give a clear indication of this effect.

Based on the computed spring season deflections and the preceding assumptions, the modulus of elasticity of the combined surface and base layer at any number of axle load applications was determined by using the BISAR computer program. The moduli values needed for the analysis of pavement response to road rater loading were determined in the following way. First, road

rater deflections were taken at the top of each constituent layer during construction. The deflection values were then corrected to correspond with spring season conditions by using the PennDOT method of correction (16). Based on these corrected deflections, the modulus of elasticity of each layer was computed by using the BISAR computer program. The change in modulus of elasticity with number of axle load applications was determined by using these initial moduli values in conjunction with the variation in modulus of elasticity for the Benkelman beam deflections already determined. It was assumed that the ratio of modulus of elasticity for Benkelman beam loading to modulus for road rater loading remains constant for each constituent layer. The initial values for modulus of elasticity for road rater loading and Benkelman beam loading for each pavement section analyzed are given below (1 MPa = 145 lbf/in²):

Layer	Benkelman Beam	Road Rater
Combined surface and base by section		
1B	7 586	11 034
1C	6 896	9 655
1D	6 896	10 345
2	8 276	11 724
6	13 793	16 552
7	13 793	17 241
8	7 586	8 965
9	6 896	10 345
14	8 276	8 965
H	12 414	13 793
Subbase	331	379
Subgrade	55	69

Response

The response of the test pavements was analyzed for both traffic and road rater loadings by using the BISAR computer program and the material properties obtained above. In the analysis, the surface and base courses were combined into a single layer, and only spring weather conditions were considered. The traffic loading used was an 80-kN (18 000-lb) dual-wheel axle load and a tire pressure of 55 kPa (80 lbf/in²).

The critical responses analyzed were maximum tensile strain in the surface and base layers, maximum vertical compressive strain in the subgrade, and maximum surface deflection. These critical responses were considered because maximum tensile strain and maximum surface deflection have been associated with fatigue cracking whereas maximum vertical compressive strain has been related to rutting.

Results of the analysis give relations between the pavement response measured by means of a Benkelman beam and that measured by means of a model 400 road rater operated at 25-Hz frequency. For pavements that contain bituminous concrete base, the ratio of Benkelman beam deflection to road rater maximum deflection is proximately 14.5. The maximum tensile and maximum compressive strains under 80-kN (18 000-lb) axle loads are both about 12.5 times those that occur under road rater loading. These two strain relations are useful for evaluating pavement behavior when a road rater is used.

The relation between maximum tensile strain (ϵ_t) under road rater loading and SCI is shown in Figure 5. This relation indicates that maximum tensile strain is directly proportional to SCI. Figure 6 shows the relation between maximum surface deflection (δ_{max}) and the ratio of BCI to the product of maximum surface deflection and maximum vertical compressive strain at the top of the subgrade (ϵ_c), i.e., BCI/($\delta_{max}\epsilon_c$). Based on Figures 5 and 6,

Figure 5. Road rater maximum tensile strain as a function of surface curvature index.

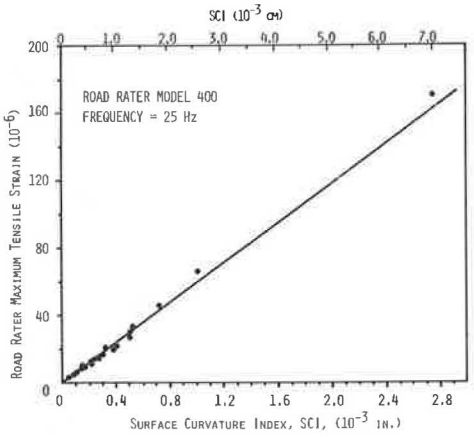

Figure 6. Relation between BCI/$\delta_{max}\epsilon_c$ and δ_{max}.

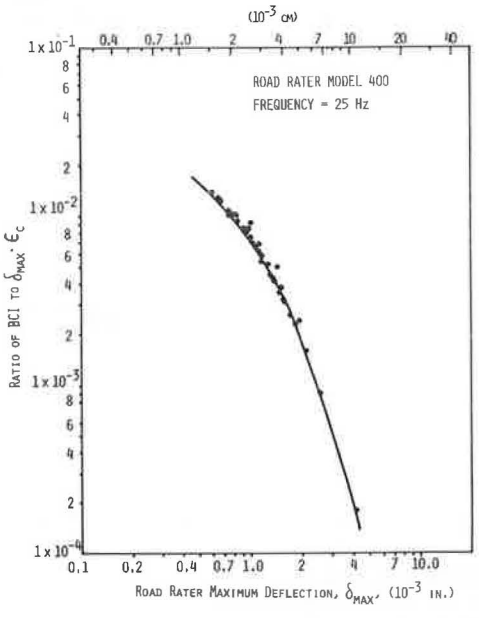

$$\epsilon_t = 59.0(SCI) \quad (10)$$

and

$$\log \epsilon_c = 2.1 + \log(BCI) + (0.6 + 1.7 \log \delta_{max}) \log \delta_{max} \quad (11)$$

where δ_{max}, SCI, and BCI are in 0.0025 cm (0.001 in) and ϵ_t and ϵ_c are in micrometers per millimeter.

The results of the analysis indicate that SCI can be related to maximum tensile strain in the base course whereas BCI is strongly related to maximum compressive strain at the top of the subgrade. By using Equations 10 and 11, it is possible to calculate maximum tensile strain in the base course and maximum compressive strain at the top of the subgrade under road rater loading from the profile of measured surface deflection. Then maximum tensile and compressive strains under 80-kN (18 000-lb) axle loads can be estimated. These two maximum strains are important factors in the evaluation of pavement performance.

Figure 7. Variation of maximum tensile strain under road rater loading with number of equivalent 80-kN (18 000-lb) axle loads.

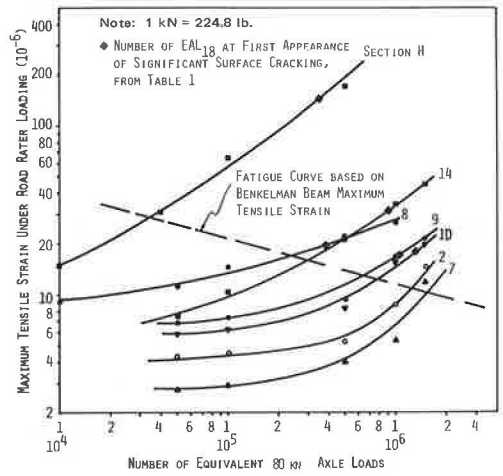

Figure 8. Number of equivalent 80-kN (18 000-lb) axle loads required for crack to propagate through base and surface layers.

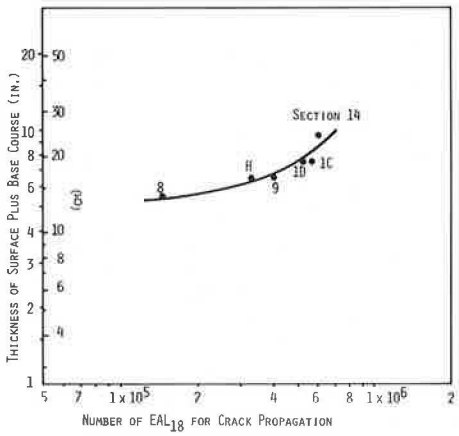

CRITERIA FOR EVALUATION OF PAVEMENT PERFORMANCE

Evaluation criteria are developed by plotting maximum tensile strain in the base course under road rater loading against the number of 80-kN (18 000-lb) axle load applications for pavement sections that contain bituminous concrete base (Figure 7). Note that the data for tensile strain were analyzed based on deflections in the spring season. Figure 7 indicates that maximum tensile strain increases with an increase in the number of 80-kN axle load applications. At any tensile strain, the number of repetitions of 80-kN axle loads required to cause fatigue failure can be determined by first converting the road rater strains to Benkelman beam strains and then substituting the Benkelman beam strain values into the fatigue equation. As the maximum tensile strain increases with traffic, the number of load applications required to cause fatigue failure will decrease as shown in Figure 7.

Figure 7 also shows the number of 80-kN (18 000-lb) axle loads at the first appearance of significant surface cracking (taken from Table 1). The difference in the number of axle loads between the appearance of cracking and the initiation of a crack at the bottom of the base layer is the number of axle loads required for the crack to propagate through the base and surface layers. As expected, the number of axle loads for crack propagation increases as the thickness of the surface plus the base layer increases (Figure 8).

The evaluation of pavement performance is usually based on maximum surface deflection. Many researchers, however, have found that maximum surface deflection alone is not sufficient to indicate pavement performance. For instance, Ford and Bissett (18) found that the ratio of the radius of the deflection basin to maximum surface deflection is a better criterion for evaluating pavement performance. Dehlen (5) found distinct relations between both maximum deflection and minimum radius of curvature and the condition of the pavement surface. Kung (19) concluded that the slope of a deflection basin is highly correlated with the condition of the pavement surface. Leger and Autret (20) proposed that the product of maximum deflection and minimum radius of curvature is a valuable indicator of pavement condition. All of these findings were the results of studies of pavements in specific environmental and traffic conditions. Precaution should be taken, therefore, in directly applying these findings to other environmental, structural, and traffic conditions.

These research findings were developed primarily for 80-kN (18 000-lb) axle loads. Few findings of this type are available for road rater loading. The rapidly increasing use of the road rater in pavement evaluation has created a heavy demand for research findings in this area.

The pavement response data analyzed here have been used to plot maximum surface deflection (i.e., deflection at road rater sensor 1), SCI, the ratio of SCI to maximum deflection (SCI/δ_{max}), and several other possible combinations against number of 80-kN axle loads. In these graphs, the numbers of axle loads required to initiate cracking in the base courses were entered, and a line was drawn to connect these numbers. It was found that the ratio of SCI to maximum surface deflection gives a better relation between layer thickness and number of axle loads to fatigue failure. Figure 9 shows the variation of the SCI/δ_{max} ratio with axle load application for bituminous concrete sections. The figure shows that fatigue cracks are initiated in the base course of bituminous concrete sections when the ratio SCI/δ_{max} is in a range of 0.15 to 0.25.

According to this finding, there is a critical SCI to maximum surface deflection ratio. When that critical value is reached, cracks will start to develop at the

Figure 9. SCI/δ_{max} ratio under road rater loading versus equivalent 80-kN (18 000-lb) axle loads.

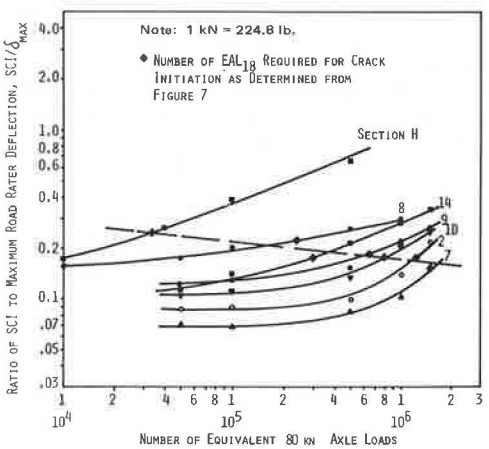

bottom of the base course and the base course will begin to lose its structural integrity. As a consequence, the rate of decrease in pavement serviceability will accelerate, and major repair of the pavement system may soon become necessary. Therefore, the critical value of the SCI to maximum deflection ratio could possibly be used as a criterion for determining the need for pavement overlay.

Note that, because the distance between sensors 1 and 2 is exactly 0.3 m (1 ft), the SCI value can be related to the minimum radius of curvature (R) of the deflection basin. Assume that the deflection curve between sensors 1 and 2 is circular, as shown in Figure 10. $R^2 = 1^2 + (R - SCI)^2$; $2R \cdot SCI = 1 + (SCI)^2$; $R = \frac{1}{2}[(1/SCI) + SCI]$. Because the units SCI and R are usually 0.0025 cm (0.001 in) and 0.3 m (1 ft) respectively, the following equation (empirically derived in U.S. customary units) results:

$$R = \tfrac{1}{2}\left(\{1/[SCI \times (10^{-3}/12)]\} + SCI \times (10^{-3}/12)\right) \quad (12)$$

or

$$R \cong (6 \times 10^3)/SCI \quad (13)$$

in feet. Thus, the ratio SCI/δ_{max} is essentially a measure of the reciprocal of the product of the radius of curvature and the maximum deflection, which is the factor proposed by Leger and Autret (20).

SUMMARY AND CONCLUSIONS

The road rater is a relatively new instrument for evaluating pavement performance. There is a need to predict the future performance of a pavement by using road rater deflections.

In this study, the BISAR computer program was used to analyze the response of experimental pavements to 80-kN (18 000-lb) axle loads and road rater loading. The experimental pavements contained four different types of base course material, but only pavements containing bituminous concrete base were analyzed. Equations were developed that interrelate various pavement responses and permit determinations of maximum tensile strain in the base course and maximum compressive strain at the top of the subgrade—strains attributable to 80-kN axle loads from the road rater deflection basin.

Based on a fatigue property determined in the laboratory, a permissible ratio of SCI to maximum deflection measured at road rater sensor 1 was determined for pavements that contain bituminous concrete base. This value may be used to evaluate pavements for rehabilitation purposes.

ACKNOWLEDGMENTS

The study presented here was conducted as part of a Pennsylvania Department of Transportation research project and a project sponsored by the Pennsylvania Department of Transportation in cooperation with the Federal Highway Administration. Their support is gratefully acknowledged. We wish to express our gratitude to the National Crushed Stone Association for loaning us the repeated-load test apparatus for laboratory testing and to the Asphalt Institute for its cooperation in conducting some of the fatigue tests. W. P. Kilareski, S. A. Kutz, B. A. Anani, and P. J. Kersavage assisted in collecting and reducing the field data.

Figure 10. Surface curvature index and minimum radius of curvature.

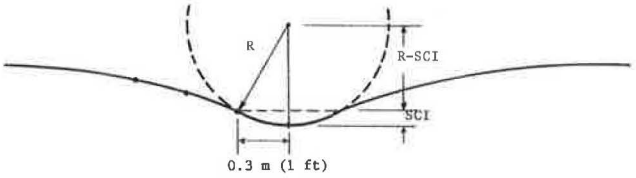

REFERENCES

1. The WASHO Road Test: Part 2—Test Data, Analyses, and Findings. HRB, Special Rept. 22, 1955.
2. Proc., 41st Convention of the Canadian Good Roads Association, 1960.
3. E. Zube and R. Forsyth. Flexible Pavement Maintenance Requirements as Determined by Deflection Measurements. HRB, Highway Research Record 129, 1966, pp. 60-79.
4. E. Prandi. The Lacroix-L.C.P.C. Deflectograph. Proc., 2nd International Conference on Structural Design of Asphalt Pavements, 1967, pp. 1059-1068.
5. G. L. Dehlen. Flexure of a Road Surfacing, Its Relation to Fatigue Cracking, and Factors Determining Its Severity. HRB, Bulletin 321, 1962, pp. 26-39.
6. R. R. James. Recoverable Deformation in a Flexible Pavement. Univ. of Auckland, ME thesis, 1970.
7. Owners Manual on Operation and Maintenance Instructions for Model RR-400 Road Rater. Foundation Mechanics, Inc., 1971, 25 pp.
8. F. H. Scrivner, G. Swift, and W. M. Moore. A New Research Tool for Measuring Pavement Deflection. HRB, Highway Research Record 129, 1966, pp. 1-11.
9. Pavement Evaluation. National Roads Board, New Zealand State Highways, RRU Bulletin 21, 1974.
10. M. C. Wang and T. D. Larson. Performance Evaluation for Bituminous-Concrete Pavements at the Pennsylvania State Test Track. TRB, Transportation Research Record 632, 1977, pp. 21-27.
11. A. C. Bhajandas, G. Cumberledge, and G. L. Hoffman. Flexible Pavement Evaluation and Rehabilitation. Transportation Engineering Journal, ASCE, Vol. 13, No. TE1, Jan. 1977, pp. 75-102.
12. G. Peterson and L. W. Shepherd. Deflection Analysis of Flexible Pavements. Utah State Department of Highways, Final Rept., Jan. 1972.
13. E. S. Lindow, W. P. Kilareski, G. Q. Bass, and T. D. Larson. Construction, Instrumentation, and Operation. Pennsylvania Transportation Institute, Pennsylvania State Univ., University Park, Interim Rept. PTI 7505, Vol. 2, 1973.
14. W. P. Kilareski, S. A. Kutz, and G. Cumberledge. Modification Construction and Instrumentation of an Experimental Highway. Pennsylvania Transportation Institute, Pennsylvania State Univ., University Park, Interim Rept. PTI 7607, April 1976.
15. M. C. Wang, T. D. Larson, and W. P. Kilareski. Field Data Reduction—The Pennsylvania Transportation Research Facility. Pennsylvania Transportation Institute, Pennsylvania State Univ., University Park, Interim Rept. PTI 7715, July 1977.
16. G. Cumberledge, G. L. Hoffman, A. C. Bhajandas, and R. J. Cominsky. Moisture Variation in Highway Subgrades and the Associated Change in Surface Deflections. TRB, Transportation Research Record 497, 1974, pp. 40-49.
17. R. E. Root. Results of Laboratory Tests on Materials from the Pennsylvania State University Pavement Durability Test Track Facility. Asphalt Institute, College Park, MD, Cycle 1, Dec. 1973.
18. M. C. Ford and J. R. Bissett. Flexible Pavement Performance Studies in Arkansas. HRB, Bulletin 321, 1962, pp. 1-15.

19. K. Y. Kung. A New Method in Correlation Study of Pavement Deflection and Cracking. Proc., 2nd International Conference on Structural Design of Asphalt Pavements, 1967, pp. 1037-1046.
20. P. H. Leger and P. Autret. The Use of Deflection Measurements for the Structural Design and Supervision of Pavements. Proc., 3rd International Conference on Structural Design of Asphalt Pavements, 1972, pp. 1188-1205.

Publication of this paper sponsored by Committee on Pavement Condition Evaluation.

Evaluation of Concrete Pavements With Tied Shoulders or Widened Lanes

Bert E. Colley, Claire G. Ball, and Pichet Arriyavat, Portland Cement Association

Field and laboratory pavements were instrumented and load tested to evaluate the effect of widened lanes, concrete shoulders, and slab thickness on measured strains and deflections. Eight slabs were tested in the field and two in the laboratory. Pavement slabs were 203, 229, or 254 mm (8, 9, or 10 in) thick. Other major design variables included the width of lane widening, the presence or absence of dowels or of a concrete shoulder, joint spacing, and the type of shoulder joint construction. Generally, there was good agreement between measured strains and values calculated by using Westergaard's theoretical equations. Concrete shoulders were effective in reducing the magnitude of measured strains and deflections. A chart is presented to show the allowable reduction in thickness of the outer lane of the main-line pavement when there is a tied concrete shoulder. Lane widening of about 406 mm (16 in) was as structurally effective as a concrete shoulder in reducing edge strains and deflections. However, it should be remembered that a concrete shoulder provides the added advantage of draining runoff farther from the pavement edge. Because of the possibility of load encroachments on a widened lane, it is recommended that lanes be widened by a minimum of 0.46 m (1.5 ft) plus any additional width required to avoid encroachment. Under the conditions considered, tied-butt, tied and keyed, and keyed-joint constructions were equally effective in reducing load-induced pavement strains and deflections.

Existing pavements represent a major investment of highway funds. A road can seldom be abandoned or replaced. Every year many kilometers of pavements require rehabilitation to cope with increased traffic. Overlays are built for the purpose of restoring pavement serviceability and improving structural capacity, but this practice is expensive and alternative solutions are needed.

One alternative to resurfacing is the use of a widened lane or a paved concrete shoulder. This type of construction could be used not only to strengthen existing pavements but also to strengthen new pavements and thus defer rehabilitation. Another approach for the design of new pavements that include a tied concrete shoulder would be to reduce the thickness of the outer lane of the main-line pavement.

In addition to strengthening a pavement, concrete shoulders and lane widening provide a benefit not obtained by resurfacing in that runoff water is drained farther away from the wheel paths of traffic. A recent study for the Federal Highway Administration (1) determined that accumulation of water in the joint between an asphalt shoulder and a concrete pavement was a major factor in reducing pavement performance. Because of this problem, several states have installed costly longitudinal and transverse drainage systems. Thus, concrete shoulders and widened lanes have the potential for curing many drainage problems as well as providing additional slab strength.

Many design features contribute to pavement life. The effect of some of these features can be evaluated analytically. For example, analytical tools can be used to determine the effect of pavement thickness or subbase strength on pavement life. Thus, when analytical procedures are available, the engineer can combine a knowledge of pavement life with data on construction and maintenance cost to provide the most economical design.

Analytical tools often are unavailable or require the use of unknown or unverified coefficients. For example, tied shoulders reduce load deflections and stresses, but the amount of the reduction is a function of the unknown continuity across the joint between the pavement edge and the shoulder. In these cases, the most direct method of evaluating design features is a planned series of field data measurements extended by laboratory tests and analytical procedures. This paper reports on a project that incorporated these features. The principal objective of the project was to determine the effect of widened lanes, tied concrete shoulders, and slab thickness on measured strains and deflections. Field and laboratory pavements were instrumented, and measurements of load strains and deflections were obtained. The measured data were then analyzed to determine the effects of the variables on pavement life.

PAVEMENT TEST SECTIONS

Field measurements were obtained on four experimental pavement projects located in the state of Minnesota. All fieldwork was done under a contract between the Minnesota Department of Transportation and the Portland Cement Association (PCA).

Project 1 is a roadway 8.23 m (27 ft) wide that consists of a 4.57-m (15-ft) wide inside lane, a 3.66-m (12-ft) wide outside lane, and a 3.05-m (10-ft) wide outside tied and keyed concrete shoulder. Shoulders are tied at 762-mm (30-in) spacing by no. 5 tie bars 762 mm

long. Shoulder thickness is 152 mm (6 in). The pavement is composed of plain concrete slabs 229 mm (9 in) thick that have skewed joints at a repeated random spacing of 3.96, 4.88, 4.27, and 5.79 m (13, 16, 14, and 19 ft). Dowel bars were placed only in the 3.66-m outside traffic lane. Dowels are no. 8 round bars spaced at 305 mm (12 in) on centers; the first dowel is located 152 mm (6 in) in from the pavement edge. Panels selected for testing were located at stations 539+16 and 540+10.

Project 2 is a roadway 8.23 m (27 ft) wide with a 3.05-m (10-ft) wide outside tied and keyed concrete shoulder. Dowel size and location are the same as for project 1. The pavement thickness is 203 mm (8 in). Panels selected for testing were located at stations 519+80 and 521+81.

Project 3 is a roadway 8.23 m (27 ft) wide with a 4.57-m (15-ft) wide inside lane and a 3.66-m (12-ft) wide outside lane. The pavement is composed of reinforced concrete slabs 229 mm (9 in) thick that have skewed joints at a spacing of 8.23 m. Dowel bars were placed only in the 3.66-m portion of main-line pavement in both traffic lanes. The dowels are no. 8 round bars spaced 305 mm (12 in) on centers. Panels selected for testing were located at stations 985+53 and 987+11.

Project 4 is a roadway 7.62 m (25 ft) wide with a 3.66-m (12-ft) wide inside lane and a 3.96-m (13-ft) wide outside lane. The pavement is composed of plain concrete slabs 203 mm (8 in) thick that have skewed joints at a repeated random spacing of 3.96, 4.88, 4.27, and 5.79 m (13, 16, 14, and 19 ft). Dowel bars were placed only in the inner 3.66 m of the 3.96-m outside traffic lane. The dowels are no. 8 round bars spaced 305 mm (12 in) on centers. Panels selected for testing were located at stations 870+64 and 872+21.

Projects 1, 2, and 3 are located on TH-90 between Albert Lea and Fairmont, Minnesota. Project 4 is located on TH-14 near Rochester, Minnesota. None of the projects had been opened to traffic before testing.

Two test sites were selected on each project for instrumentation and data recording. Sites were located within 60.96 m (200 ft) of each other to facilitate load testing and data acquisition. Care was taken to ensure that the sites selected were representative of the project and were similar in joint opening. The field test pavements were 203 or 229 mm (8 or 9 in) thick and either had or did not have a tied and keyed concrete shoulder 152 mm (6 in) thick.

Supplementary data were obtained from two pavement slabs constructed and tested at the PCA laboratories. These slabs included tied and keyed, keyed, and tied-butt shoulder joints. The laboratory slabs were 254 mm (10 in) thick and had shoulders that were also 254 mm thick. They were constructed indoors directly on a soft clay subgrade.

The indoor test area was equipped with thermostatically controlled heaters to provide a uniform temperature of 18°C (65°F). Overhead steel frames provided reaction for loading test specimens. The testing area was 30.48 m (100 ft) long and 7.32 m (24 ft) wide. The subgrade was a clay soil 1.52 m (5 ft) thick compacted to American Association of State Highway and Transportation Officials (AASHTO) standard density at 2 percent above optimum moisture. The k value of the subgrade (modulus of subgrade reaction), determined from tests of plates 762 mm (30 in) in diameter, was 758 kPa (110 lbf/in^2).

For the slabs constructed and tested in the laboratory, the tied and keyed and tied-butt shoulder joints were included in a slab that was 9.14 m (30 ft) long and 3.66 m (12 ft) wide. Shoulder width was 2.13 m (7 ft). To provide continuity at doweled transverse joints, sections of concrete 2.74 m (9 ft) in length were cast at each end of the slab. The untied and keyed construction was tested in a slab 4.57 m (15 ft) long that had one doweled and one undoweled transverse joint.

INSTRUMENTATION

All pavement test sections were instrumented to measure load-induced strains and deflections. In addition, field sections were instrumented to measure air and slab temperatures and slab curling (a change in the vertical profile of the slab that results from changes in slab temperature).

Type and Location

Figure 1 shows locations of strain and deflection instrumentation used on field pavement slabs that included both a widened lane and a tied concrete shoulder. Curl measurements were obtained at deflectometer locations, and temperatures were measured in instrumented test blocks. Test blocks were placed in the subbase adjacent to the pavement at least 12 h before load testing. Air temperatures were monitored by a thermocouple that was shaded from the direct sun. Details on types of instrumentation, methods of installation, and monitoring equipment used are given elsewhere (2).

Monitoring Equipment

Data were monitored by equipment housed in a mobile instrument van. The equipment consisted of 38 channels of heat stylus recorders, a 14-channel magnetic tape recorder, a 50-channel temperature recorder, a portable strain indicator, and a portable temperature recorder.

TEST PROCEDURES

Trucks used to apply load to field pavement slabs were supplied by the Minnesota Department of Transportation. The trucks were an 89-kN (20 000-lb) single-axle, a 151-kN (34 000-lb) tandem-axle, and a 187-kN (42 000-lb) tandem-axle. Before testing, axle weights were checked and loads were adjusted to obtain uniform distribution to the rear wheels. Prints of the contact area for each of the rear tire assemblies were obtained for use in data analysis. All pertinent dimensions of axle and wheel spacing were also obtained.

Effects of axle weight and load location on strains and deflections were recorded as the trucks moved at creep speed in the wheel paths shown in Figure 1. Wheel-path

Figure 1. Instrumentation on field pavement slabs with widened lanes and tied concrete shoulders.

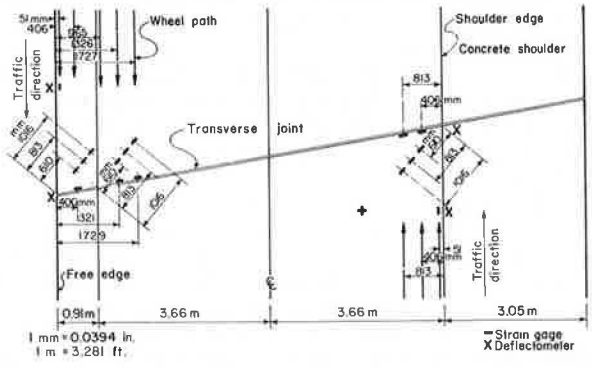

locations are shown as the distance from the pavement edge to the sidewall of the outside tire.

Instrumentation readouts for three loads operating in different wheel paths were obtained continuously during the day at each test site. Information for correcting data for the effects of temperature curling was obtained by hourly reading of selected instruments.

For indoor slabs, static loads were applied at edges, corners, and interiors. Loads were transmitted to slabs through a steel plate 406 mm (16 in) in diameter that rested on a rubber pad. Because slab temperature was kept constant, no correction for temperature was necessary.

RESULTS

Data for edge strain in slabs 229 mm (9 in) thick located at stations 539+16 and 540+10 are shown in Figure 2. Although strains were measured only on the top surface of the pavement, it is common engineering practice to assume a straight-line distribution of stress in a pavement slab. In this paper, therefore, bottom strains are assumed to be equal in magnitude and opposite in sign to measured top strains.

The close spacing of the data points for the two slabs shows that there was good agreement between strains obtained at the two test sites. As expected, edge strains decreased as the distance of the load from the edge was increased. In addition, based on data for the 51-mm (2-in) load position, strains measured at the shoulder edge were about 27 percent less than those measured at the free edge.

Figure 2. Edge strain at test stations 539+16 and 540+10.

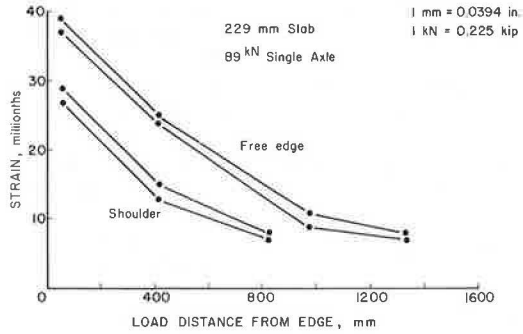

The effect of load and axle configuration on the magnitude of strain may be demonstrated by comparing free-edge strains at the 51-mm (2-in) load position for the three loads. These strains were 38, 30, and 36 millionths for the 89-, 151-, and 187-kN (20 000-, 34 000-, and 42 000-lb) loads respectively. Thus, strain decreased as load was changed from an 89-kN single-axle load to a 151-kN tandem-axle load but increased as the tandem-axle load was increased to 187 kN.

Tables 1 and 2 give a summary of the data for the effect of axle loads on strain for two slab thicknesses. The values reported were obtained by dividing the strain obtained for the selected axle load by the strain for the 89-kN (20 000-lb) single-axle load. Average ratios for all data were 1.0, 0.84, and 1.0 for the 89-, 151-, and 187-kN (20 000-, 34 000-, and 42 000-lb) axle loads respectively. These ratios are in good agreement with the values of 1.0, 0.80, and 0.99 obtained at the AASHO Road Test for slabs 229 mm (9 in) thick (4).

Maximum strains measured for an 89-kN (20 000-lb) single-axle load at corner, edge, interior, and transverse joint are shown in Figure 3. These data were obtained for slabs 203 mm (8 in) thick located at stations 519+80 and 521+81, but they are representative of trends measured at all test slabs that included paved shoulders. These trends were characterized by the fact that free-edge loading produced the largest measured strains. In general, free-edge strains were 36 to 50 percent greater than interior strains. In contrast, strains for cases of corner, tied shoulder, and transverse joint loadings were generally within 10 percent of strains measured at the interior load position.

Edge strains at test sites without shoulders were also

Figure 3. Maximum strains at test stations 519+80 and 521+81.

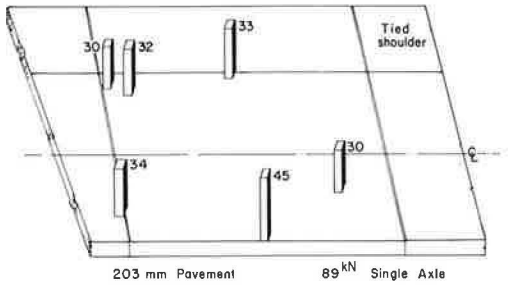

Table 1. Effect of axle load on strain in 203-mm (8-in) slab.

Load (kN)	Strain Ratio[a] Free Edge 519+80	Free Edge 521+81	Shoulder 519+80	Shoulder 521+81	Strain Ratio[a] Free Edge 870+64	Free Edge 872+21	Free Widened Edge 870+64	Free Widened Edge 872+21
89	1.00	1.00	1.00	1.00	1.00	1.00	1.00	1.00
151	0.86	0.87	0.88	0.85	0.79	0.83	0.82	0.84
187	1.05	1.00	1.06	1.06	1.00	1.00	1.11	1.05

Note: 1 kN = 225 lb.

[a] Obtained by dividing strain for the selected axle load by strain for the 89-kN (20 000-lb) axle load.

Table 2. Effect of axle load on strain in 229-mm (9-in) slab.

Load (kN)	Strain Ratio[a] Free Edge 539+16	Free Edge 540+10	Shoulder 539+16	Shoulder 540+10	Strain Ratio[a] Free Edge 985+53	Free Edge 987+11	Free Widened Edge 985+53	Free Widened Edge 987+11
89	1.00	1.00	1.00	1.00	1.00	1.00	1.00	1.00
151	0.79	0.78	0.72	0.70	0.90	0.92	0.87	0.88
187	0.95	0.95	0.83	0.89	1.03	1.00	0.97	0.98

Note: 1 kN = 225 lb.

[a] Obtained by dividing strain for the selected axle load by strain for the 89-kN (20 000-lb) axle load.

the maximum measured values. However, strains measured at the transverse joint and corner locations were sometimes greater than interior strains by 30 percent or more.

Measurements of edge strain shown in Figure 4 were taken from a laboratory-tested 254-mm (10-in) slab that had a 254-mm shoulder. Load strains obtained from the laboratory slabs were larger than those obtained from field slabs although the data followed the same trends. But indoor slabs were on a soft clay subgrade, and loads were applied at the edge rather than 51 mm (2 in) in from the edge. It will be shown later that there was good agreement between measured and theoretical edge strains for all slabs tested.

One significant difference between the data for indoor and field tests was the amount of reduction in edge strain that resulted from the addition of a shoulder. The indoor slab designs showed an average strain reduction of 37 percent compared with an average reduction of 28 percent for the outdoor designs. A theoretical analysis indicated that this difference is due to the use of a 254-mm (10-in) thick shoulder with indoor slabs rather than the 152-mm (6-in) thick shoulder with outdoor slabs.

To determine the benefit of dowels versus aggregate interlock, separate comparisons were made for test sites with and without shoulders. At field sites with shoulders, joint strains were reduced by an average of 4 percent when dowels were used. In the only laboratory comparison made to determine the benefit of dowels—the case of a slab with a shoulder—there was no reduction of strain at the doweled joint. For the one field site without shoulders, strains at joints with dowels were reduced by an average of 12 percent. These reductions are small, but it should be remembered that the pavements had not been opened to traffic. The value of dowels will increase as aggregate interlock is reduced by increased pavement age and traffic applications.

The effect of load placement on edge deflection is shown in Figure 5. As expected, edge deflections decreased rapidly as the load was moved inward from the pavement edge. In contrast to measured strains, however, deflections always increased as the total axle load increased. A summary of the effect of axle load on deflection for all edge measurements is given in Tables 3 and 4. Average deflection ratios for axle loads of 89, 151, and 187 kN (20 000, 34 000, and 42 000 lb) were 1.0, 1.15, and 1.45 respectively. At the AASHO Road Test (4), the ratios were 1.0, 1.42, and 1.75.

The larger deflections for tandem-axle loads measured at the AASHO Road Test may partially result from the times when the data were taken. Measurements were made both during the day and at night. In Minnesota, measurements were made only during the day. Upward curl is greater during the night and the early morning than it is during the day. In addition, the slab is unsupported over a greater distance inward from the pavement edge. Because the wheels of a tandem-axle vehicle are spread over a larger area than are those of an

Figure 4. Edge strain in laboratory test slab.

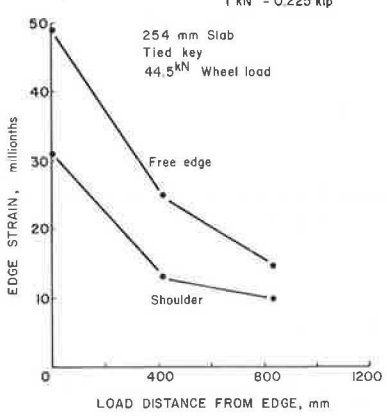

Figure 5. Edge deflection versus distance of load from the pavement edge.

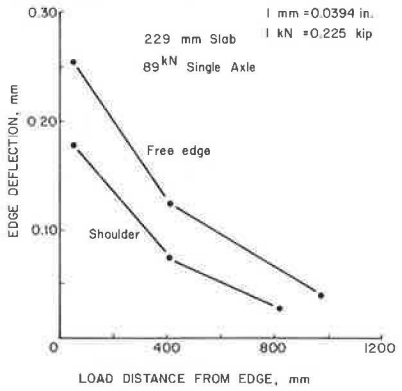

Table 3. Effect of axle load on deflection in 203-mm (8-in) slab.

Load (kN)	Deflection Ratio[a]				Deflection Ratio[a]			
	Free Edge		Shoulder		Free Edge		Free Widened Edge	
	519+80	521+81	519+80	521+81	870+64	872+21	870+64	872+21
89	1.00	1.00	1.00	1.00	1.00	1.00	1.00	1.00
151	1.17	1.14	1.13	1.10	1.27	1.00	1.08	1.15
187	1.58	1.36	1.38	1.30	1.45	1.50	1.58	1.46

Note: 1 kN = 225 lb.

[a] Obtained by dividing deflection for the selected axle load by deflection for the 89-kN (20 000-lb) axle load.

Table 4. Effect of axle load on deflection in 229-mm (9-in) slab.

Load (kN)	Deflection Ratio[a]				Deflection Ratio[a]			
	Free Edge		Shoulder		Free Edge		Free Widened Edge	
	539+16	540+10	539+16	540+10	985+53	987+11	985+53	987+11
89	1.00	1.00	1.00	1.00	1.00	1.00	1.00	1.00
151	1.25	1.15	1.14	1.23	1.10	1.33	1.11	0.91
187	1.46	1.54	1.43	1.49	1.50	1.56	1.56	1.09

Note: 1 kN = 225 lb.

[a] Obtained by dividing deflection for the selected axle load by deflection for the 89-kN (20 000-lb) axle load.

equivalent single-axle vehicle, the larger length of non-supported slab is deflected more by tandem axles.

The use of a tied and keyed shoulder reduced edge deflections by an average of 32 percent. This is a larger reduction than the 27 percent obtained based on strain measurements. However, it has been demonstrated that deflections are more influenced than strains by warping and curling. So it is possible that the presence of the shoulder reduced drying shrinkage and that this resulted in less warping. The smaller warping was more effective in reducing edge deflections than in reducing edge strains.

Measured deflections for corner loading were greater than those for edge loading. The larger corner deflections are due to the loss in continuity and the greater upward warping that occur at joints. Corner deflections were 226 percent larger than edge deflections.

ANALYSIS OF DATA

Comparison of Theoretical and Measured Data

Theoretical stresses and deflections were calculated by using influence charts (5). These charts, which are based on Westergaard's equations, permit the calculation of edge stresses and deflections caused by loads placed inward from the edge. Stresses were converted to strains by using a concrete modulus of elasticity of 34.5 GPa (5 million lbf/in^2). The k values used for computations were 33 and 109 MN/m^3 (120 and 400 lb/in^3) for the laboratory and field tests respectively. The value of 109 MN/m^3 used for field tests was estimated on the basis that the in-place subbase k was 41 MN/m^3 (150 lb/in^3). At the time of testing, however, there was a freezing index of 9, which is sufficient to freeze subsoils. Thus, a k value of 109 MN/m^3 was selected.

Comparisons of measured and theoretical values are given in Table 5. The data show generally good agreement between measured and theoretical values. Based on averages, measured strains were 4 percent greater than theoretical strains. However, measured deflections were on the average 12 percent larger than theoretical deflections. The larger variation for deflections is consistent with data previously presented. These data indicated that deflections are more influenced by warping than are strains.

The field data may be used to determine the effect of pavement thickness on measured strains and deflections. For example, increasing slab thickness from 203 to 229 mm (8 to 9 in) decreased edge strains by 16 percent and edge deflections by 21 percent. These values are used later for comparison with reductions in strain and deflection obtained when a shoulder was added to the pavement.

Concrete Shoulders

Strain and deflection measurements were obtained at free edges and shoulder edges. Based on these measurements, average percentage reductions in strain and deflection attributable to the presence of a shoulder were computed for slabs 203, 229, and 254 mm (8, 9, 10 in) thick. Strain reductions were 26.5, 29.0, and 37.0 percent respectively.

Good agreement has been shown between theoretical and measured strains and deflections. Therefore, influence charts were used to compute theoretical percentage reductions in strain or deflection as a result of increasing pavement thickness. These data were plotted, and then the graph was entered at the value of the measured reduction to determine the increase in slab thickness required to reduce strains by the same magnitude as that obtained by the construction of a tied concrete shoulder. The same type of analysis was made by using measured deflections. The results showed that, to obtain the reduction in deflection achieved by adding a shoulder, thickness would have to be increased by 66, 84, and 107 mm (2.6, 3.3, and 4.2 in) for the 203-, 229-, and 254-mm (8-, 9-, and 10-in) slabs respectively. To achieve equal reductions in strain, pavement thickness would have to be increased by 43, 56, and 86 mm (1.7, 2.2, and 3.4 in) for the 203-, 229-, and 254-mm slabs respectively.

The same data can be used to determine an allowable reduction in thickness in the outer traffic lane of a mainline pavement when a tied concrete shoulder is incorporated in the design. In Figure 6, the conventional or "as-built" pavement design thickness is plotted versus the effective thickness with a concrete shoulder. The

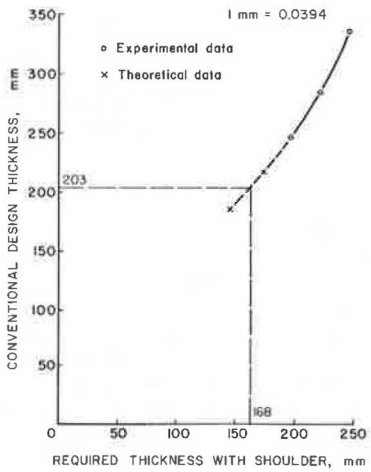

Figure 6. Reduction in outer lane thickness with addition of tied concrete shoulder.

Table 5. Comparison of theoretical and measured data for edge and interior strains and edge deflection.

Test Location	Thickness (mm)	Load (kN)	Strain: Edge (millionths) Measured	Strain: Edge (millionths) Theoretical	Strain: Interior (millionths) Measured	Strain: Interior (millionths) Theoretical	Edge Deflection (mm) Measured	Edge Deflection (mm) Theoretical
Field	203	89	45	45	30	29	0.31	0.27
		151	38	35	21	21	0.36	0.32
		187	46	45	26	26	0.47	0.43
	229	89	38	38	28	26	0.25	0.20
		151	33	30	21	19	0.28	0.25
		187	38	38	25	24	0.36	0.32
Laboratory	254	89	48	49	27	26	0.38	0.41

Note: 1 mm = 0.039 in; 1 kN = 225 lb.

solid, curved line that passes through the three experimental data points has been extended by extrapolation. The validity of the extrapolation is demonstrated by the close agreement between the extended portion of the curve and the two points computed by using Westergaard's equation for edge load.

On the chart, the curved line is entered on the abscissa of the determined conventional design thickness. In the example (Figure 6), the conventional design thickness has been assumed to be 203 mm (8 in). A horizontal line is drawn to intersect the curve and is then extended vertically downward to the ordinate. The value of 168 mm (6.6 in) obtained at the intercept is the pavement thickness of the outer lane that could be permitted if a tied concrete shoulder were used instead of a 203-mm-thick pavement without a shoulder.

Another method of evaluating the benefit of a concrete shoulder is to determine the added life expectancy of the pavement that is attributable to the reduction in edge stress. This is done by using the following equation developed at the AASHO Road Test (6):

$$\log W_{2.5} = 5.789 + 3.42 \log (S_c/\sigma) \quad (1)$$

where

$W_{2.5}$ = number of applications of stress σ,
S_c = 28-d flexural strength of the concrete, and
σ = predicted stress in the concrete caused by external loading.

The life expectancy of the pavement is increased because, at a reduced level of stress, the pavement can carry a greater number of traffic loads before reaching a level of terminal serviceability. Thus, if traffic remained constant with time, the life of the pavement would be extended.

Values of W were computed by substituting experimental data into the equation. The results show that the addition of a shoulder would extend the life of the 203-, 229-, and 254-mm (8-, 9-, and 10-in) pavements by factors of 3.2, 3.3, and 3.6 respectively.

Lane Widening

Experimental data were used to determine the effectiveness of lane widening in reducing pavement strains. An example of the procedure followed is shown in Figure 7. The data, which are the average of load strains measured at the free edge for test sites located at stations 539+16 and 540+10, show the decrease in measured edge strain as the load was moved inward from the edge. The dashed line represents the measured interior strain for the load being considered—a tensile strain that occurs at the bottom of the slab directly under the load.

By projecting downward from the intersection of the lines for interior and edge strain in Figure 7, it can be determined that an edge strain of 28 millionths was obtained when the load was 305 mm (12 in) in from the pavement edge. This means that, if the slab was widened by 305 mm, no further strain reduction could be obtained by additional widening. As the cross-hatching shows, the case of edge loading produced the largest strain until the load was 305 mm from the edge, and after that the strain directly under the load was larger. Results from a similar analysis for each of the test sites are given below (1 kN = 225 lb and 1 mm = 0.04 in):

Test Station	Load (kN)	Required Widening (mm)
985+53	89	305
987+11	151	356
	187	330
870+64	89	279
972+21	151	356
	187	330
539+16	89	305
540+10	151	305
	187	305
519+80	89	406
521+81	151	381
	187	559

With one exception, widening requirements varied from 279 to 406 mm (11 to 16 in).

Based on this analysis, it would appear that a lane widening of 406 mm (16 in) would be sufficient. This would be true, however, only if vehicles did not encroach on the widening.

To investigate the probability of encroachment, data from two studies of traffic distribution are shown in Figure 8. The data shown by the curve on the right were obtained by Taragin of the Federal Highway Administration in 1958 (7). These data, which are still used in pavement design, show that the highest frequency of travel and mean travel path distance occurred at slightly more than 0.61 m (2 ft) from the pavement edge. In addition, only about 4 percent of the traffic drove closer to the edge than 305 mm (12 in). The data for the curve on the left were obtained by Emery of the Georgia Department of Transportation in 1974 (8). In this case, 53 percent of the traffic traveled within 305 mm of the pavement edge. In addition, 9 percent of the traffic was observed to be driving in a 381-mm (15-in) wide wheel path that began 76 mm (3 in) inward from the pavement edge and extended outward to include 305 mm of the shoulder. Because these data were obtained from pavements that had asphalt shoulders, there was a highly visible delineation between pavement and shoulder. Therefore, it is

Figure 7. Effect of lane widening at test stations 539+16 and 540+10.

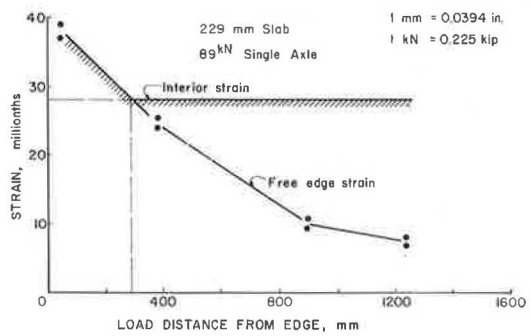

Figure 8. Traffic distribution: frequency versus wheel path.

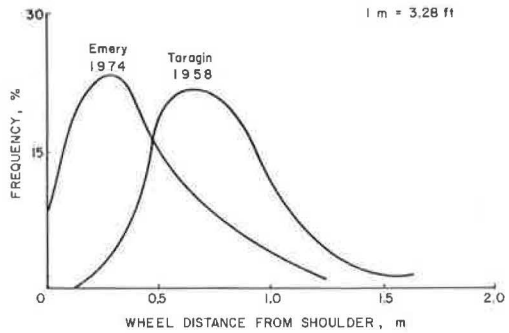

highly improbable that a painted white stripe located 406 mm (16 in) from the pavement edge will prevent encroachment. If pavement widening is to be structurally effective, determination of the minimum width should include consideration of the effects of load encroachments.

Shoulder Joint Design

Because all shoulder joints in the field projects used a tied and keyed design, laboratory slabs were constructed with keyed, tied and keyed, and tied-butt joints. Tie bars were 16 mm (0.7 in) in diameter and 965 mm (38 in) long and were spaced at 762-mm (30-in) centers.

Load strains and deflections were measured at the free edge and the shoulder edge for each design. These data were used to compute the percentage reduction in strain and deflection that occurred as a result of the presence of a shoulder. Figure 9 shows that edge strains and deflections were reduced by an average of 38 and 43 percent respectively. The small percentage difference in the performance of the three types of joints is not considered significant.

Although the keyed joint without tie bars was effective in reducing strains and deflections, its use would not be recommended in construction of outside lanes because of the possibility of shoulder joint separation. Such a separation might result from lateral traffic forces and differential vertical movements in the subgrade.

The excellent performance of the tied-butt joint suggests that this type of construction could reduce costs. Joints of this design, however, may lose some of their effectiveness under accumulated traffic loadings.

CONCLUSIONS

Pavement slabs were instrumented and load tested to determine the effects of concrete shoulders, widened lanes, and slab thickness on measured strains and deflections. The following results were obtained:

1. There was good agreement between measured strains and deflections and those computed by using Westergaard's theoretical equations.
2. The 152-mm (6-in) thick concrete shoulders of the 203- and 229-mm (8- and 9-in) thick highway slabs reduced edge strains by 28 percent.
3. Measured reductions in edge strain are used to demonstrate that the outer lane main-line pavement thickness may be reduced when a tied concrete shoulder is used. As an example, a conventional design of 203-mm (8-in) thickness could be reduced to 168 mm (6.6 in) with the addition of a tied concrete shoulder 152 mm (6 in) thick.

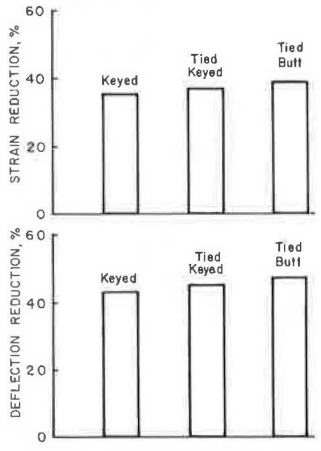

Figure 9. Percentage reductions in strain and deflection attributable to presence of a shoulder (by type of joint).

4. The effectiveness of concrete shoulders in reducing edge deflections was equivalent to increasing slab thickness by 66, 84, and 107 mm (2.6, 3.3, and 4.2 in) for the 203-, 229-, and 254-mm (8-, 9-, and 10-in) pavements respectively.
5. Lane widening was as effective as concrete shoulders in reducing strains and deflections.
6. A 254-mm (10-in) concrete shoulder was only slightly more effective in reducing edge strains and deflections than a 152-mm (6-in) shoulder.
7. Tied and keyed, tied-butt, and keyed joint construction were equally effective in reducing strains and deflections. However, it should be remembered that tied-butt joints might lose some effectiveness with accumulated traffic loadings.
8. In addition to reducing strains and deflections, tied concrete shoulders direct surface runoff away from the pavement edge.

ACKNOWLEDGMENTS

All fieldwork was conducted under a research contract with the Minnesota Department of Transportation. Minnesota Department of Transportation project supervision was provided by F. W. Thorstenson, director of materials, research, and standards; L. E. Warren, chief of concrete engineering; and R. M. Canner, Jr., research planning engineer. Field testing was coordinated by J. C. Hale, senior highway technician for the Minnesota Department of Transportation.

The project was conducted under the guidance of W. Gene Corley, director of engineering, Portland Cement Association. Special thanks are extended to PCA technicians Richard D. Ward and Fred Blaul for conducting the laboratory and field tests.

REFERENCES

1. P. J. Nussbaum and E. C. Lokken. Portland Cement Concrete Pavements—Performance, Design and Construction Practices. Federal Highway Administration, U.S. Department of Transportation, April 1977, 89 pp.; NTIS, Springfield, VA.
2. B. E. Colley, C. G. Ball, and P. Arriyavat. Evaluation of Concrete Pavements With Lane Widening, Tied Concrete Shoulders, and Thickened Pavement. Minnesota Department of Transportation, Sept. 1977.
3. H. J. Treybig, W. R. Hudson, and A. Abou-Ayyash. Application of Slab Analysis Methods to Rigid Pavement Problems. Center for Highway Research, Univ. of Texas at Austin, Research Rept. 56-26, May 1972.
4. AASHO Road Test Report 5—Pavement Research. HRB, Special Rept. 61E, 1962.
5. G. Pickett, M. E. Raville, W. C. Janes, and F. J. McCormick. Influence Charts for Concrete Pavements. Engineering Experiment Station, Manhattan, KA, Oct. 1951.
6. G. Langsner, T. S. Huff, and W. J. Liddle. Use of Road Test Findings by AASHO Design Committee. HRB, Special Rept. 73, 1962, pp. 399-414.
7. A. Taragin. Lateral Placement of Trucks on Two-Lane and Four-Lane Divided Highways. Public Roads, Vol. 30, No. 3, Aug. 1958.
8. D. K. Emery, Jr. Paved Shoulder Encroachment and Transverse Lane Displacement for Design Trucks on Rural Freeways. Preliminary report presented to Committee on Shoulder Design, TRB, Jan. 1974.

Publication of this paper sponsored by Committee on Shoulder Design.

Use of Freeway Shoulders to Increase Capacity

William R. McCasland, Texas Transportation Institute, Texas A&M University

The Texas State Department of Highways and Public Transportation approved for testing the concept of increasing roadway capacity on urban freeways by restriping the main-line pavement to create narrower lane widths and encroaching on the shoulder to create additional lanes for travel. Two sections of the US-59 Southwest Freeway in Houston were selected for study. The effectiveness of reconfiguring the main lanes was examined from the following aspects: operational characteristics of peak-period flow, driver acceptance of use of the shoulder lane, accident experience, benefit-cost analysis, and design and maintenance requirements. Expected improvements in operations during peak periods as a result of increased capacity were achieved. One section did not reach the anticipated level of improvement because of low driver use of the shoulder lane, and an analysis determined the need for a change in the length of that section. Accident experience was significantly reduced as a result of the modifications, and the benefit-cost analysis was extremely favorable to this type of low-cost improvement. The results of the study support the application of the use of shoulder and narrow freeway lanes for travel through bottleneck sections of urban freeways.

Travel demands on urban freeways continue to increase, and state highway departments are unable to build new facilities fast enough to prevent the development and spread of traffic congestion. Techniques that reduce or control travel demand—such as ramp control, priority operations for high-occupancy vehicles, and modal shifts—are being developed and implemented, but demand continues to increase. Low-cost, temporary measures to increase the capacity of urban freeway systems are needed.

Texas, like most states, has programs to identify and eliminate bottlenecks on urban freeways by widening bridges and pavements, relocating ramps, constructing continuous frontage roads, and eliminating geometric features that reduce capacity. These improvement programs will be accelerated as time and money permit, but the type of improvement discussed in this paper is designed to solve or alleviate capacity problems immediately and at low cost. California is conducting a similar program (1, 2, 3, 4), and a recent state-of-the-art report suggests using shoulders on freeways for travel (5). This project in Houston, one of the first to be undertaken by the Texas State Department of Highways and Public Transportation (SDHPT), has unique design and traffic requirements that contribute to knowledge about freeway operations and design.

STUDY SITE

The Southwest Freeway (US-59) in Houston is a radial freeway that varies in design from 6 to 10 lanes. At the interchange of the I-610 Freeway, average daily traffic (ADT) on both intersecting freeways exceeds 200 000 vehicles, and traffic demand immediately adjacent to the interchange exceeds the capacity for several hours of the day. Major reconstruction will be necessary to relieve the congestion, but temporary relief was provided to this section of US-59 in 1976 when the SDHPT designed and implemented a reconfigured cross section for the freeway to provide another lane for travel by narrowing the existing main lanes and encroaching on the emergency shoulder. The added lane was opened on May 1, 1976, and accommodated travel 24 h/d. Emergency parking areas are provided on both sides of the roadway except on bridge structures where the right shoulder has been totally preempted for travel.

The study site on the southbound lanes of US-59 is divided into the following two sections by the directional interchange with I-610 (Figure 1):

1. Section 1 (Weslayan to I-610)—The section is 1.9 km (1.2 miles) long with a cross section before restriping of 3.05 × 14.6 × 3.05 m (10 × 48 × 10 ft) made up of four 3.6-m (12-ft) concrete lanes and two 3.05-m (10-ft) asphalt concrete shoulders. The cross section was restriped to 3.05 × 16 × 1.7 m (10 × 52.5 × 5.5 ft) to make five 3.2-m (10.5-ft) lanes, a 3.05-m (10-ft) half median, and a 1.7-m (5.5-ft) right shoulder (Figure 2). The right shoulder was eliminated at the two bridges over the railroad and New Castle intersection.
2. Section 2 (I-610 to Westpark)—The section is 3.06 km (1.9 miles) long with a cross section before restriping of 3.05 × 14.6 × 3.05 m (10 × 48 × 10 ft) made up of four 3.6-m (12-ft) concrete lanes and two 3.05-m (10-ft) asphalt concrete lanes from I-610 to Chimney Rock. At Chimney Rock the cross section reduces to 3.05 × 10.97 × 3.05 m (10 × 36 × 10 ft) by dropping a lane and carrying three 3.6-m (12-ft) lanes from Chimney Rock to Westpark. The cross sections were restriped to 3.05 × 16 × 1.7 m (10 × 52.5 × 5.5 ft) and 3.05 × 12.8 × 1.2 m (10 × 42 × 4 ft) respectively (Figures 2 and 3) to create a 3.05-m (10-ft) half median, five 3.2-m (10.5-ft) lanes, and a 1.7-m (5.5-ft) right shoulder upstream of Chimney Rock and four 3.2-m (10.5-ft) lanes and a 1.2-m (4-ft) right shoulder downstream. The right shoulder was eliminated at the bridges over Rice Boulevard and Chimney Rock.

Emergency parking can be accommodated on the narrow right shoulder along sections 1 and 2 by encroaching on the turf area of the outer separation.

RESULTS

Operational Characteristics

Section 1

Section 1 is the last bottleneck upstream of the I-610 interchange. Traffic demand for this section comes from the four main lanes and two high-volume entrance ramps at the Edloe and Weslayan interchanges. The freeway lanes are congested upstream from the New Castle exit ramp for a distance of more than 3.2 km (2 miles), and ramp queues at Edloe and Weslayan often exceed 100 vehicles.

The capacity of the bottleneck is approximately 7600 vehicles/h, but peak-hour flow rates of 7800 vehicles/h were observed as the traffic occasionally encroached on the shoulder upstream of the New Castle exit ramp.

After the conversion from four to five lanes of travel, peak-hour volume through the bottleneck was unchanged, and the total number of vehicles in the 2-h peak increased by only 3 percent, as given below:

Condition	Peak Hour	2-h Peak
Before restriping	7870	14 180
After restriping	7830	14 600

Figure 1. Study sections 1 and 2 of southbound US-59, Southwest Freeway, in Houston.

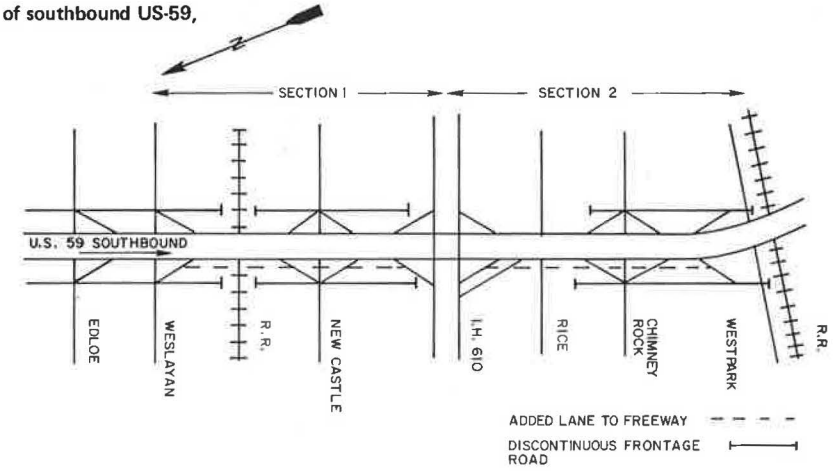

Figure 2. Reconfiguration of cross section from four to five lanes.

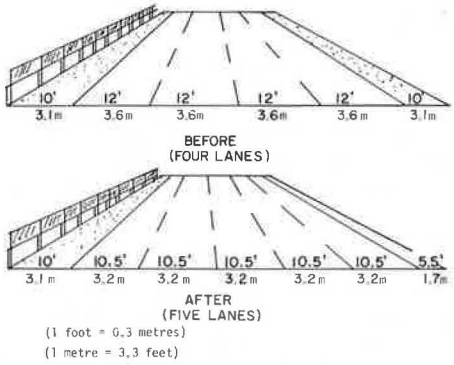

Figure 3. Reconfiguration of cross section from three to four lanes.

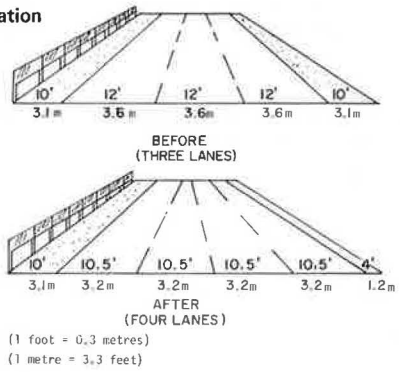

Lane use indicated that traffic did not use the added lane effectively enough to increase flow rates through the bottleneck section. The level of service was improved within the section, but total delay was not significantly reduced. The bottleneck was shifted approximately 100 m (330 ft) upstream of the merge point of the Weslayan entrance ramp.

Section 2

The Westpark overpass has a geometric design that would usually result in a bottleneck: horizontal and vertical curvature, no shoulders, and discontinuous frontage roads. But the volumes on upstream ramps have established the bottleneck section between the Chimney Rock entrance and the Westpark exit ramps. High traffic demand is maintained at this bottleneck by the high volumes that enter the section from the main lanes and the I-610 connection ramps upstream of the lane drop at Chimney Rock. Heavy congestion and queuing are maintained throughout the peak period.

The capacity of the bottleneck was 5800 vehicles/h, but peak-hour flows of 6000 vehicles/h were observed as the Westpark exiting traffic encroached on the shoulder.

In contrast to section 1, the addition of one lane for travel from the I-610 interchange had a significant impact on traffic volumes (Figure 4). The peak-hour volumes and throughput of the section increased, and the bottleneck shifted downstream to the Westpark overpass:

	Section 2 Bottleneck		
Item	Before Restriping	After Restriping	Increase (%)
Vehicles per peak hour	5 800	7 100	22.5
Vehicles per 2-h peak	11 600	13 800	19.0

	Section 2 Throughput		
Item	Before Restriping	After Restriping	Increase (%)
Vehicles per peak hour	7 250	8 400	15.9
Vehicles per 2-h peak	14 450	16 400	13.5
Vehicle kilometers per peak hour	16 130	19 430	20.4
Vehicle kilometers per 2-h peak	32 770	37 900	15.6

Some of the increase in vehicle kilometers is the result of the improvement in traffic flow through this section. Traffic that used the Chimney Rock exit and frontage road to bypass freeway congestion now remains on the freeway. This results in a reduction of traffic demand on the congested Chimney Rock-Frontage Road intersection.

The high flow rates and volumes through the Westpark overpass bottleneck (12 000 vehicles/h for 2 h) were not expected (Figure 5). However, several counts have confirmed these results, and the following factors are offered in explanation:

1. Truck volumes are very low (1.3 percent).
2. Volumes of small vehicles are high (20 percent).
3. Speeds of vehicles approaching and leaving the overpass are maintained at a high level throughout the peak period because of high-volume, high-speed exit ramps on both sides of the overpass.

Figure 4. Result of adding one lane to section 2: 1- and 2-h traffic volumes in p.m. peak period.

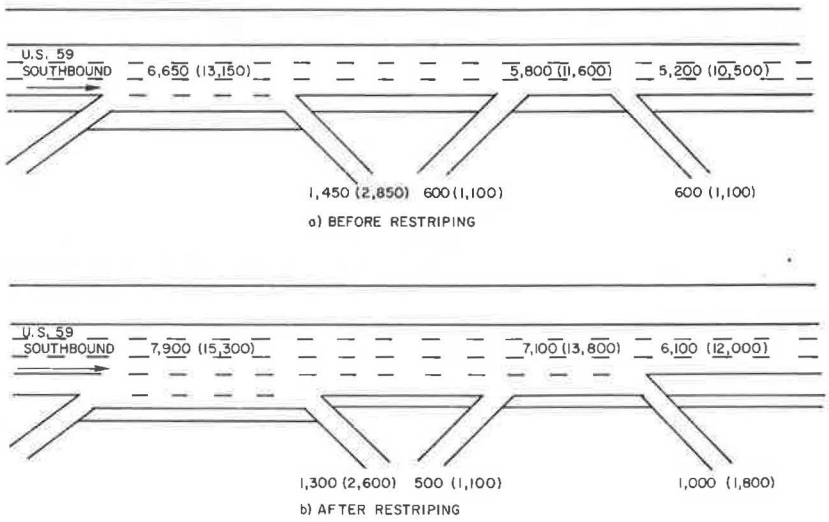

Figure 5. Traffic volume on US-59 southbound at Westpark in p.m. peak period.

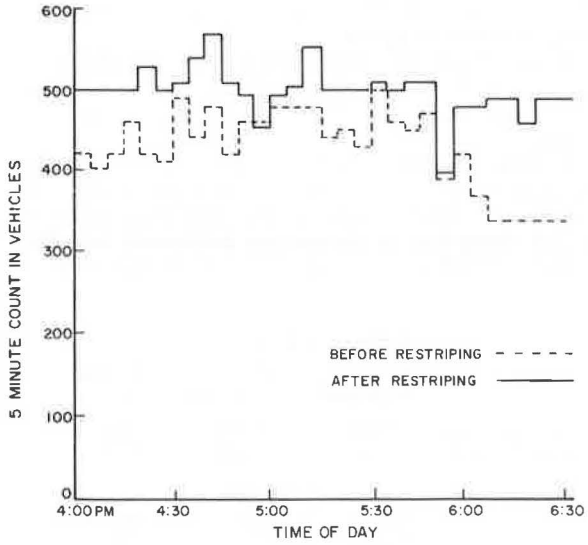

4. The traffic volume that uses the added lane upstream of the Westpark exit is high.
5. Demand for the three through lanes at the Westpark exit ramp is high throughout the peak period. Some vehicles merge into the through lanes from the added lane at or near the termination of the lane at the Westpark exit ramp.
6. Although the overpass has a 5 percent grade and is on a 3° horizontal curve, sight distance, lateral clearances, and design features are adequate for high-volume, high-speed operation.
7. Driving performance may be more efficient when vehicles enter a section of freeway that has lanes of standard width after traveling several minutes in a section that has narrow lanes.
8. The population of motorists who use this freeway could be classified as aggressive drivers who tend to overdrive traffic conditions. This results in better operational efficiency but also an accident rate higher than that of other freeways used by less aggressive motorists.

To determine the effects of added capacity on traffic delays, traffic demand for these sections over the 2-h period was assumed to be constant before and after restriping. The demand curve is represented by the input curve shown in Figure 6. The output curve is the sum of the volumes at the Westpark overpass and the Westpark and Chimney Rock exit ramps. The output curve before restriping indicates traffic congestion between 4:20 and 6:10 p.m. Output after restriping causes the length of the congestion period to be reduced by 20 min to 5:50 p.m. and the total amount of delay to be reduced by 1100 vehicle-h/d.

Although the demand curve was assumed to be unchanged to measure the effects on traffic delays, traffic volumes after 1 year of operation have actually increased. Peak-period demand increased by 14 percent whereas ADT increased by 8.7 percent. The increase in peak-period traffic is especially significant when it is compared with the 2 percent increase experienced the year before restriping. As a result of this increase in traffic volumes, the length of the congestion period has

Figure 6. Input-output flow rates for US-59 southbound between I-610 and Westpark overpass in p.m. peak period.

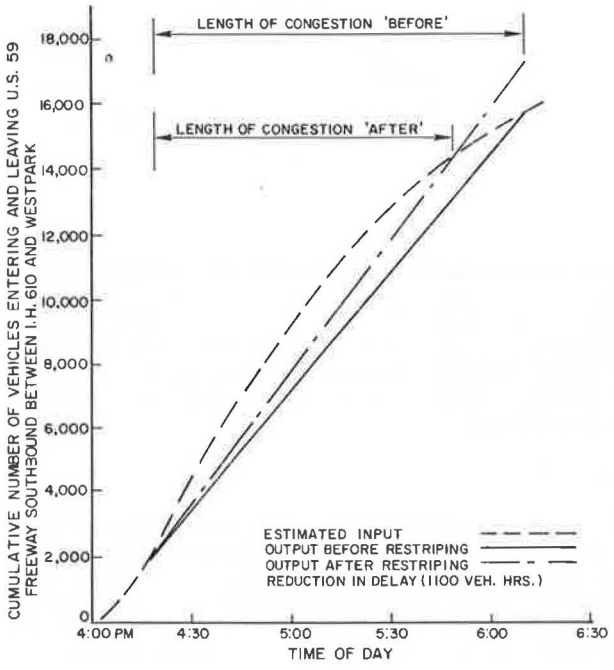

stayed the same or increased slightly, but the section accommodates 1950 more vehicles during the 2-h peak period.

The level of service has been improved, particularly for exit ramp traffic. However, traffic demand for the section has increased and still exceeds the capacity of the bottleneck, and congestion develops throughout the peak period.

Driver Acceptance of Use of Shoulder Lane

The key to a successful freeway reconfiguration is the use of the added lane. In this project, the lane was composed partly of the right shoulder and partly of the main-line pavement. Several factors against its use are (a) the texture and contrast of the two pavement materials, (b) the restrictive lateral clearance on the approaches to bridges, and (c) the condition of the riding surface. Factors in favor of its use are (a) the high percentage of local traffic, particularly during the peak periods; and (b) the high volumes of traffic throughout the day. To test the effectiveness of low-cost design, no major construction or maintenance activities were conducted to minimize the adverse factors during the first year of the project. If the concept proved to be successful, a more permanent design was to be implemented.

Section 1

The number of vehicles in 2-h and peak-hour traffic volumes for the various traffic movements shown in Figure 7 are given below:

Movement	Peak Hour	2-h Peak
$R_1 + R_2$	450	770
R_3	140	320
F_1	970	1700
L_1	470	710
L_2	640	1310

No special signing was used to designate the shoulder lane for travel. Lane arrows were used downstream of the Weslayan entrance ramp to encourage full use by entering traffic, but only 30 percent remained in the lane (see movement R_3 in Figure 7). The contrast between the concrete acceleration lane taper and the asphalt concrete shoulder appeared to guide the entering traffic out of the shoulder lane. Peak-period use by main-line traffic (F_1) was high, but the traffic entered the lane too late to improve upstream flow rates. This movement will be improved by extending the lane upstream to the next entrance ramp (Edloe), which will enable most of the 1700 vehicles that originate upstream of the Weslayan ramp and use the shoulder lane (movement F_1) to weave into that lane before they reach the bottleneck section.

The lane is available for 24 h, but it is used primarily during the peak period when all other lanes become congested. ADT in the lane is 8155 vehicles, approximately 25 percent of which uses the lane during the peak period (Figure 8).

Section 2

Use of the shoulder lane at the second study site was much greater. Although the lane was "black and white" pavement, the riding surface and the lateral clearances were better than those of section 1. The high exiting volumes at the Chimney Rock and Westpark exits account for much of the success of this lane. ADT is 13 445 vehicles, approximately 20 percent of which uses the lane during the peak period (Figure 8). The greater use in the off-peak period is a measure of the acceptability of the design in comparison to that of section 1.

Accident Experience

Total accident experience for sections 1 and 2 in the 2 years before restriping is compared below with accident experience for 1 year after restriping (1 km = 0.62 mile):

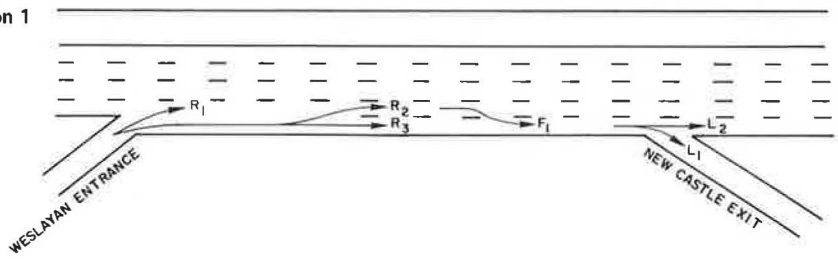

Figure 7. Peak-period use of shoulder lane: section 1 of Southwest Freeway.

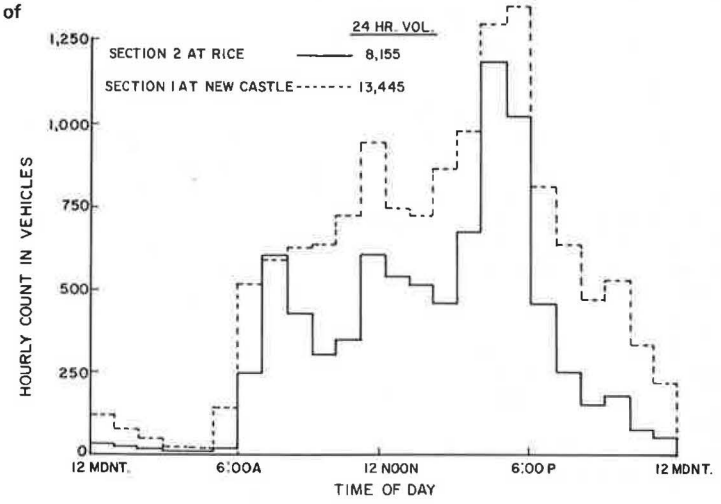

Figure 8. Use of shoulder lane over 24-h period: sections 1 and 2 of Southwest Freeway.

Item	1	2	Total
Accidents per year			
Number before restriping (2-year average)	128	205	333
Number after restriping (1-year average)	120	196	316
Percentage decrease	6	4	5
Accidents/100 million vehicle-km			
Number before restriping	207	229	220
Number after restriping	173	197	187
Percentage decrease	16	14	15

These accident frequencies and rates indicate that section 1 had the better accident experience for the 24-h period. After the shoulder lane was added, accident rates for both sections decreased significantly when they were tested at the 95 percent level of confidence for the Poisson comparison of means test (6) (figures for percentage decrease in accidents/100 million vehicle-km are significant at the 95 percent confidence level for the Poisson test).

Analysis of accident experience during the peak 2-h period when there is the greatest use of the added lane indicates much greater reductions in frequency and rate of accidents for the two sections (1 km = 0.62 mile):

Item	1	2	Total
Accidents per year			
Number before restriping (2-year average)	43	38	81
Number after restriping (1-year average)	22	33	55
Percentage decrease	49	13	32
Accidents/100 million vehicle-km			
Number before restriping	602	370	465
Number after restriping	279	292	287
Percentage decrease	54	21	38

The rate for section 1 and the combined rate for sections 1 and 2 are reduced significantly when they are tested at the 95 percent level of confidence for the Poisson comparison of means test (6) (figures for percentage decrease in accidents/100 million vehicle-km are significant at the 95 percent confidence level for the Poisson test). Although the accident rate for section 2 is reduced by 21 percent, it does not satisfy the test because of the low number of accidents before restriping (38).

The accident rate for section 2 was much lower than that for section 1 before restriping because section 2 had less congestion during the peak period 2 years ago. Travel demands and congestion have greatly increased in section 2 but have remained somewhat constant in section 1. In addition, the small number of accidents varies greatly from year to year.

Benefit-Cost Analysis

The benefits of restriping had not been realized in section 1 at the time this paper was written. It was estimated, however, that the extension of the lane to the Edloe entrance would result in a significant reduction in vehicle delay.

As a result of the added lane, section 2 achieved a 13.5 percent increase in the number of vehicles that exit the section in a 2-h period. The estimated savings in total travel time were calculated to be 1100 vehicle-h/d for 14 600 vehicles with an occupancy rate of 1.3 persons/vehicle. A cost of $5.51/vehicle-h for private vehicles was used to calculate a savings of $6061/weekday or $1 515 250/year [1975 prices taken from Buffington and McFarland (7)].

Fuel savings resulted from a reduction in travel time. Each vehicle saved an average of 4.52 min. This represents a time difference of 9 min at a speed of 32 km/h (20 mph) and 4.48 min at 64 km/h (40 mph) over a distance of 4.83 km (3 miles). Running cost at 32 km/h (20 mph) is $0.0613/vehicle-km ($0.0987/vehicle-mile); at 64 km/h (40 mph), it is $0.04/vehicle-km ($0.0644/vehicle-mile) or

($0.0613 - $0.04)/vehicle-km ($0.0987 - $0.0644)
÷ vehicle x 14 600 vehicles x 4.83 km
= $1502.34 operating cost savings/d or $375 585/year (1)

Approximately 75 percent of the operating costs are attributed to fuel. Therefore, the number of liters of gasoline conserved each year by the improvement can be estimated as follows (1 L = 0.26 gal):

($375 585)(0.75)(L/$0.125) = 2 253 510 L (2)

Similar calculations of benefits can be made for noise and air pollution and traffic accidents, but those categories were not included in this analysis. Therefore, total annual benefits are $1 890 835.

The cost of restriping the lanes was $38 700. The project required relocating two lighting standards and three roadside warning signs; modifying a metal guard beam section and two curb inlets; removing sections of curb, traffic buttons, and paint; applying asphalt overlay strip to smooth pavement-shoulder transition; stabilizing shoulders; and applying paint stripes. Lane lines were restriped after three months at a cost of $471, and additional lane markings and lane arrows were added at the Weslayan ramp at a cost of $157.

Some maintenance was required in the outer separation that had been used as emergency parking areas. Inadequate shoulder strength during wet weather caused the material to rut badly. Costs for this work were absorbed in normal maintenance activities, but the extra expense should be included as an annual cost of maintaining the installation.

The benefit/cost ratio for this project was $1 890 835/$39 328 or 48.1. Annual costs to maintain the system have not been calculated but should be considerably less than $40 000. At some time in the future, however, the shoulders will deteriorate and have to be replaced. If only the shoulders were to be replaced, the estimated cost would be $275 600 or $39 245/year. This is calculated for an interest rate of 7 percent and a time period of 10 years by using the uniform series capital recovery calculation.

Design and Maintenance Requirements

Cross sections with uniform lane widths of 3.2 m (10.5 ft) were designed because of the following considerations:

1. The median shoulder width was maintained at 3.05 m (10 ft) because of the small, mountable curb and drainage inlets in the median.
2. A paved right shoulder was desired where it was practical.
3. The volume of large vehicles that used this freeway during peak periods was very low.
4. The minimum desirable width for travel on freeways was considered to be 3.2 m.

The cross sections were changed in a 250-m (820-ft) transition zone. The old stripes and delineator buttons were removed by maintainer blades and sandblasting, and new paint stripes were placed. The paint tended to wear quickly because of vehicle encroachment and accumulation of oil and dirt. New stripes placed after 3 months of operation have worn well, but better delineation by means of new stripes and buttons will be provided after 15 months of operation.

The shoulder lanes have held up well under the increasing volume of traffic. The turf area in the outer separation that has been used for emergency parking has become rutted and requires considerable maintenance. New stabilized shoulders will be provided in those areas. The longitudinal joint between the main-line pavement and the old shoulder pavement has widened and requires maintenance. However, the quality and the safety of the ride over the joint has not been substantially reduced.

CONCLUSIONS

1. Adding a traffic lane in a bottleneck section of a freeway produces benefits in travel time, safety and quality of operation, and the volume of traffic that can be accommodated.
2. Such solutions are generally accepted by the public.
3. The additional capacity in a converted roadway section reduces accident rates and thus offsets any increase in accident potential attributable to narrow lanes and fewer emergency parking areas.
4. Additional capacity can be achieved at low cost by reconfiguring existing roadway and parking pavements. Benefit/cost ratios for these projects are very favorable.
5. Reconfigured roadways require additional maintenance to provide adequate lane delineation, structural integrity of the shoulder lane, and emergency parking areas.

ACKNOWLEDGMENTS

I wish to express my appreciation to Musa J. Misleh of the Houston district of SDHPT for his assistance in collecting the accident data for this study and to Jocille Johnson for her contributions to the manuscript.

This paper discusses one phase of a research project conducted by the Texas Transportation Institute and SDHPT in cooperation with the Federal Highway Administration. The contents reflect my views, and I am responsible for the facts and the accuracy of the data presented. The contents do not necessarily reflect the official views or policies of the Federal Highway Administration. This report does not constitute a standard, specification, or regulation.

REFERENCES

1. A. C. Estep and K. Moskowitz. Getting the Most out of a Freeway System. TRB, Special Rept. 153, 1975, pp. 10-18.
2. W. R. Green. Freeway Reconditioning. California Department of Transportation, Paper presented to AASHTO, July 1975.
3. F. Rooney. Restriping Freeways for Added Lanes. California Division of Highways, 1972.
4. G. Endo and J. J. Spinello. Evaluation of Santa Monica Freeway Viaduct Widening (Westbound Interstate Route 10). California Department of Transportation, 1973.
5. J. M. Portigo. State-of-the-Art Review of Paved Shoulders. TRB, Transportation Research Record 594, 1976, pp. 57-64.
6. J. C. Laughland and others. Methods for Evaluating Highway Safety Improvements. NCHRP, Rept. 162, 1975.
7. J. L. Buffington and W. F. McFarland. Benefit-Cost Analysis: Updated Unit Cost and Procedures. Texas Transportation Institute, Texas A&M Univ., Research Rept. 202-2, 1975.

Publication of this paper sponsored by Committee on Shoulder Design.

Structural Evaluation of PCC Shoulders

Jihad S. Sawan and Michael I. Darter, Department of Civil Engineering, University of Illinois

A structural evaluation of portland cement concrete (PCC) shoulders has been conducted. The influence of the major design variables on the behavior of shoulders under load was determined by using a finite element analysis program and data from field surveys of several PCC shoulders. The major design variables studied include slab thickness and tapering, foundation support and loss of support, joint spacing, lane-shoulder tie, shoulder width, and design and condition of the adjacent lane. Results of analytical and field studies show that each of these variables can have a significant effect on the performance of PCC shoulders and also on the performance of the adjacent traffic lane. A minimum slab thickness of 15 cm (6 in) is recommended, but certain design situations—i.e., poor foundation support, need for significant load transfer support at the lane edge, heavy traffic, or a narrow shoulder—require greater thickness. The required thickness should be determined from structural analysis. To achieve the greatest structural benefits for the traffic lane and the shoulder, load transfer efficiency at the longitudinal joint should be greater than about 50 percent. Field studies indicate that this efficiency can be attained by providing tie bars across the longitudinal joint. Shoulder width should be at least 91 to 152 cm (3 to 5 ft) to contribute a significant structural benefit. A shoulder joint spacing of 4.6 m (15 ft) is recommended to minimize joint spalling and blowups and slab cracking. If the shoulder is designed properly, significant improvement in the performance of the traffic lane for both new construction and rehabilitation as well as long-term, low-maintenance performance of the PCC shoulder can be achieved.

Portland cement concrete (PCC) shoulders have been constructed for many years on some urban expressways but for only about the past 12 years on rural highways. They were first constructed on an experimental basis but have more recently become a part of regular construction. Because no structural design procedure is available, design has been based on engineering judgment and on the performance of a few experimental sec-

tions. The purpose of this study is to improve shoulder design by determining the effects of the major design variables on PCC shoulder performance and also the effect of shoulder design on the adjacent traffic lane. The evaluation includes the placement of PCC shoulders for the purpose of rehabilitating existing pavements and also as part of new pavement construction.

Shoulders are an integral part of today's major highways and are required to provide structural support to (a) encroaching traffic loads from the adjacent traffic lane, (b) emergency parking, and (c) regular traffic if the shoulder is used as a detour around a closed lane or as an additional lane during peak traffic hours. Shoulder design has been inadequate in the past (usually because of an effort to minimize construction costs); this has often led to considerable distress and required major maintenance.

The influence of many of the major variables in the design of PCC shoulders has not been previously determined. To study their influence, a program of finite element slab analysis was used to compute critical stresses and deflections for several shoulder and lane design configurations. Surveys of several experimental PCC shoulders have also provided field data about some of the design variables. The guidelines for improved design presented in this study were formulated based on the study results for both rehabilitation and new construction.

DESIGN CONSIDERATIONS

The two major engineering objectives in shoulder design are to (a) provide a shoulder that will structurally support encroaching traffic loads for long-term, low-maintenance performance, and (b) provide a shoulder that will reduce the rate of deterioration of the adjacent lane of pavement (usually the heaviest traveled truck lane). If both objectives can be accomplished economically, placing PCC shoulders during new construction or replacing deteriorated shoulders on existing highways with PCC shoulders can be very beneficial.

The major design variables for PCC shoulders are (a) slab thickness and tapering of thickness, (b) joint spacing, (c) foundation support and loss of foundation support, (d) tie between the shoulder and the traffic lane (including load transfer of the longitudinal joint), (e) width of the shoulder slab, and (f) design and condition of the adjacent traffic lane. The shoulder must withstand both repeated moving loads and static loads from parked vehicles. Both of these conditions involve edge loading caused by heavy trucks. Because the edge-loading condition is the most critical in fatigue damage (3), the stresses and deflections that result from that condition are referred to in this study as critical stresses and deflections. The actual amount of loading is relatively unknown but probably varies widely within a given project and from project to project. The effects of moisture and of loss of support caused by pumping and settlement should also be considered because of edge-loading conditions.

Several studies have been made of the critical effect of edge loadings on the performance of all types of PCC pavements. Recent field and analytical studies have concluded that edge loading results in transverse cracking of jointed concrete slabs and edge punchouts of continuously reinforced concrete pavement (CRCP) (1, 2, 3, 4). Studies of traffic encroachment have shown that much more edge loading of traffic-lane slabs and shoulder encroachment occur than was previously believed (5, 6). Structural design procedures that will attempt to consider these major design variables are being developed at the University of Illinois.

EFFECT OF DESIGN VARIABLES ON PERFORMANCE

The influence of the major design factors on the structural performance of PCC shoulders is determined by using a finite element program that was originally developed by Huang and Wang (7) but has been modified at the University of Illinois to handle problems such as PCC shoulder design. Stresses computed in the program have been found to agree very closely with stresses computed from measured strains at the AASHO Road Test (3).

Shoulder Thickness

The effect of the thickness of a PCC shoulder on the critical tensile stress caused by an encroaching 80-kN (18 000-lb) single-axle wheel load is shown in Figure 1. The design configuration is typical and has a traffic lane 20.3 cm (8 in) thick, 3.6 m (12 ft) wide, and 4.6 m (15 ft) long. The PCC shoulder is 3 m (10 ft) wide and ranges in uniform thickness from 10.2 to 30.5 cm (4 to12 in). Three different load transfer efficiencies are shown for the lane-shoulder longitudinal joint. If the load transfer efficiency is 0 percent, there is no tie between the shoulder and the lane and they act independently. If the efficiency is 100 percent, there is complete load transfer (i.e., the deflection of the loaded side of the joint is equal to the deflection of the unloaded side). Transfer of moment across the joint is zero in both cases because joints transfer very little, if any, moment.

As thickness increases from 10 to 31 cm (4 to 12 in), tensile stress decreases. The rate of decrease is much more rapid for slabs less than 20 cm (8 in) thick when load transfer efficiency is low (0 to 50 percent). When the shoulder is not tied to the lane (efficiency = 0 percent), the stresses approach or exceed the range of flexural strength of PCC for slabs less than 20 cm thick. Stresses greater than about 3450 kPa (500 lbf/in^2) will result in cracking of the shoulder after only a few heavy load applications.

The effect of load transfer at the joint is significant. If there is reasonable load transfer (50 percent) and slab thickness (≥20 cm), the effect of increased thickness on stress is reduced at the lane-shoulder joint. Parked trucks impose a wheel load at the outside edge of the shoulder where the load transfer is of course 0 percent. Thus, the thickness design of PCC shoulders should consider both loading positions and the number of applications at each position.

Shoulder Width

The width of the shoulder affects both critical stress and deflections in the shoulder slab. Figures 2 and 3 show these effects for a range of design conditions. The load efficiency is 0 percent, thickness varies from 15.2 to 30.5 cm (6 to 12 in), and foundation support varies from poor for saturated clay [k = 1.38 kg/cm^3 (50 lb/in^3)] to excellent for a thick stabilized subbase [k = 13.84 kg/cm^3 (500 lb/in^3)]. Deflection increases very rapidly for a width of less than about 1.5 m (5 ft). For poor foundations, narrow PCC shoulders experience high deflections and thickness has only minimal effect. Thickness has a more significant effect on deflections in the case of wider shoulders (B > 1.5 m).

The effect of width on critical stress is shown in Figure 3. For example, for a slab that is 20 cm (8 in) thick, widening the shoulder from 0.9 to 1.5 m (3 to 5 ft) reduces stress by 20 percent, and widening the shoulder from 1.5 to 3 m (3 to 10 ft) causes a decrease of only 5 percent. The effect of shoulder width is about the same regardless of slab thickness. Thus, for structural pur-

Figure 1. Effect of shoulder thickness and lane-shoulder tie on tensile stresses at bottom of PCC shoulder.

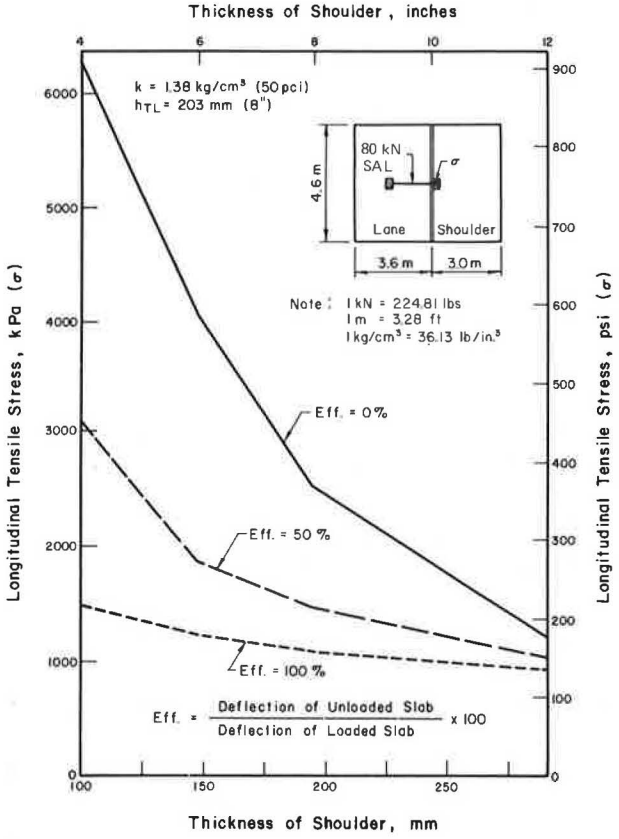

poses, a shoulder wider than 1.5 m has a minimal effect on the critical stresses caused by encroaching truck traffic near the longitudinal joint. If a narrow shoulder is required, the critical stress can be reduced to allowable levels by increasing the thickness of the shoulder slab and joint efficiency. For example, a 3-m-wide shoulder of 20-cm thickness has a tensile stress of 2550 kPa (370 lbf/in^2) under an encroaching truck wheel load (Figure 3). If the shoulder were to be constructed only 0.9 m (3 ft) wide, the thickness required for the same stress would be 25 cm (10.1 in).

Tapering of the PCC shoulder has been used on some existing projects. The taper would not have much effect on the critical stress near the longitudinal joint if the full shoulder thickness were carried about 0.9 to 1.5 m (3 to 5 ft). The thickness could then be tapered to the outside edge of the shoulder. But critical stresses caused by trucks that park on the shoulder with their wheels at the outer edge limit the taper to some acceptable edge thickness. The outside shoulder edge will probably receive far fewer load applications than the inside edge near the traffic lane, but these high free-edge stresses must be considered in design.

Foundation Support and Loss of Support

The effect of foundation support on deflections and stresses in the shoulder is shown in Figures 2, 4, and 5. Foundation support—measured by the k value, which has a significant effect on deflection—is shown in Figure 2. A poor foundation [k = 1.38 kg/cm^3 (50 lb/in^3)] has a very large deflection in comparison with a moderate foundation [k = 5.5 kg/cm^3 (200 lb/in^3)]. Large shoulder deflections may result in settlements and pumping problems. A stiff foundation [k = 13.8 kg/cm^3 (500 lb/in^3)]

Figure 2. Effect of encroachment of truck wheel loads on deflection of PCC shoulder for various conditions of support and thickness.

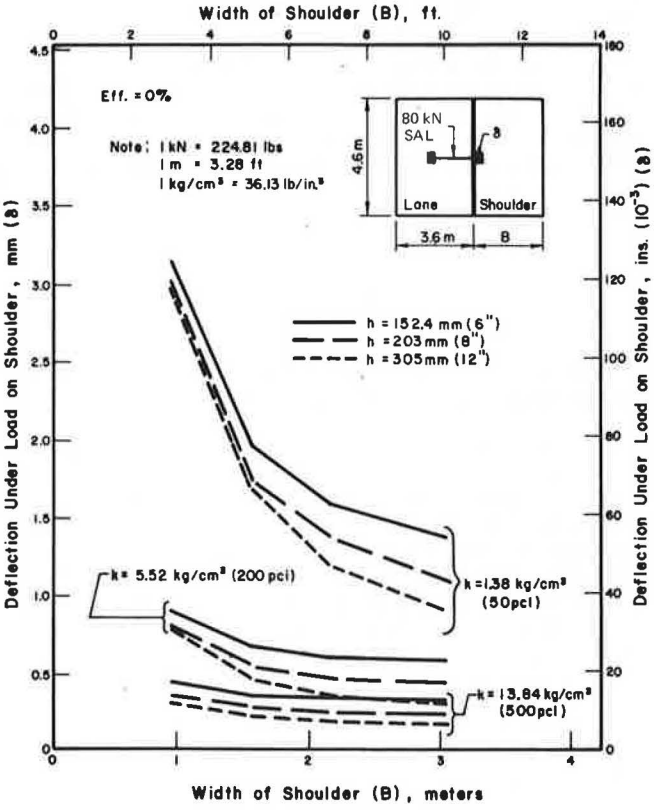

Figure 3. Effect of thickness and width of PCC shoulder on tensile stresses at bottom of shoulder.

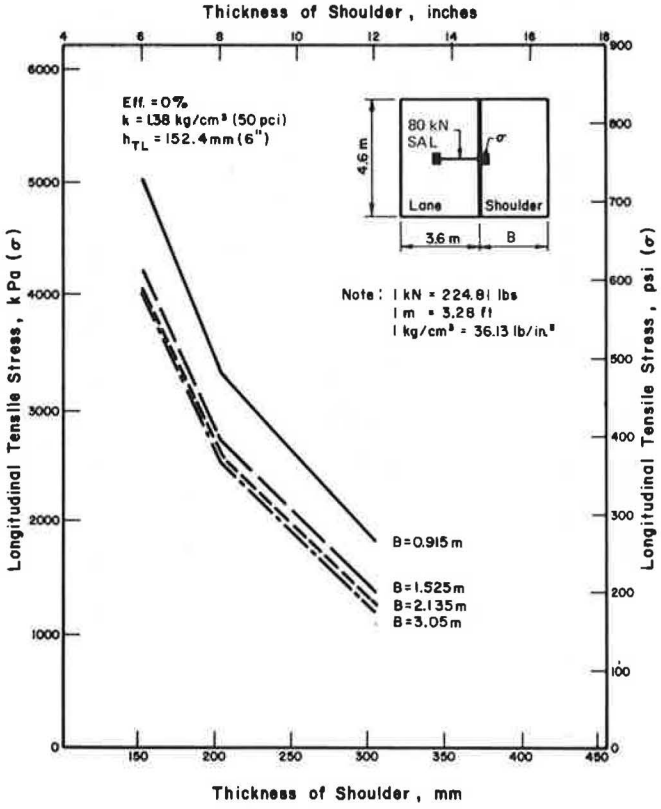

Figure 4. Effect of encroachment of truck wheel loads on tensile stresses at bottom of PCC shoulder for various conditions of support and thickness.

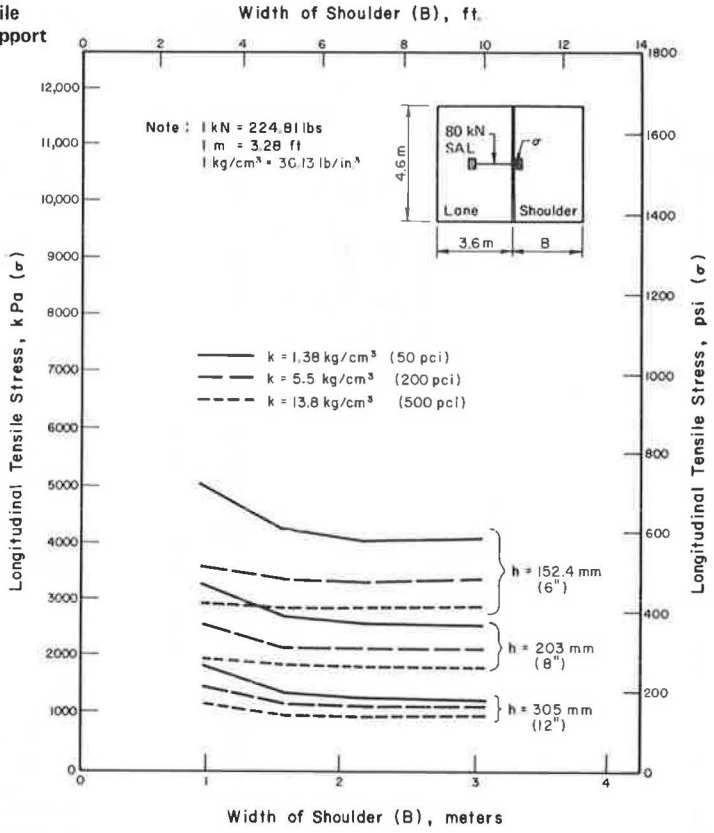

Figure 5. Effect of loss of support on tensile stresses at bottom of PCC shoulder.

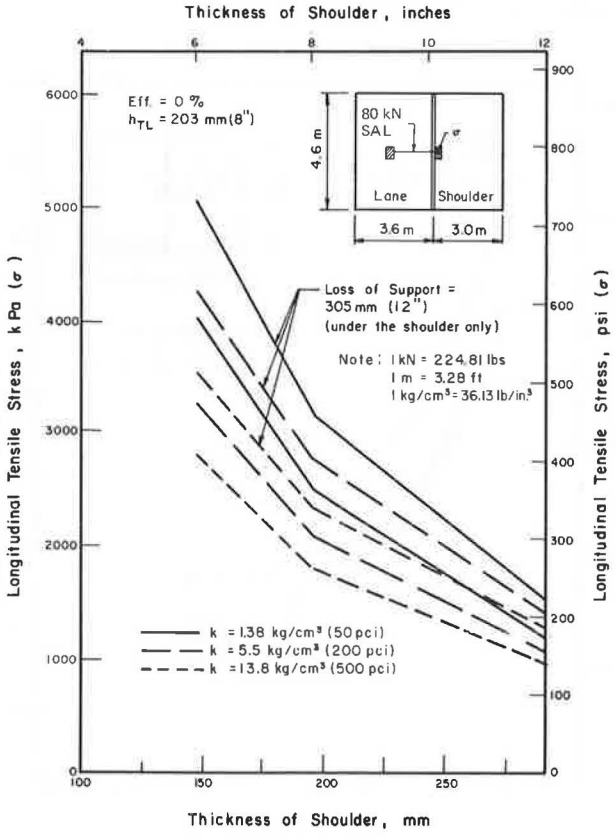

reduces the deflections to 20 percent of those for a poor foundation.

The influence of foundation support on critical stress for a range of design variables is shown in Figure 4. Stresses are not as sensitive to foundation support as are deflections but, as foundation support increases, critical stresses decrease. The effect is much greater for thin shoulder slabs than for thicker slabs. For example, a shoulder 15 cm (6 in) thick and 3 m (10 ft) wide shows the following critical stresses for the three conditions of foundation support (1 kPa = 0.145 lbf/in^2):

Support	Critical Stress (kPa)	Ratio to Poor
Poor	4137	1.00
Moderate	3309	0.80
Stiff	2758	0.67

These data show that foundation support has a significant effect on critical stress, especially for the poor condition.

The effect of loss of support beneath the shoulder edge near the lane-shoulder joint is shown in Figure 5. A loss of support of 30 cm (12 in) could be caused by, for example, the settlement of a subsurface drain trench beneath the shoulder. In such a case, the increase in critical stress is about 25 percent. This can be adjusted for by increasing shoulder slab thickness by approximately 3.5 cm (1.4 in) for an original 15-cm (6-in) shoulder, for example.

Lane-Shoulder Tie and Load Transfer

The extent of the tie between the traffic lane and the shoulder affects load transfer, separation of the shoul-

Figure 6. Effect of joint spacing of PCC shoulder on joint spalling.

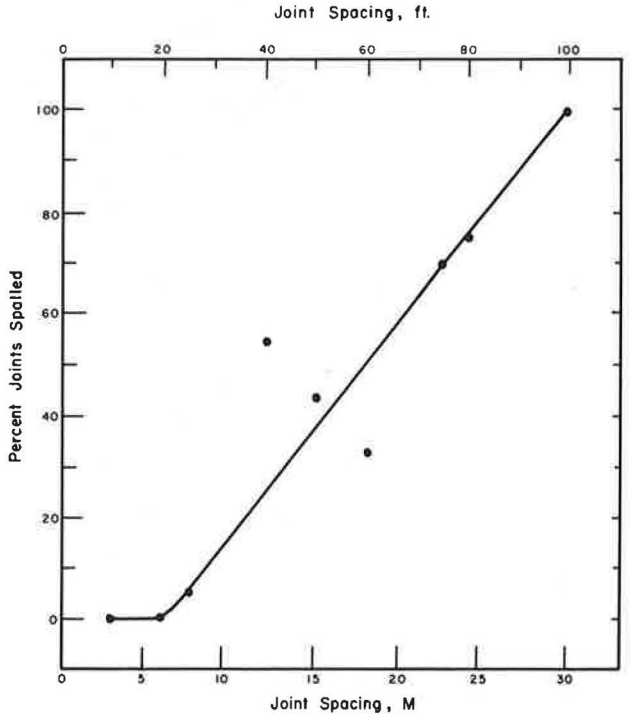

Figure 7. Effect of joint spacing of PCC shoulder on transverse cracking.

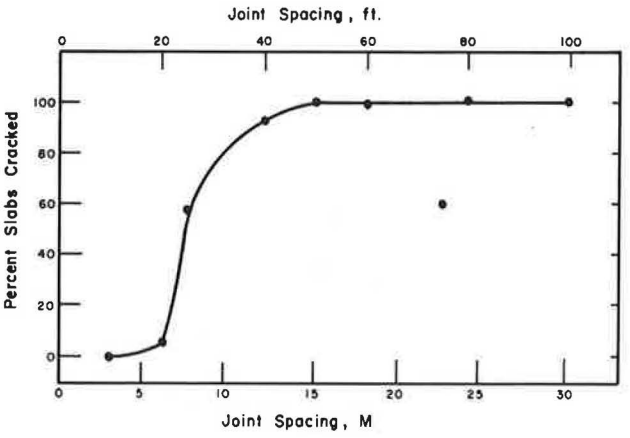

der from the lane, and settlement of the shoulder. The effect of the lane-shoulder tie (as indicated by joint load transfer or efficiency) on critical stress in the shoulder is shown in Figure 1. At the 10- to 20-cm (4- to 8-in) range of thickness, the extent of joint efficiency has a very large effect on stress. Changing from 0 to 50 percent efficiency reduces stress by a factor of 2.1 and to 100 percent by a factor of 3.3 for a 15-cm (6-in) shoulder slab. The reduction in critical stress from 0 to 50 percent efficiency is most significant.

Joint Spacing

The effect of joint spacing on the performance of PCC shoulders is shown in Figures 6 and 7. These are based on data obtained from a field survey of three sections of plain PCC shoulders located in Illinois. The sections, which are 9 to 12 years old, are located on Ill-116, I-74, and I-80 (9, 10). The traffic lanes were composed of CRCP, jointed reinforced concrete pavement (JRCP), and composite (asphalt over JRCP) pavement. Most of the sections were tied by rebars to the main-line pavement.

Figure 6 shows the effect of joint spacing on the percentage of joints spalled. As the shoulder joint spacing exceeds 6.1 m (20 ft), the proportion of spalled shoulder joints increases rapidly to the point where, at a spacing of 30 m (100 ft), all joints are spalled. The relation between shoulder joint spacing and percentage of shoulder slabs cracked is shown in Figure 7. Again, as the joint spacing exceeds 6.1 m, a very rapid increase in slab cracking occurs. A number of the transverse cracks had spalled. In addition, many blowups were found in sections that had joint spacings of about 12 to 18 m (40 to 60 ft), and one blowup was found for a joint spacing of 6.1 m.

Other field surveys on main-line pavements and experimental field tests have shown the benefits of using small joint spacings (2, 3).

Effect of PCC Shoulder on Traffic Lane

A PCC shoulder may have an influence on the performance of the adjacent traffic lane. Figure 8 shows the influence of a shoulder on critical edge stress in the traffic lane. As load transfer efficiency increases from 0 percent (no effect) to 100 percent, the critical edge stress decreases by about 50 percent. The decrease is more rapid for up to 50 percent efficiency. The influence of the PCC shoulder on traffic-lane deflections is shown in Figure 9. If the joint has 100 percent efficiency, the deflection decreases by about 50 percent for this example.

Figure 10 shows the influence of both shoulder width and load transfer efficiency on critical stress. The width of the shoulder has a large influence in reducing stress in the traffic lane for a width of up to 0.9 m (3 ft). Beyond that width there is almost no effect. The strong influence of joint load transfer is again indicated. These analytical results show that PCC shoulders should have a beneficial influence on the performance of adjacent traffic lanes if load transfer is reasonable.

Table 1 gives the results of field surveys conducted along the entire length of two projects that included PCC shoulders. Both projects had been constructed about 10 years before and contained CRCP in the main traffic lanes. All types of distress were recorded in the traffic lane adjacent to the shoulders. In general, extensive structural distress was found in the portions of both projects that did not contain PCC shoulders, and little distress was found in the portions that contained the shoulders. On the I-74 project, there was evidence of extensive pumping in areas that did not include PCC shoulders.

Joint separation and settlement of the shoulders were also determined on the three projects. On I-74, it was found that sections that had tie bars experienced virtually no joint separation whereas sections that did not have tie bars experienced joint separation that ranged between 12.7 and 25.4 mm (0.5 and 1 in). On I-80, all the sections with PCC shoulders that were surveyed are tied to the traffic lane. Joint separation was very small [<5 mm (<0.2 in)].

The survey on Ill-116 showed that the sections that had tie bars had a joint separation of less than 5 mm (0.2 in) whereas the section that had a longitudinal keyway had a joint separation of up to 12.5 mm (0.5 in). The section that had neither tie bars nor keyway had a joint separation of up to 25.4 mm (1 in). Thus, tie bars are absolutely required to maintain a tight joint so that

high load transfer efficiency can be maintained over a long time period.

DESIGN GUIDELINES

Slab Thickness

PCC shoulder thickness has a very significant influence on critical stress caused by encroaching traffic loads (Figure 1). Two load positions must be considered to determine required thickness: (a) the inside edge near the lane-shoulder longitudinal joint and (b) the outside free edge. The inside edge of the longitudinal joint is subjected to many more load applications than the outside edge, but if the shoulder is tied to the lane so that there is reasonable load transfer, stress on the inside edge will be significantly reduced—from 4000 to 2000 kPa (580 to 290 lbf/in^2) for a 15-cm (6-in) shoulder that has 50 percent joint efficiency (Figure 1). Because the reduction in stress is so large, it is believed that the outer free edge may control design thickness when a reasonable lane-shoulder tie is provided. Fatigue analyses are being conducted to verify this point and to provide a rational design procedure for determining adequate thickness. A minimum thickness of 15 cm is currently recommended because thinner slabs loaded

Figure 8. Effect of concrete shoulder on critical edge stress for varying joint load transfer efficiency.

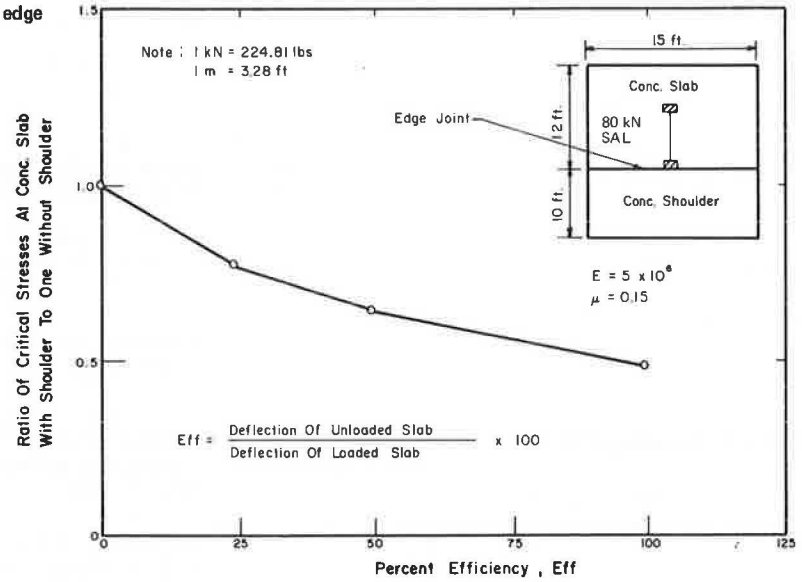

Figure 9. Effect of lane-shoulder tie on deflection of PCC traffic lane.

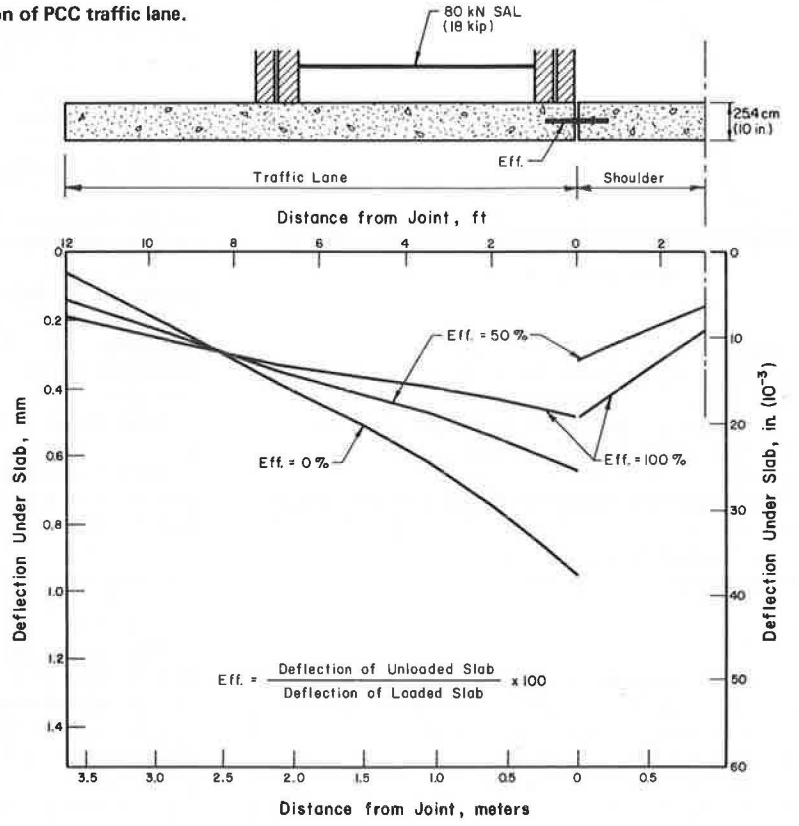

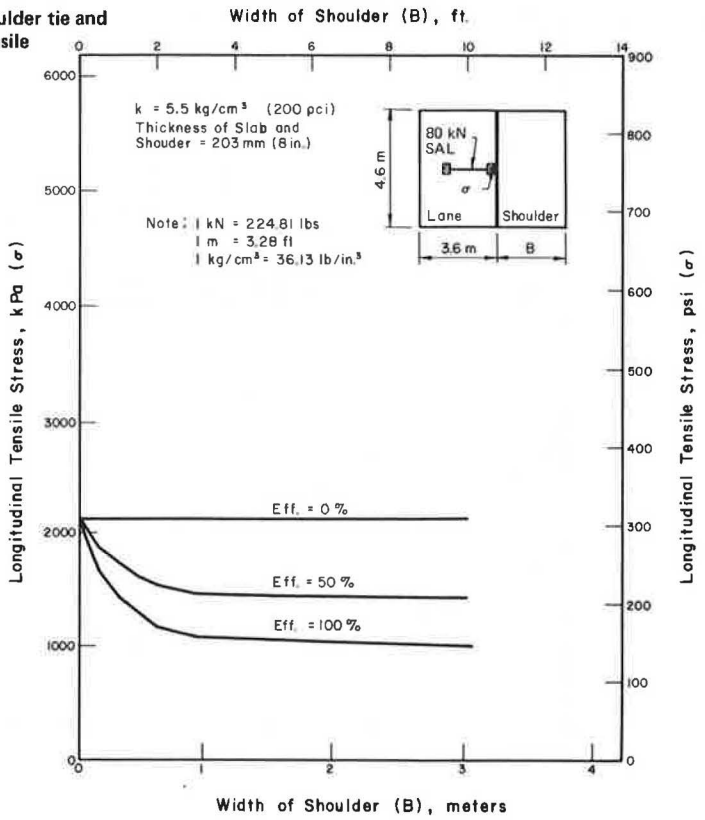

Figure 10. Effect of lane-shoulder tie and width of PCC shoulder on tensile stress of traffic lane.

Table 1. Distress in traffic lane for two CRCP projects that have PCC shoulders along a portion of their length.

		Portion Without PCC Shoulders			Portion With PCC Shoulders		
Project	Age (years)	Length (km)	Edge Punchouts per Kilometer	Wide Cracks per Kilometer	Length (km)	Edge Punchouts per Kilometer	Wide Cracks per Kilometer
I-80	9	3.54	3.7	4.9	1.12	0.7	3.1
I-74	10	3.11	2.5	1.0	0.5	0	0

Note: 1 km = 0.62 mile.

by typical heavy trucks develop very high stresses and tend to crack after only a few such applications. Whether thicker shoulders may be required depends on truck traffic, the amount of structural support desired for the traffic-lane edge, foundation support, load transfer at the joint, and shoulder width.

The table below gives a summary of performance data from the two Illinois highway projects (1 cm = 0.39 in, 1 m = 3.3 ft, and 1 kN = 225 lb):

Parameter	I-74	I-80
Age (years)	10	9
Thickness of traffic lane	18-cm CRCP	20-cm CRCP
Thickness of PCC shoulder	15 cm	20 cm at joint, tapering to 15 cm at outside edge
Range of joint spacing	3-30.5 m	6.1 m
Tie	Tie bars and no tie bars (no. 4 bars 76 cm long, spaced 76 cm center to center)	Anchor bars
Mean average daily traffic in adjacent truck lane	950	2140
80-kN equivalent single-axle loads in adjacent lane (over life of pavement)	2 700 000	7 000 000
Percentage of slabs cracked		5
3.05-m joint spacing	0	
6.10-m joint spacing	5	
7.60-m joint spacing	60	
12.10-m joint spacing	90	
15.25-m joint spacing	100	
18.30-m joint spacing	100	
24.40-m joint spacing	100	
30.50-m joint spacing	100	

Both pavements (especially I-80) carried heavy truck traffic. The 50 percent slabs cracked on I-74 is cause for concern; the long 7.6-m (25-ft) joint spacing had an effect on the cracking because similar, adjacent 3-m (10-ft) long slabs did not show any cracking. The 20- to 15-cm (8- to 6-in) tapered shoulders on I-80 performed very well under heavy traffic: Only 5 percent of the slabs cracked.

Although tapering the shoulder thickness between the two edges has been thought to save on concrete, it may not be the best design for the following reasons:

1. The critical stress load position is probably the outside free edge because of parked trucks or moving traffic that uses the shoulder as a detour around a closed lane.
2. Tapering tends to put the entire pavement section

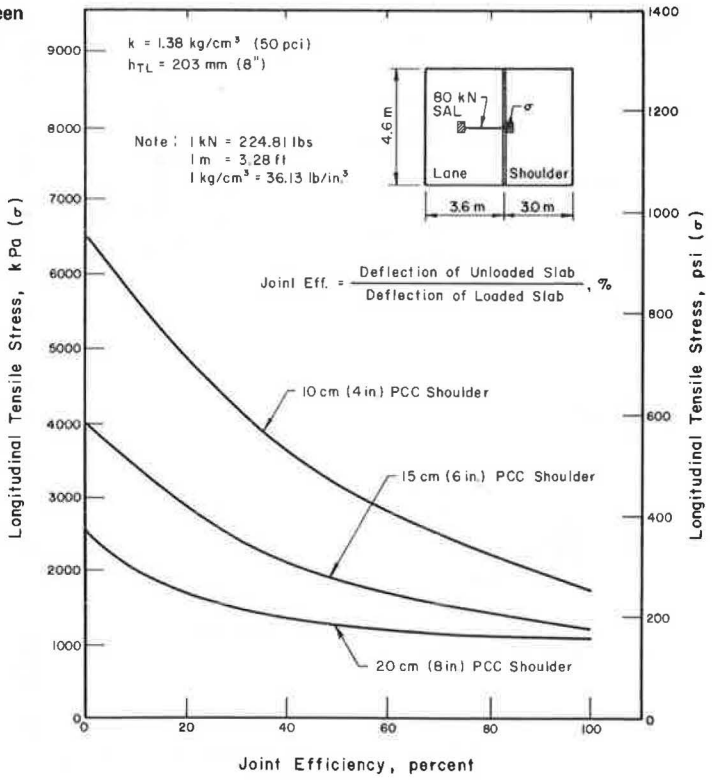

Figure 11. Effect of joint efficiency (tie between traffic lane and shoulder) on tensile stresses in bottom of PCC shoulders.

Table 2. Field data on I-74 and I-80 PCC shoulders to determine efficiency of longitudinal lane-shoulder joint.

Project	Shoulder Design	Mean Edge Deflection (mm)		Load Transfer Efficiency (d)
		Traffic Lane	Shoulder	
I-74[a]	Tie bars, keyway, and granular subbase	0.1143	0.1118	97.8
	Tie bars, keyway, and no subbase	0.1448	0.1016	70.2
	Keyway and granular subbase but no tie bars	0.2108	0.0330	16.0
I-80[b]	Tie bars and intermediate granular subbase	0.2311	0.0889	38.5
	Tie bars and coarse granular subbase	0.2464	0.0762	31.0
	Tie bars and no subbase	0.2159	0.1016	47.0

Note: 1 mm = 0.039 in.

[a] Ten-year-old PCC shoulders. [b] Nine-year-old PCC shoulders.

in a "bathtub" so that water is trapped in the structural section.

3. It is doubtful whether the additional grading required for tapering results in any construction-related cost saving.

Shoulder Width

Required shoulder width is generally dictated by geometric and safety considerations. However, the width influences stresses and deflections in the shoulder and the adjacent traffic lane if they are tied together. The width of a tied shoulder should be at least 91 to 152 cm (3 to 5 ft) to provide maximum structural benefits (stress and deflection) to the traffic lane and shoulder. A narrower shoulder could be used (with load transfer) to help reduce edge stresses in the traffic lane, but a thicker PCC shoulder slab is required.

Lane-Shoulder Tie

The lane-shoulder tie is an effective way of reducing critical stress and deflection and preventing separation at the joint. The effect of joint efficiency (or the extent of load transfer) on the critical shoulder stress is shown in Figure 11 for a typical design situation. A tie system that provided at least 50 percent load transfer would reduce critical stress to acceptable levels. The shape of the curves in the figure shows that there is really only a small advantage in providing more than 50 percent load transfer.

There are essentially three methods of obtaining this level of load transfer along the longitudinal joint:

1. Use of a keyed joint and tie bars that hold the joint very tight,
2. Use of tie bars that hold the joint very tight, and
3. Use of steel dowels.

Tie bars or anchor bolts have been used on most PCC shoulders constructed up to this time.

Field studies were conducted to determine load transfer efficiency in the I-74 and I-80 experimental shoulders (Table 2). On both projects, the procedure used was similar to that used at the AASHO Road Test (13) where the outside of dual tires was 7.5 to 15 cm (3 to 6 in) from the edge of the traffic-lane slab and the beam probe was at the edge of the traffic lane and the edge of the shoulder (creep speed deflection).

On I-74, deflections were measured by using the

Benkelman beam and a single-axle load of 84.4 kN (19 000 lb). After 10 years in service [2.7 million 80-kN (18 000-lb) equivalent single-axle loads (ESAL)], the load transfer efficiency for tied shoulders with a keyway ranged from 70 to 98 percent. Those without tie bars had very low efficiency (16 percent) because of lane-shoulder separation.

After 9 years of service (7 million 80-kN ESAL), load transfer efficiency on I-80 for tied shoulders without a keyway (butt joint) ranged from 31 to 47 percent (Table 2). The I-80 joint had opened an average of about 10 mm (0.4 in), and some of the bars had ruptured. Thus, joint design on I-80 did not provide a long-term joint efficiency of 50 percent or greater.

Laboratory tests by the Portland Cement Association showed that steel tie bars are effective in extending the endurance of aggregate interlock and keyed joints under repeated loading. Load transfer efficiency after about 5 million load applications was greater than 70 percent for aggregate interlock, keyway, and smooth joints, all of which had steel ties (12). Dowels have been shown to provide very high load transfer efficiency (>80 percent) even if the joint separates somewhat (11). Thus, as Figures 10 and 11 show, if a tied shoulder is used and at least 50 to 70 percent load transfer efficiency is attained, stresses in both the traffic lane and the shoulder are significantly reduced (by 30 and 55 percent respectively). One problem that has been noticed is that when PCC shoulders are on high fills the outer edge tends to settle; as a result, some joints have separated because the tie bars pulled out from the PCC or the steel ruptured. Consideration should therefore be given to increasing the number of tie bars for greater load transfer and to prevent separation.

Foundation Support

The PCC shoulder can be placed directly on the subgrade soil, a granular subbase, or a stabilized subbase. These foundation conditions can generally be considered poor, moderate, and stiff respectively. Analysis shows that PCC shoulders that have poor support [$k \cong 1.38$ kg/cm^3 (50 lb/in^3)] show large deflections and stresses. Providing a moderate level of support [$k \cong 5.5$ kg/cm^3 (200 lb/in^3)] appears to be justified. Using a stiffer foundation support is not very effective in further reducing deflections or stresses. Field results in Illinois have shown little difference in the performance of sections that have granular subbases and those that have fine-grain soil subbases. However, continuous drainage should be considered when subbases are selected to avoid a bathtub cross section.

Slab Length

Based on results from the field survey, a maximum slab length of 3.6 m (15 ft) is recommended. The reason for this choice can be seen in Figures 6 and 7, which clearly show that using a slab longer than 3.6 to 6.1 m (15 to 20 ft) will result in joint spalling and increased transverse cracking. Short slab lengths eliminate the need for steel reinforcement and reduce joint movement to an amount small enough that it does not force cracks to open up on the adjacent traffic lane in either CRCP or JRCP.

Effect of Shoulder on Traffic Lane

The shoulder affects stress and deflection of the traffic lane (a) through the load transfer of the longitudinal joints and (b) by minimizing the potential for edge pumping. Figures 8, 9, and 10 show that the efficiency of load transfer between the traffic lane and the shoulder is of significant importance to the traffic lane. Figures 8 and 10 show that critical edge stresses for the traffic lane could be reduced by more than 30 percent if a 50 percent joint efficiency were used. Figure 9 shows that edge deflection for the traffic lane could be reduced by about a third if there were 50 percent joint efficiency. Reduction of stresses and deflections would therefore improve the performance of the traffic lane (Table 1). Figures 8, 9, and 10 indicate that, to improve the performance of the traffic lane, optimum design of a shoulder would require providing maximum load transfer across the longitudinal joint (≥50 percent) and adequate shoulder thickness [≥15 cm (≥6 in)], width [>0.9 m (>3 ft)], and foundation support [≅ 5.5 kg/cm^3 (≅ 200 lb/in^3)]. Provision of a PCC shoulder either on new construction or for rehabilitation of an existing shoulder is expected to have a beneficial effect if these design requirements are met.

The condition and the design of the existing traffic lane should be determined. If distress associated with edge traffic loadings is occurring, special consideration should be given to providing high load transfer and adequate shoulder thickness to reduce critical stresses and deflections in the traffic lane.

CONCLUSIONS

Analytical and field studies have shown that PCC shoulders can be designed to (a) provide long-term, low-maintenance performance and (b) help to reduce the amount of distress in the adjacent traffic lane. The influence of major design variables on shoulder behavior under load was determined by using a finite element analysis program and data from field surveys of several PCC shoulders. Improvements in design practice are recommended. Additional work is under way at the University of Illinois to develop structural design procedures that consider the effect of repeated loadings on the shoulder so that slab thickness can be determined more adequately. Work is also under way to determine the amount of load transfer across various longitudinal joint designs.

ACKNOWLEDGMENTS

This investigation was conducted at the University of Illinois at Urbana-Champaign. We wish to thank the sponsor—the Federal Highway Administration, U.S. Department of Transportation.

REFERENCES

1. S. A. LaCoursiere, M. I. Darter, and S. A. Smiley. Evaluation of Performance and Maintenance of CRCP in Illinois. Univ. of Illinois, Project 901, interim rept., 1977, in preparation.
2. M. I. Darter and E. J. Barenberg. Zero-Maintenance Pavement: Results of Field Studies on the Performance Requirements and Capabilities of Conventional Pavement Systems. Federal Highway Administration, Technical Rept. FHWA-RD-76-105, 1976.
3. M. I. Darter. Design of Zero-Maintenance Plain Jointed Concrete Pavement: Vol. 1—Development of Design Procedures. Federal Highway Administration, Technical Rept. FHWA-RD-77-111, 1977.
4. M. I. Darter. Design of Zero-Maintenance Plain Jointed Concrete Pavement: Vol. 2—Design Manual. Federal Highway Administration, Technical Rept. FHWA-RD-77-112, 1977.
5. D. K. Emery, Jr. Transverse Lane Placement for Design Tracks on Rural Freeways. Office of Road

Design, Georgia Department of Transportation, preliminary rept., 1974.
6. R. G. Hicks, R. D. Barksdale, and D. K. Emery. Design Practices for Paved Shoulders. TRB, Transportation Research Record 594, 1976, pp. 48-56.
7. Y. H. Huang and S. T. Wang. Finite-Element Analysis of Concrete Slabs and Its Implications for Rigid Pavement Design. HRB, Highway Research Record 466, 1973, pp. 55-69.
8. E. C. Lokken. What We Have Learned to Date From Experimental Concrete Shoulder Projects. HRB, Highway Research Record 434, 1973, pp. 43-53.
9. Portland Cement Concrete Shoulders. Illinois Division of Highways, Project IHR-404, interim rept., July 1970.
10. L. J. McKenzie. Experimental Paved Shoulders on Frost Susceptible Soils. Illinois Department of Transportation, Project IHR-404, final rept., March 1972.
11. W. B. Stelzenmulter, L. L. Smith, and T. J. Larson. Load Transfer at Contraction Joint in Plain Portland Cement Concrete Pavements. Florida Department of Transportation, Research Rept. 90-D, April 1973.
12. C. G. Ball and L. D. Childs. Tests of Joints for Concrete Pavements. Portland Cement Association, 1975.
13. The AASHO Road Test: Report 5—Pavement Research. HRB, Special Rept. 61E, 1962.

Publication of this paper sponsored by Committee on Shoulder Design.